The role of reactive oxygen species in thyroid radio-carcinogenesis

Fabio Hecht Castro Medeiros

THE ROLE OF REACTIVE OXYGEN SPECIES IN THYROID RADIO-CARCINOGENESIS

Thèse de doctorat de l'Université Paris-Saclay
et de l'Universidade Federal do Rio de Janeiro
préparée à Université Paris Sud

Programa de Pós-Graduação em Ciências Biológicas
Instituto de Biofísica Carlos Chagas Filho
École doctorale n°568 BIOSIGNE
Signalisations et réseaux intégratifs en biologie
Spécialité de doctorat: Aspects moléculaires et cellulaires de la biologie

Thèse présentée et soutenue à Rio de Janeiro, le 28/03/2018, par

M. Fabio Hecht Castro Medeiros

Composition du Jury :

M. Antônio Carlos Campos de Carvalho Professeur, Universidade Federal do Rio de Janeiro	Président
Mme. Françoise Miot Professeur, Université Libre de Bruxelles	Rapporteur
M. Leonardo Teixeira Karam Directeur de Recherche, INCA	Examinateur
M. Filippo Rosselli Directeur de Recherche, CNRS (UMR8200)	Examinateur
Mme. Corinne Dupuy Directrice de Recherche, CNRS (UMR8200)	Directrice de thèse
Mme. Denise Pires de Carvalho Professeur, Universidade Federal do Rio de Janeiro	Directrice de thèse

Université Paris-Saclay
École doctorale n°568
BIOSIGNE - Signalisations et réseaux intégratifs en biologie

Universidade Federal do Rio de Janeiro
Instituto de Biofísica Carlos Chagas Filho
Programa de Pós-Graduação em Ciências Biológicas (Fisiologia)

FABIO HECHT CASTRO MEDEIROS

THE ROLE OF REACTIVE OXYGEN SPECIES IN THYROID RADIO-CARCINOGENESIS

Rio de Janeiro,
2018

FABIO HECHT CASTRO MEDEIROS

THE ROLE OF REACTIVE OXYGEN SPECIES IN THYROID RADIO-CARCINOGENESIS

Doctoral thesis presented to *Programa de Pós-Graduação em Ciências Biológicas, Instituto de Biofísica Carlos Chagas Filho, Universidade Federal do Rio de Janeiro* and *École Doctorale Biosigne, Faculté de Médicine, Université Paris-Saclay* as a requisite for the title of PhD.

Supervisors: Corinne Dupuy (Université Paris-Saclay) and Denise Pires de Carvalho (Universidade Federal do Rio de Janeiro)

Rio de Janeiro,

2018

FABIO HECHT CASTRO MEDEIROS

THE ROLE OF REACTIVE OXYGEN SPECIES IN THYROID RADIO-CARCINOGENESIS

Doctoral thesis presented to *Programa de Pós-Graduação em Ciências Biológicas, Instituto de Biofísica Carlos Chagas Filho, Universidade Federal do Rio de Janeiro* and *École Doctorale Biosigne, Faculté de Médicine, Université Paris-Saclay* as a requisite for the title of PhD.

Approved in: March 28th, 2018

Antônio Carlos C. de Carvalho, DSc Universidade Federal do Rio de Janeiro	Corinne Dupuy, PhD Université Paris-Saclay
Denise Pires de Carvalho, DSc Universidade Federal do Rio de Janeiro	Filippo Rosseli, PhD Université Paris-Saclay
Françoise Miot, PhD Université Libre de Bruxelles	Leonardo Teixeira Karan, DSc Instituto Nacional do Câncer

ACKNOWLEDGEMENT

I would like to express my gratitude to my two PhD mentors; Denise Pires de Carvalho and Corinne Dupuy. Thank you very much for the trust, for the patience, for the daily lessons and for the passionate scientific conversations that led to the development of this project. You are both great inspirations to my academic career.

I must also mention all people who made my stay in France so pleasant. To all members of the UMR8200 at Gustave Roussy Cancer Campus, thank you for the friendly environment, the kindness and your helpful assistance both in scientific issues and daily life tasks. To all fellows in Dupuy's team: Naima, Rabii, Camille and all other students with who I shared the benches, thank you very much. Raphael Corre, a friend inside and outside the lab, thanks for being available and helpful when I needed help in lab experiments or even in the multiple times in which we needed help to move from one apartment to another. Special thanks to all students and post-docs from IGR, specially Camille, Filipe, Tangui, Barbara, Alice, Noémie and all others. I'll miss our afterworks at Saint Hilaire! The luso-franco-brazilian community; Teresa, Júlio, Luiz, Clarissa and Adrien. Thanks for the companionship throughout those two long winters. Special recognition to Ruy Louzada, thanks for being by our side at all times, including the best and worst moments of this experience.

To all students, professors and technicians from LFEDR, the place where I have spent my days for almost a decade, thank you very much. Your optimism and hard work, despite the clear despise of our current government for science and education, are truly inspirational.

I must express my very profound gratitude to my beloved family, Sérgio, Fátima, Pedro, Liana, Lili, Gabriel and Lívia, for providing me with unfailing support and continuous encouragement throughout my years of study and through the process of writing this thesis. This accomplishment would not have been possible without you.

Finally, I must acknowledge the person who, amongst all, was the most important contributor to the development of this thesis: my lab and life partner, Juliana

Cazarin. Having you by my side during all this years have been amazing. Without your care and unlimited support I would never have made it so far. Thank you for everything!

"*It is a capital mistake to theorize before one has data. Insensibly one begins to twist facts to suit theories, instead of theories to suit facts*."

Sir Arthur Conan Doyle (1891)
in "A Scandal in Bohemia"

ABSTRACT

HECHT, Fabio. **The role of reactive oxygen species in thyroid radio-carcinogenesis. Rio de Janeiro**, 2018. Doctoral thesis - Universidade Federal do Rio de Janeiro, Rio de Janeiro, Brazil and Université Paris-Saclay, Orsay, France, 2018.

Papillary thyroid cancers (PTC) are the most common endocrine tumors and account for 2-3% of all human cancers. The most relevant genetic alterations found in these tumors are mutations in the genes BRAF and RAS, and chromosomal translocations in RET, a proto-oncogene activated in 15-20% of PTCs. These oncogenic translocations, known as RET/PTCs, result from the fusion of RET with unrelated partner genes. Ionizing radiation is a major risk factor for RET/PTC formation, however, the molecular mechanisms involved in these radioinduced translocations just begun to be unveiled. In the past few years, our group has reported a critical role for reactive oxygen species (ROS) in the formation of RET/PTC in thyroid cells *in vitro* and has also shown that irradiation can elicit a persistent oxidative stress caused by the upregulation of the NADPH Oxidase DUOX1 that leads to DNA damage, mediating at least part of the effects of radiation. However, how could ROS lead to the formation of RET/PTC is not fully understood. Children are at significantly higher risk of developing radio-induced thyroid tumors, specially RET/PTC positive, probably due to the intense proliferation rate of their follicular thyroid cells. This epidemiological observation prompts the assumption that replication dynamics may be involved in RET/PTC formation. Indeed, it has been shown that the pharmacological induction of replicative stress can stimulate the *in vitro* formation of RET/PTC in thyroid cells. Thus, to investigate whether replicative stress might contribute for the long-term effects of irradiation on DNA damage and RET/PTC formation, we analyzed the effects of radiation in NTHY-ori3.1 thyroid cell lineage in terms of oxidative and replicative stress and replication dynamics. Our results confirm that irradiation triggers two waves of oxidative stress: first, a strong but transient oxidative burst takes place minutes after irradiation and next, a persistently increased oxidative stress that starts only 2 days after irradiation. These two peaks of oxidative stress lead to two peaks of DNA damage. Irradiation caused little or no effect on proliferation nor on cell cycle progression. However, several protein markers of replicative stress, such as pATR, pATM, pChk1 and pRPA are induced three days after irradiation. Moreover, replication dynamics analysis revealed a diminished replication speed that has been reversed by antioxidants, suggesting that oxidative stress may contribute to replication defects. Finally, using ChIP-qPCR, we observed that the genes involved in RET/PTC1 translocation present more double-stranded breaks than RET/PTC-unrelated genes 3 days after irradiation. Hence, we propose that replicative stress is potentially involved in the etiology of RET/PTC-positive tumors.

RESUMÉ

HECHT, Fabio. **The role of reactive oxygen species in thyroid radio-carcinogenesis.** Rio de Janeiro, 2018. Doctoral thesis - Universidade Federal do Rio de Janeiro, Rio de Janeiro, Brazil and Université Paris-Saclay, Orsay, France, 2018.

Les cancers papillaires de la thyroïde (PTC) sont les tumeurs endocrines les plus courantes et représentent 2-3% de tous les cancers humains. Les altérations génétiques les plus pertinentes trouvées dans ces tumeurs sont des mutations dans les gènes BRAF et RAS, et des translocations du gène RET. Ces translocations oncogéniques, connues sous le nom de RET/PTC, résultent de la fusion de RET avec des gènes partenaires non-apparentés. L'exposition aux radiations ionisantes est le facteur de risque le plus important pour la formation de RET/PTC. Durant ces dernières années, notre groupe a mis en évidence un rôle crucial des espèces réactives de l'oxygène (ROS) dans la formation de RET/PTC dans des cellules thyroïdiennes in vitro et a notamment montré que l'irradiation (IR) induit l'établissement d'un stress oxydatif persistant du aux ROS produites par la NADPH Oxydase DUOX1, laquelle est induite à post-IR. Cela conduit à des dommages à l'ADN. Les enfants présentent un risque significativement plus élevé de développer des cancers radio-induits de la thyroïde exprimant RET/PTC, probablement en raison du taux de prolifération élevé des cellules. Ceci suggère que la dynamique de réplication pourrait être impliquée dans la formation de la translocation RET/PTC1. En effet, il a été montré que l'induction pharmacologique d'un stress réplicatif peut favoriser la formation de RET/PTC in vitro dans les cellules thyroïdiennes. Ainsi, pour déterminer si un stress réplicatif peut contribuer aux effets à long terme de l'irradiation: à savoir une persistance des lésions de l'ADN et la formation de RET/PTC1, nous avons analysé les effets à post-IR dans les cellules NTHY-ori3.1. Nos résultats confirment qu'une irradiation des cellules aux rayons X à la dose de 5 Gy induit deux vagues de stress oxydatif: une première vague forte mais transitoire qui se produit dans les minutes qui suivent l'irradiation et une deuxième vague dont l' augmentation débute 2 jours après l'irradiation pour persister ensuite. Ces deux pics de stress oxydatif conduisent à deux pics de dommages à l'ADN. L'irradiation des cellules à cette dose n'a aucun effet sur la prolifération et sur la progression du cycle cellulaire. Cependant, plusieurs marqueurs de stress réplicatif sont exprimés trois jours après l'irradiation. Par ailleurs, l'analyse de la dynamique de réplication révèle une diminution de la vitesse de réplication à post-IR qui est contrecarrée par les antioxydants, suggérant qu'un stress oxydatif peut contribuer à un stress réplicatif. Enfin, par ChIP-QPCR, nous observons que les gènes impliqués dans RET/PTC1 présentent plus de cassures double brin que des gènes endogènes, et ce, trois jours après l'irradiation. Ainsi, nous proposons qu'un stress réplicatif induit par un stress oxydatif pourrait être potentiellement impliqué dans l'étiologie des tumeurs RET/PTC-positives.

RESUMO

HECHT, Fabio. **The role of reactive oxygen species in thyroid radio-carcinogenesis.** Rio de Janeiro, 2018. Doctoral thesis - Universidade Federal do Rio de Janeiro, Rio de Janeiro, Brazil and Université Paris-Saclay, Orsay, France, 2018.

O câncer papilífero de tireoide é o tumor endócrino mais comum e corresponde a 2-3% de todos os cânceres humanos. As alterações genéticas mais relevantes relacionadas a esse tumor são mutações nos genes BRAF e RAS e translocações do gene RET, um proto-oncogene ativado em 15-20% dos tumores papilíferos. Essas translocações, conhecidas como RET/PTC, resultam da fusão de RET com diversos outros genes. A radiação ionizante é um importante fator de risco para a formação de RET/PTC, no entanto, o mecanismo molecular responsável por essa translocação radioinduzida ainda não foi elucidado. Nos últimos anos, nosso grupo demonstrou um papel crítico exercido pelas espécies reativas de oxigênio na formação de RET/PTC em células tireoidianas *in vitro* e também mostrou que a irradiação promove um estresse oxidativo persistente causado pelo aumento de expressão da NADPH Oxidase DUOX1, levando à dano ao DNA, mediando assim parte dos efeitos da radiação. No entanto, como o ROS leva à formação de RET/PTC ainda não é compreendido. Crianças possuem um risco significativamente mais alto de desenvolver tumores tireodianos após a irradiação, especialmente RET/PTC positivos, provavelmente em função da intensa proliferação das células tireodianas. Essa associação sugere que a replicação esteja envolvida na formação de RET/PTC. De fato, foi observado que a indução farmacológica de estresse replicativo pode estimular a formação *in vitro* de RET/PTC em células tireodianas. Portanto, para investigar se o estresse replicativo contribui com os efeitos da irradiação no longo prazo sobre o dano ao DNA e formação de RET/PTC, nós investigamos o papel da radiação sobre o estresse oxidativo e replicativo, além da dinâmica de replicação de linhagem de células tireodianas NTHY-ori 3.1. Nossos resultados confirmam que a irradiação desencadeia duas ondas de estresse oxidativo: primeiramente, um forte, mas transitório pico de espécies reativas de oxigênio é observado minutos após a irradiação, seguido por um novo e persistente pico que só é observado a partir de dois dias após a irradiação. Esses dois picos de estresse oxidativo resultam em dois picos de dano ao DNA. A irradiação causou pouco ou nenhum efeito na proliferação ou na progressão do ciclo celular. No entanto, vários marcadores de estresse replicativo foram observados três dias após a irradiação, como pATR, pATM, pChk1 e pRPA. Além disso, a análise da dinâmica de replicação mostrou uma diminuição na velocidade da replicação que foi revertida por antioxidantes, sugerindo que o estresse oxidativo contribui para distúrbios dos mecanismos replicativos. Por fim, utilizando ChIP-qPCR, nós observamos que os genes envolvidos na translocação RET/PTC possuem mais quebras duplas do que genes endógenos, dias após a irradiação. Portanto, propomos que o estresse replicativo está potencialmente envolvido na etiologia dos tumores RET/PTC positivos.

LIST OF FIGURES

LIST OF TABLES

LIST OF APPENDIX

LIST OF ABBREVIATIONS

γH2AX	Gamma-phosphorylated histone variant H2AX
2-AP	2-aminopurine
8-oxo-G	7,8-dihydro-8-oxo-guanine
A	Adenine
ALK	Anaplastic lymphoma kinase
APC	Adenomatous polyposis coli
APE1	AP endonuclease 1
APH	Aphidicolin
ARID1B	AT-rich interactive domain 1B
ATC	Anaplastic thyroid cancer
ATM	ATM Serine/threonine kinase, formerly called ataxia-telangiectasia mutated
ATP	Adenosine triphosphate
ATR	ATR Serine/threonine-protein kinase, formerly called ataxia telangiectasia and Rad3-related protein
BCA	bicinchoninic acid
BDP1	B double prime 1, subunit of RNA polymerase III transcription initiation factor IIIB
BER	Base excision repair
Bq	becquerel
BRAF	B-Raf proto-oncogene, serine/threonine kinase
BrdU	Bromodeoxyuridine
C	Cytosine
CCDC6	Coiled-coil domain containing 6, formerly called H4 or D10S170
CCND2	Cyclin D2
cdc25a	Cell division cycle 25A
CDH4 C	Cadherin 4
CDK1	Cyclin dependent kinase 1
cDNA	Complementary DNA
CFS	Common fragile sites

CHEK1	Checkpoint kinase 1
CHEK2	Checkpoint kinase 2
CldU	5-Chloro-2′-deoxyuridine thymidine analog
cm	centimeters
DAPI	4',6-diamidino-2-phenylindole
dATP	Deoxyadenosine triphosphate
DCF	2',7'-dichlorofluorescein
dCTP	Deoxycytidine triphosphate
DDR	DNA damage response
dGTP	Deoxyguanosine triphosphate
DNA	Deoxyribonucleic acid
dNTP	Deoxyribonucleotide triphosphate
DPI	Diphenyleneiodonium
DTT	Dithiothreitol
DUOX1	Dual Oxidase 1
DUOX2	Dual Oxidase 2
ECACC	European Collection of Authenticated Cell Cultures
EDTA	Ethylenediamine tetraacetic acid
EGTA	Ethylene glycol-bis(β-aminoethyl ether)-N,N,N',N'-tetraacetic acid
EIF1AX	Eukaryotic translation initiation factor 1A, X-linked
eNOS	Endothelial nitric oxide synthase
ETC	Electron transport chain
EZH1	Enhancer of zeste 1 polycomb repressive complex 2 subunit
FANCD2	Fanconi anemia complementation group D2
FBS	Fetal bovine serum
FGFR2	Fibroblast growth factor receptor 2
FISH	Fluorescence in situ hybridization
FRA3B	Fragile site 3B
FTC	Follicular thyroid cancer
FUdR	Floxuridine
g	Gravitational force
GAPDH	Glyceraldehyde-3-phosphate dehydrogenase
GDNF	Glial cell line-derived neurotrophic factor
GFP	Green fluorescent protein

Gy	Gray
H_2-DCF-DA	2',7'-dichlorodihydrofluorescein diacetate
H2AX	Histone variant H2AX
H2DCF	Dihydrodichlorofluorescein
HEPES	Hydroxyethyl piperazineethanesulfonic acid
HPLC	High-performance liquid chromatography
HR	Homologous recombination
HRAS	HRas proto-oncogene, GTPase
HRP	Horseradish peroxidase
HU	Hydroxyurea
IdU	5-Iodo-2′-deoxyuridine
IgG	Immunoglobulin G
IP	Propidium Iodide
kb	Kilobases
KV	Kilovolts
LTK	Leukocyte receptor tyrosine kinase
MAPK	Mitogen-activated protein kinase
MCM	replicative minichromosome maintenance helicase
MEN1	Multiple Endocrine Neoplasia Type 1
MEN2A	Multiple endocrine neoplasia type 2
MET	MET proto-oncogene, receptor tyrosine kinase
mRNA	Messenger ribonucleic acid
MTC	Medullary thyroid cancer
MUTYH	MutY glycosylase homologue
MYH13	Myosin heavy chain 13
NADPH	Nicotinamide adenine dinucleotide phosphate
NCOA4	Nuclear receptor coactivator 4, formerly known as ELE1
NF1	Neurofibromin 1
NIS	Sodium-Iodide Symporter
NOX4	NADPH Oxidase 4
NTRK	Tropomyosin receptor kinase
OGG1	8-oxo-G DNA glycosylase 1
PBS	Phosphate-buffered saline
PCNA	Proliferating cell nuclear antigen

PCR	Polymerase chain reaction
PFA	Paraformaldehyde
PI3K	Phosphoinositide 3-kinase
PPARG	Peroxisome proliferator activated receptor gamma
PPM1D	Protein phosphatase, Mg2+/Mn2+ dependent 1D
PRDX2	Peroxiredoxin 2
PTC	Papillary thyroid cancer
PTEN	Phosphatase and tensin homolog
qPCR	Quantitative polymerase chain reaction
RAD17	RAD17 checkpoint clamp loader component
RAS	Ras proto-oncogene, GTPase
RB1	RB transcriptional corepressor 1
RET	Rearranged during transfection
RFS	Rare fragile sites
RNA	Ribonucleic acid
RNR	Ribonucleotide reductase
rNTPs	Ribonucleotides
ROS	Reactive oxygen species
RPA	Replication protein A
RPMI	Roswell Park Memorial Institute
rRNA	Ribosomal ribonucleic acid
SASP	Senescence-associated secretory phenotype
SDS-PAGE	Sodium dodecyl sulfate polyacrylamide gel electrophoresis
SPOP	Speckle type BTB/POZ protein
ssDNA	single-stranded DNA
T	Thymine
TBS	Tris-buffered saline
TCGA	The Cancer Genome Atlas
TG	Thyroglobulin
THADA	THADA, armadillo repeat containing
TP53	Tumor protein p53
Trab	TSH receptor antibodies
TSH	Thyroid-stimulating hormone
TSHR	Thyroid-stimulating hormone receptor

TTP	Thymidine triphosphate
WRN	Werner syndrome RecQ like helicase
YFP	Yellow fluorescente protein
ZFHX3	Zinc finger homeobox 3

SUMMARY

1. INTRODUCTION

1.1. Thyroid cancer

Thyroid cancers are the most common endocrine tumors and account for 2-4% of all human cancers. In 2018, 7.57 new cases of thyroid cancer are expected per 100,000 women and 1.49 per 100,000 men in Brazil (INSTITUTO NACIONAL DE CÂNCER, 2017). Thyroid cancer incidence is growing worldwide in a rate superior to any other cancer type (AMERICAN CANCER SOCIETY, 2013). In France, the incidence has jumped from 2.8 in 1980 to 13.8 in 2012 per 100,000 women, while in men it has increased from 1.1 to 5.5 per 100,000 within the same interval of time (BINDER-FOUCARD *et al.*, 2013). The same increase has been observed in several other countries, like the United States where incidence has tripled since 1975 (FAGIN; WELLS, 2016). Many authors suggest that the increased incidence rates are, in fact, due to over diagnosis of very small (< 1cm) and clinically irrelevant microcarcinomas that are now being revealed by the widespread use of high resolution ultrasonography and improved scrutiny for thyroid nodules. However, the increase in the incidence was observed in tumors of all sizes, including large tumors that have always been easily diagnosed with simple neck palpation or elementary radiologic techniques (CHEN, A. Y.; JEMAL; WARD, 2009; MORRIS; MYSSIOREK, 2010). So, it is likely that although the improved detection of microcarcinomas boosts the incidence rates, the world is truly facing a real increase in thyroid cancer incidence. Although the thyroid cancer incidence increased, mortality rates decreased due to the indubitable advances in patient care and drug development in the past decades, but also because of the over diagnosis. Microcarcinomas were found at a very high frequency (up to 36%) during autopsy studies, suggesting the existence of a large reservoir of small and clinically-irrelevant thyroid tumors in the general population (FRANSSILA; HARACH, 1986). The detection of those microcarcinomas by extensive screening boosts incidence rates, however, as they are usually not life-threatening, their diagnosis will ultimately dilute death rates.

The pattern of the age-stratified incidence of thyroid cancer diverges from most other cancers. The great majority of non thyroid cancers are rare in children and young adults, increasing exponentially in frequency in older people. A few others, such as

retinoblastomas, are virtually restricted to the first years of life. However, thyroid cancer shows neither of these patterns: incidence increases during adolescence and early adult life and declines in elderly. In the United States, the incidence rises until about the age of 45 years, when it seems to stabilize and it starts to decline after the age of 75 years (WILLIAMS, 2015). The Cancer Research UK, which has a user-friendly and visual appealing data bank of cancer statistics in the United Kingdom, shows similar results (Figure 1).

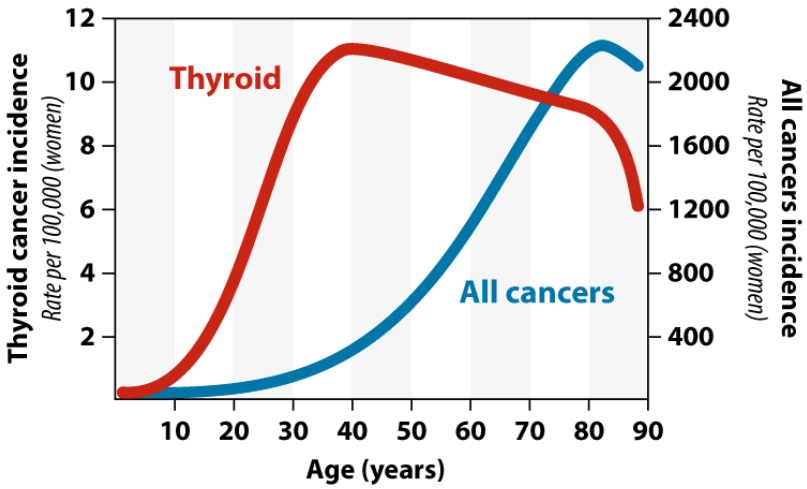

Figure 1. Age-related incidence of thyroid cancer. Cancer Research UK data of all cancers (excluding non-melanoma skin cancer) and thyroid cancers incidence per 100,000 women in the United Kingdom between 2012 and 2014 versus year at diagnosis (Adapted from UK, 2012-2014, ICD-10 C73). Statistics for all cancers were obtained in: http://www.cancerresearchuk.org/health-professional/cancer-statistics/incidence/age#heading-Zero (Accessed in July 2017). Statistics for thyroid cancer were obtained in: http://www.cancerresearchuk.org/health-professional/cancer-statistics/statistics-by-cancer-type/thyroid-cancer/incidence#collapseOne (Accessed in July 2017).

The general term “thyroid cancer” comprises a collection of distinctive diseases with completely different etiologies and clinical features. Thyroid cancer may arise from the two main cellular types of the thyroid tissue: the thyrocytes, that are the follicular cells responsible for thyroid hormone biosynthesis, or the parafollicular cells or C cells, responsible for calcitonin secretion.

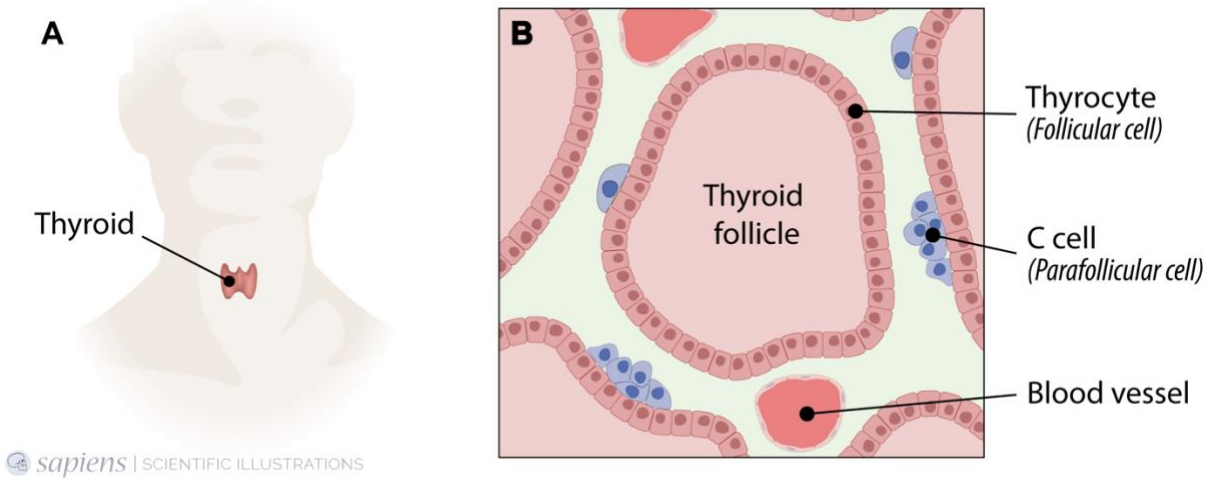

Figure 2. Anatomy and histology of the thyroid gland. Schematic representation of the anatomic position of the thyroid gland in anterior neck (A) and thyroid histology (B) depicting thyrocytes (thyroid hormone-producing follicular cells) and C cells (parafollicular cells).

Neoplastic follicular cells may evolve into the well-differentiated papillary (PTC) or follicular thyroid (FTC) cancers and the undifferentiated anaplastic thyroid cancers (ATC), while neoplastic parafollicular cells are the origin of medullary thyroid cancer (MTC). Papillary carcinomas are by far the most prevalent type of thyroid cancer, accounting for nearly 85% of cases (FAGIN; WELLS, 2016). This histological type was initially thought to be a single entity; however, multiple driver mutations were discovered enlightening the existence of molecular subgroups with distinct biological features and clinical outcomes. The most clinically relevant genetic alterations found in thyroid papillary cancers are point mutations and/or translocations in effector genes of the mitogen-activated protein kinase (MAPK) pathway: *BRAF*, *RAS* and *RET*.

1.2. Molecular profiling of thyroid neoplasia

BRAF^{V600E} is by far the most prevalent oncogene, accounting for 40-60% of cases while mutations in *RAS* represent approximately 13%. The prevalence of genomic alterations involving *RET* in PTC varies enormously between different series, ranging from as low as 2.5% (ZOU; SHI; FARID, 1994) in one series to astonishing 73% in another (RHODEN *et al.*, 2006), but its average is around 15-20% according to most authors (FAGIN; WELLS, 2016). These huge variations can be attributed to

ethnical and geographic variations, detection method sensitivity (ZHU *et al.*, 2006) and even the improper mixing of tumors with different etiologies. For example, as we will discuss in greater detail later, ionizing radiation exposure predisposes to *RET* chromosomal translocations. Thus, cohorts comprising radiation-exposed patients might display higher prevalence of this translocation than cohorts composed mostly or totally by patients with sporadic non radioinduced cancer. Another important information to consider is that the predominant molecular profile of thyroid tumors seems to be changing over time to an even stronger predominance of *BRAF* point mutations (ROMEI *et al.*, 2012), so the averaging of studies conducted 30 years apart may lead to great discrepancies. Other gene fusions involving *BRAF* and other tyrosine kinase receptors (such as *NTRK*, *ALK* and *PPARG*) are far less prevalent.

The remaining cancer cases mostly had no known driver mutations, but high-throughput next-generation sequencing technologies and bioinformatics enabled researchers to further characterize these tumors. The publication by The Cancer Genome Atlas of a genome-wide analysis of almost 500 papillary thyroid tumors not only extended the set of known PTC driver alterations but reduced the portion of PTC cases with undetermined oncogenic driver mutations from 25% to 3.5% (Figure 3). In this specific work, a substantially low RET/PTC prevalence was reported (CANCER GENOME ATLAS RESEARCH NETWORK, 2014).

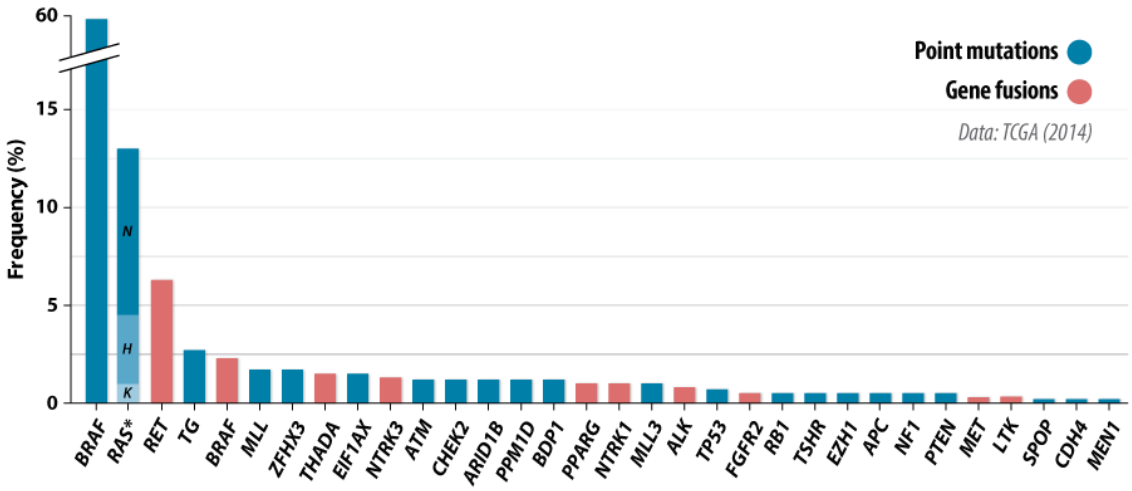

Figure 3. Frequency of recurrent mutations and fusions in thyroid papillary carcinoma from the The Cancer Genome Atlas (TCGA). Data extracted from TCGA's report (2014) analyzing 496 papillary thyroid tumors. (RAS* represents all RAS subtypes combined. KRAS = 1%, HRAS = 3.5%, NRAS = 8.5%). Adapted from Cancer Genome Atlas Research Network, 2014.

The typical observation of a single driver mutation per thyroid tumor led several authors to state that these PTC-related mutations are mutually exclusive (CANCER GENOME ATLAS RESEARCH NETWORK, 2014; FAGIN; WELLS, 2016; IYAMA *et al.*, 2017; SOARES *et al.*, 2003) despite the reports of a small number of cases in which dual mutations (*BRAF* and *RET* alterations within the same tumor) were observed, remarkably in recurrent papillary tumors (HENDERSON *et al.*, 2009; ZHU *et al.*, 2006).

The name *RET* is a reference to the term ‘Rearranged during transfection’, an allusion to its discovery. In 1985, Takahashi and colleagues reported a new transforming gene detected during the transfection of NIH 3T3 cell lineage with high molecular weight DNA from human T-cell lymphoma and coined the name *RET* (TAKAHASHI; RITZ; COOPER, 1985). *RET* is a 53 kb proto-oncogene located in the long arm of chromosome 10(q11.21) that encodes a tyrosine-kinase receptor that stimulates proliferation, cell growth, differentiation and survival upon activation by ligands of the GDNF (glial cell line-derived neurotrophic factor) family. The activation process of this receptor includes dimerization and subsequent trans-autophosphorylation of specific tyrosine residues (ARIGHI; BORRELLO; SARIOLA, 2005)

RET expression in the thyroid follicular cells is considered to be extremely low or even nonexistent (NIKIFOROV, 2008). This gene is strongly expressed in organs derived from the neural crest (like thyroid C cells) and urogenital cells. This expression profile reflects its important role in the normal development of the central and peripheral nervous systems, as well as the excretory system (for example, in the development of the Wolffian duct and ureteric bud epithelium) (ARIGHI; BORRELLO; SARIOLA, 2005). Mice with a homozygous deletion of *RET* die soon after birth due to renal agenesis and lack of enteric neurons in the digestive tract (SCHUCHARDT *et al.*, 1994). Thus, RET gain of function point mutations are a common cause of familial and sporadic medullary thyroid cancer, since it is constitutively expressed in thyroid C cells.

1.3. The RET/PTC translocation

Several types of genomic alterations have already been described in the *RET* gene and its role in cancer development has been extensively studied for more than 20 years. There are two main pronto-oncogene activation pathways for *RET*: point mutations and chromosomal translocations.

The very first report of a point mutations in *RET* has been made in 1993 during investigations of the molecular background of the multiple endocrine neoplasia type 2 (MEN2A), a dominant inherited cancer syndrome that affects tissues derived from the neural ectoderm and strongly predisposes to medullary thyroid cancer (MULLIGAN *et al.*, 1993). Indeed, virtually all hereditary medullary tumors have point mutations in *RET*, with variations of the affected amino acid. Dozens of germ-line and somatic mutations are known and their implications on the development of medullary thyroid cancer are being progressively unveiled (ROMEI; CIAMPI; ELISEI, 2016).

In general terms, point mutations in *RET* will generate medullary tumors (MTC), while chromosomal translocations will lead to papillary tumors (PTC). However, this oversimplification ignores the recent finding of a novel chromosomal translocation involving the exon 12 of the *RET* gene and the exon 35 of the myosin heavy chain 13 gene (*MYH13*) identified in a patient with aggressive sporadic medullary cancer. This translocation creates a fusion transcript with high oncogenic ability when expressed ectopically in mouse models (GRUBBS *et al.*, 2015). Still, the relevance of chromosomal translocations to medullary cancer etiology is extremely small compared to its role in papillary tumors development. The vast majority of *RET* proto-oncogene activation through chromosomal translocations takes place in thyrocytes, leading to the formation of papillary tumors. Of note, to date there is no evidence of a point mutation in *RET* related to papillary tumors, probably because the gene is normally not expressed in thyrocytes.

In 1987, Fusco and colleagues reported the discovery of DNAs with transforming activity in tissue samples from human papillary thyroid tumors and their metastasis, laying the groundwork for decades of RET/PTC research (FUSCO *et al.*, 1987). A few years later, this same team cloned the transforming transcript revealing

its rearranged nature (GRIECO *et al.*, 1990) and further characterized it by discovering the genomic locus involved, revealing an intrachromosomal inversion joining two unrelated genes of the chromosome 10 (PIEROTTI *et al.*, 1992). This translocation, currently known as RET/PTC1, comprises an intrachromosomal inversion between *RET* and *CCDC6* (formerly called *H4* or *D10S170*), a gene located in locus 10(q21.2) that encodes a coiled-coil domain-containing protein ubiquitously expressed. Functional characterization of *CCDC6* in thyrocytes revealed a major role in regulating apoptosis. The loss of gene function leads to impaired apoptosis, possibly also contributing to tumorigenesis (CELETTI *et al.*, 2004). Another important recurrent translocation was discovered in the following years and was named RET/PTC3 (SANTORO, M *et al.*, 1994). It is formed by the fusion of *RET* and *NCOA4* (nuclear receptor coactivator 4, formerly known as ELE1), a gene also located in chromosome 10 **(Figure 4)**. These discoveries inaugurated a list that includes more than 27 translocations, each with its respective partner gene (ROMEI; CIAMPI; ELISEI, 2016). Interestingly, the list of *RET* translocations is still expanding. Two novel *RET* translocations (AFAP1L2/RET and PPFIBP2/RET) were recently discovered in thyroid cancers of young patients from Fukushima, where a nuclear accident took place in 2011 (IYAMA *et al.*, 2017).

Independently of the partner gene, all RET/PTC translocations are fusions between the 3' portion of *RET*, coding for the tyrosine kinase receptor, and the 5' portion of the donor gene. In all cases, it will generate a constitutively active cytoplasmic fusion protein that will promote sustained stimulus to proliferation by activating MAPK and PI3K pathways, thus increasing considerably the risk of malignant neoplasia. Experiments performed in the 90's revealed that thyroid-targeted expression of RET/PTC1 induces papillary thyroid carcinomas in mice with considerable histological resemblances to human papillary thyroid carcinomas (JHIANG *et al.*, 1996; SANTORO, M *et al.*, 1996). The transforming capacity of RET/PTC rearrangements has been also demonstrated by *in vitro* studies in which this activated oncogene transformed rat thyroid cell lineage PCCl3 cells into malignant cells (SANTORO, MASSIMO; MELILLO; FUSCO, 2006).

RET/PTC was thought to be specific to thyroid tumors due to its virtual inexistence in other analyzed tumors. A study that analyzed 528 non-thyroid neoplasia

failed to detect any *RET* activation, while thyroid tumors were positive in 10% of the cases (SANTORO, M *et al.*, 1993). However, subsequent studies challenged this theory, showing that even though rare, RET/PTC activation was capable of driving transformation in other tissues. Artificial expression of RET/PTC1 oncogene under control of CCDC6 promoter in mice efficiently creates neoplasia, remarkably in mammary tissue, although natural occurrence of RET/PTC1 in this tissue has never been described neither in mice nor in humans (PORTELLA *et al.*, 1996). Interestingly, several non-thyroid papillary tumors were analyzed for RET/PTC rearrangements and it was found that 20% of peritoneal carcinoma derived from ovarian tissue were positive for RET/PTC mRNA and protein. Nevertheless, the authors argue that RET/PTC might be a passenger mutation, meaning that it would not contribute to cancer development, resulting from the genomic instability of the *RET* gene in tumor subclones (FLAVIN *et al.*, 2009).

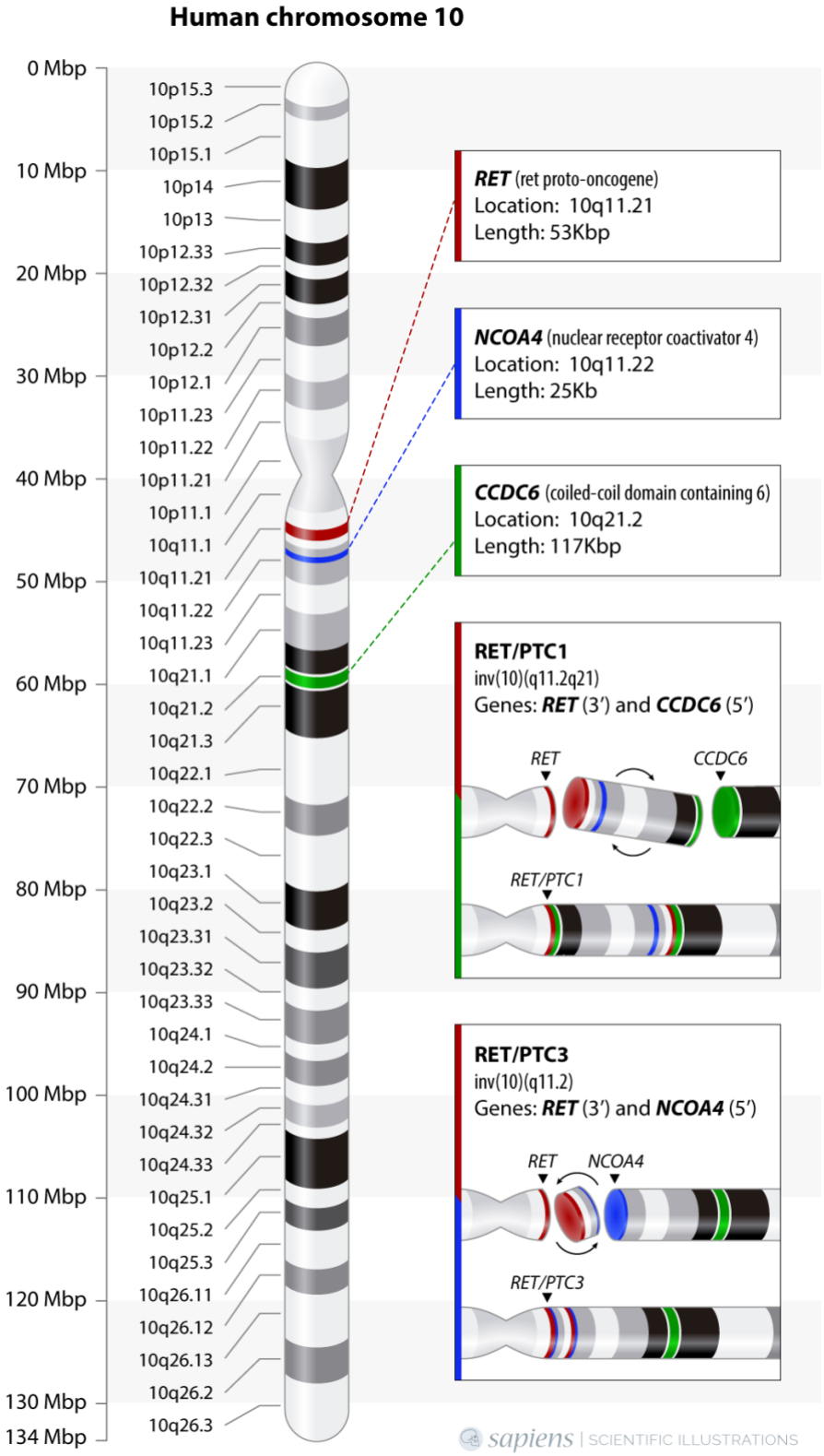

Figure 4. Schematic representation of chromosome 10. Genomic locus of the genes involved in RET/PTC1 and RET/PTC3 translocations and their theoretical fusion mechanism (Data obtained from NCBI's Map Viewer [www.ncbi.nlm.nih.gov/projects/mapview/] Accessed in July 2017).

The reason why this translocation occurs almost exclusively in the thyroid gland remains not fully understood. However, some authors propose a very interesting role for genomic conformation in this tissue (Figure 5). In contrast to other tissues (such as mammary gland), FISH analysis combined with three-dimensional microscopy revealed that *RET* and *CCDC6* are closer than it would be expected by their linear distances in the interphase nuclei of thyroid follicular cells (NIKIFOROVA, 2000).

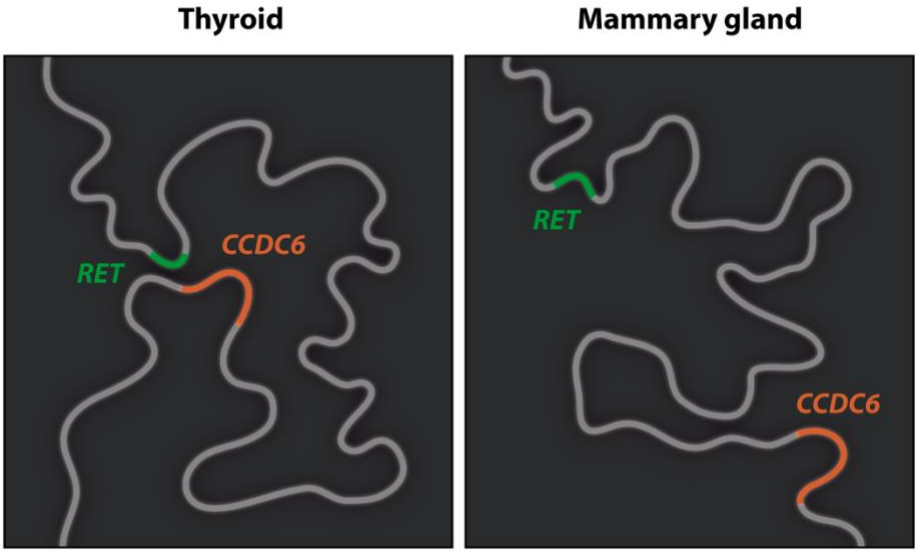

Figure 5. Schematic representation of spatial proximity between RET/PTC1 genes in different tissues. FISH and 3D microscopy-analysis revealed that *RET* and *CCDC6* are unexpectedly close in thyrocytes when compared to other tissues, suggesting a role for genomic conformation in the occurrence of this translocation.

Whether this conformational particularity of the thyroid tissue is caused by thyroid-specific transcriptional factors, epigenetic imprint or other mechanisms is still completely unknown. However, this different spatial proximity is thought to be the key factor implicated in the high frequency of translocation between these two genes observed in thyroid cells and not in other tissues (PORTELLA *et al.*, 1996).

Although our knowledge about the molecular mechanisms governing the breakage of these specific genes is slowly progressing, much more information is still needed to fully understand their functional influence on tumorigenesis and their relationship with the currently known risk factors.

1.4. Ionizing radiation and thyroid cancer

Ionizing radiation is recognized for decades as a major risk factor for papillary thyroid cancer development, especially in children and adolescents, even at doses as low as 0.1 Gy (RON *et al.*, 1995). RET/PTC translocations seem to be the most frequent genomic alteration induced by ionizing radiation (CORDIOLI *et al.*, 2015). Indeed, several authors have experimentally demonstrated the causal relation between irradiation and RET/PTC formation *in vitro* (CAUDILL *et al.*, 2005), corroborating long-standing clinical findings that show that radio-induced thyroid cancers are more likely to have RET/PTC than papillary thyroid tumors from patients with no history of radiation exposure (sporadic tumors) (ROMEI; ELISEI, 2012).

Multiple demonstrations of the carcinogenic effect of radiation can be found in the past, since early X-ray workers developed skin cancers and Marie Curie developed leukemia due to her work with radioactive isotopes (WILLIAMS, 2008a). However, this relationship has been thoroughly established by the analysis of the clinical consequences of the nuclear bombings in Hiroshima and Nagasaki during the Second World War and the Chernobyl disaster. On April 26th of 1986, the reactor number 4 of the Chernobyl Nuclear Power Plant exploded in Ukraine (at that time, USSR) after an unfortunate combination of reactor design flaws and human mistakes executed during a routine safety simulation. The steam explosion blew off the reactor and a fire in the graphite core led to the release $8x10^{18}$ Becquerels of radioisotopes, comprising nearly all the volatile isotopes in the reactor. Between 10 and 20 million people were exposed to substantial levels of radioactive fallout not only in Ukraine but also in Belarus and part of the Russian Federation. Several hundred workers of the power plant received whole-body radiation, 134 developed acute radiation syndrome and, of these, 28 died in less than 120 days (WILLIAMS, 2002). The genetic effects of the heavy contamination was observed even in wild animals, such as rodents (BARKER *et al.*, 1996) and birds (ELLEGREN *et al.*, 1997). Few years later, the first official report of the notorious increase in thyroid cancer incidence, particularly in children, was published (BAVERSTOCK *et al.*, 1992), leading to extensive international collaboration. The World Health Organization estimates that the accident caused about 4,000 thyroid cancer cases within a 20-year period (WORLD HEALTH ORGANIZATION, 2006). The reason why the thyroid gland was specially affected by

the radioactive fallout relies on the fact that although dozens of radionuclide types have been released, one was particularly dangerous for the thyroid, the β-radiation-emitting isotope ^{131}Iodine. This isotope is one of the common radioactive fission-products of nuclear fission and is therefore produced in huge amounts inside nuclear reactors. About 1.8×10^{18} Bq of ^{131}I were released, along with huge amounts of ^{132}Tellurium, that rapidly decays to ^{132}I (WILLIAMS, 2002).

The thyroid gland avidly uptakes and concentrates iodine, as it uses these ions to produce thyroid hormones. The Na-I-Symporter (NIS), responsible for the active transmembrane transport of iodide, does not differentiate between radioactive and non-radioactive isotopes, and also uptakes radioactive ions whenever they are present in the bloodstream. Consequently, this mechanism of radionuclide concentration in the thyroid causes thyrocytes to receive a dose 500–1000 times higher than the rest of the body (FAGIN; WELLS, 2016), increasing the risk of genetic damage. This particularity of the thyroid gland is exploited in the clinic, as it is deliberately used to destroy the thyroid cells in some cases of goiters and cancers.

In 1987, only one year after the Chernobyl disaster, the greatest Brazilian nuclear accident occurred in the city of Goiânia, where scrap metal collectors found an improperly disposed radiotherapy device at an abandoned medical clinic. Interested in selling the great amount of lead to a junkyard, they dismantled the device, unwillingly releasing 19 grams of radioactive ^{137}Cesium chloride salt. The owner of the junkyard became instantly fascinated by the mysterious blue glow that the unknown substance emitted in the dark, decided to keep it and, along with their relatives, amused himself by manipulating the Cesium powder for several days until symptoms started to appear. When the contamination was discovered, thousands of people were monitored and removed from contaminated areas. In later studies, blood samples from over a hundred people were collected and analyzed cytogenetically to assess the frequency of chromosomal aberrations in cultured lymphocytes. The individual absorbed dose was estimated to vary from zero up to 7 Gy. As a result, four people died due to the acute effects of radiation soon after exposure and hundreds were contaminated (INTERNATIONAL ATOMIC ENERGY AGENCY, 1988). Several studies were conducted on the affected population and, surprisingly, they failed in detecting any relation of the radiation with the prevalence of BCL2/J(H) translocations (NUNES *et*

al., 2013) or germline microsatellite mutations (COSTA *et al.*, 2011). To date, there is no epidemiological or scientific proof of radiation-related increase in the prevalence of any type of cancer despite the testimony of local habitants about numerous cancer cases and deaths thought to be related to the accident. These observations show that not only the dose, but the nature of the radiation and the biological effects of the radionuclide represent a major variable in cancer risk induction. The radiation exposure from the Chernobyl accident (^{131}I) greatly differed from that created by the atomic bombs in Japan (gamma rays and neutrons) and the Goiânia accident (^{137}Cs).

Besides the fallout of nuclear disasters and nuclear war, irradiation may also occur from the daily use of radiation as treatment for several benign conditions. In the past, diseases like the fungal infection tinea capitis, enlarged tonsils or enlarged thymus gland were often treated with radiation (Figure 6), increasing the risk of thyroid cancer even several years after the irradiation event (BOAVENTURA *et al.*, 2013; RON *et al.*, 1995; SADETZKI *et al.*, 2006). Accordingly, the main genetic alteration found in those patients was the RET/PTC rearrangement (COLLINS *et al.*, 2002). Moreover, a recent case-control study analyzed the risk for thyroid cancer in more than 300 individuals that underwent regular dental X-rays, a low-dose and often neglected source of radiation, and observed a significant increased risk with a dose-response pattern (MEMON *et al.*, 2010).

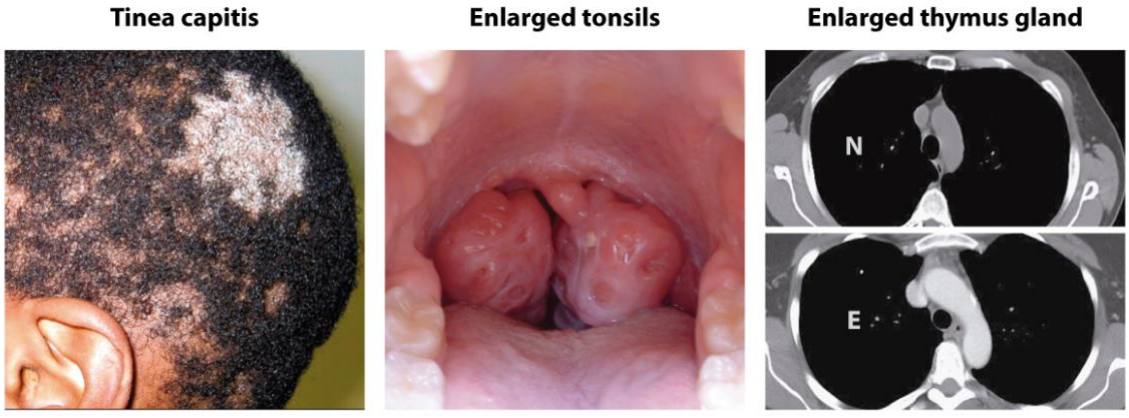

Figure 6. Main benign conditions formerly treated with radiation. Left panel: Tinea capitis, a fungal infection on the scalp (Picture from Shy, 2007). Central panel: Enlarged tonsils of a child (Picture from Lemyze & Favory, 2010). Right panel: comparison of a normal (N) and enlarged (E) thymus gland (Picture from Singla et al., 2010).

Thyroid cancer is a very rare condition in children. The documented rate of pediatric thyroid cancer in Belarus before Chernobyl was less than 1 case per 1,000,000. However, after the accident this rate skyrocketed reaching 100 per 1,000,000 in the city of Gomel (Belarus) by 1995 (WILLIAMS, 2008b). Children's thyroids are particularly vulnerable to ionizing radiation, and *RET* fusions are the main genetic alteration found in pediatric patients. While RET/PTC represents roughly 15% of sporadic papillary tumors in general population, in children it represents 48% of sporadic tumors and almost 60% of radio-induced tumors (CORDIOLI *et al.*, 2015).

Of note, while the acute effects of radiation (such as nausea, dizziness, skin burns, gastrointestinal bleeding and others) are deterministic, that is, it will certainly occur after a dose threshold, the carcinogenic effect of radiation is probabilistic, meaning that its probability increases with dose. So, radiation exposure does not condemn exposed individuals to the development of malignancies, it only increases its probability. One real-life example is the junkyard owner from Goiânia's incident, named Devair, that bare-handed manipulated the cesium salt and was one of the individuals that received the greatest dose among all victims. Still, Devair did not die as a result of radiation exposure nor developed any tumor, dying only in 1994 from radiation-unrelated causes. Although radiation surely increases the risk of cancer, not all exposed individuals will be affected. So, it is plausible that individuals that have been irradiated and remained unaffected but naturally developed radiation-unrelated sporadic tumors will be misplaced in the 'radio-induced' group in epidemiological analysis, contaminating the results.

Nevertheless, while *RET* fusions represent a relatively small share of adult sporadic tumors, it is safe to state that these translocations are an exceptionally relevant issue in pediatric thyroid cancer. However, the reason why children's thyroids are more susceptible to the formation of RET/PTC fusions is not fully understood. Many authors suggest a major role for cell proliferation rate in this issue (WILLIAMS, 2015).

In 2006, Saad and colleagues estimated the proliferation rate for over 100 thyroid glands from corpses of different ages through immunostaining for Ki67. They observed that proliferation rate is maximal during early fetal life, when up to 16% of cells are proliferative (Ki67-positive). Yet, this rate continuously decreases, reaching

only 2% between 31-35 weeks and about 0,2% at birth. This rate presents only minor changes during childhood before finally dropping again in early adult life to a stable and very low proliferation rate that remains constant throughout lifetime (SAAD *et al.*, 2006).

Table 1. Proliferation of thyrocytes during lifetime. Percentage of proliferative cells in thyroid glands of corpses from all ages were assessed using immunohistochemistry for Ki67 expression. Adapted from Saad et al., 2006.

	Age	n	Proliferative cells (%)
Intra-uterus	11-15 weeks	4	16,25
	16-20 weeks	4	11,66
	21-25 weeks	4	8,31
	26-30 weeks	4	7,64
	31-35 weeks	4	1,85
	36-40 weeks	5	0,41
Childhood	<1 year	10	0,21
	1 year	4	0,38
	2 years	4	0,27
	3-4 years	5	0,07
	5-6 years	10	0,27
	7-8 years	2	0,33
	9-10 years	4	0,26
	11-12 years	5	0,27
	13-14 years	5	0,11
	15-19 years	6	0,18
Adults	20-24 years	5	0,08
	25-29 years	6	0,11
	30-34 years	5	0,10
	35-39 years	5	0,09
	40-44 years	6	0,08
	45-49 years	5	0,09
	50-60 years	5	0,09

Data: Saad, et al., 2006 (JCEM)

A high mitotic rate in fetal life and childhood is consistent with normal development and growth. The thyroid gland mass increases from approximately 0.13 grams at the 15th gestational week to 2-4 g at birth (GUIHARD-COSTA; MÉNEZ; DELEZOIDE, 2002) and to 15–20 g in young adults, remaining stable throughout

lifetime. Yet, part of this thyroid weight gain must be attributed to colloid formation and not exclusively to cell divisions (WILLIAMS, 2015).

The low proliferation rate at early adulthood represents the cell replacement in a tissue with low cell turnover. The evaluation of cell population kinetics in human thyroid slices using ^{3}H-thymidine estimates that the S phase of a thyrocyte cell cycle lasts 10 h, indicating that thyroid undergo only about 5 cell divisions during the whole adult life (COCLET *et al.*, 1989). These features are consistent with a lifespan of 8.5 years for thyrocytes, contrasting to 1 year of hepatocytes (MARONGIU *et al.*, 2014) and only a few hours for T lymphocytes (VERSTEYHE *et al.*, 2013). This growth pattern inversely-correlated with age led several authors to instantly question whether this pattern could explain the vulnerability of children's thyroids to irradiation (Figure 7).

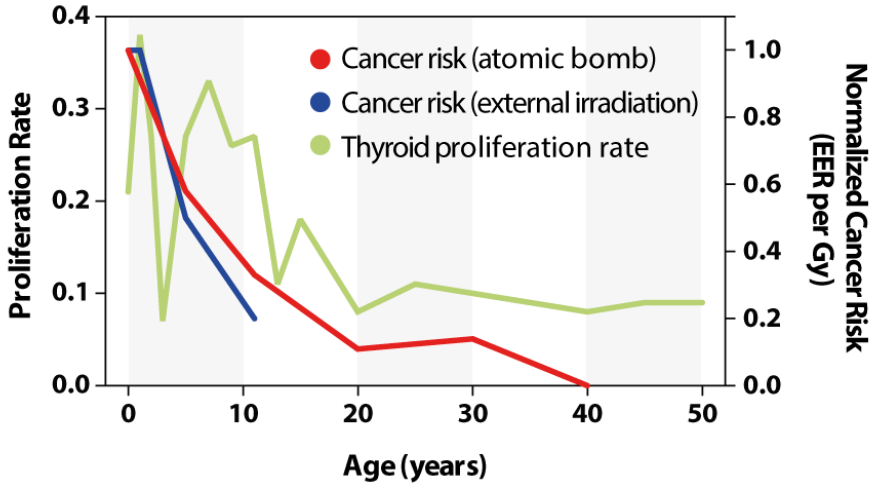

Figure 7. Thyroid proliferation rate and thyroid cancer risk varies with age. Adapted representation of thyroid proliferation rate after birth measured by Ki67 stain from corpses of different ages (green line, SAAD et al., 2006) and the excess relative risk per Gy (ERR/Gy, corrected using the risk at birth as 1.0) of a pooled analysis of 7 cohorts of patients exposed to different radiation sources (blue line, RON et al., 1995) or Japanese atomic bomb survivors (red line, AKIBA et al., 1992).

These results demonstrate an evident overall decrease trend in the proliferative rate as a function of age that correlates with the reduction of cancer risk as age of radiation exposure increases. However, this imperfect correlation presents also inconsistencies that suggest that proliferation alone cannot explain the age-related risk.

An interesting work used full-genome mRNA microarrays to analyze the transcriptome of normal thyroid tissue (contralateral) in age-matched Ukrainian children with radio-induced PTC (exposed to Chernobyl's fallout) or sporadic PTC (born after 1 March 1987). The authors reported the identification of a distinct gene expression signature of over 400 genes that allows the differentiation of the irradiated from the non-irradiated group. The gene signature found in the normal tissue of the radio-exposed group is associated with higher cell proliferation rates (DOM *et al.*, 2012). These findings suggest that a higher proliferation rate increases the susceptibility of the thyroid gland to the carcinogenic effect of radiation, although a higher proliferation rate is not imperative for PTC development since sporadic tumors arise in patients without this signature.

Other biological contexts may also contribute to better understand the relationship between proliferation and thyroid cancer, not exclusively in children. Grave's disease is the major cause of hyperthyroidism and thyrotoxicosis and is characterized by the illegitimate activation of the TSH receptor by TSH receptor antibodies (TRab), leading to intense cell proliferation and abnormal thyroid growth with consequent excessive thyroid hormone secretion (BARTALENA, 2013). Even though it is still a matter of debate, several authors state that Grave's patients have an increased risk for thyroid cancer (BOUTZIOS *et al.*, 2014; CHEN, Y.-K. *et al.*, 2013; STANIFORTH; ERDIRIMANNE; ESLICK, 2016).

Altogether, these findings insinuate that the high proliferation status during infancy or hyperplastic diseases may promote a permissive environment that may further stimulate the mitotic rate of initiated cells and increase the risk of thyroid tumor growth, similarly to the oncogenic effect of estrogen on mammary tumor cells. These studies, however, do not elucidate which molecular cancer type is induced under these conditions nor the specific molecular mechanism linking proliferation imbalance and tumorigenesis.

1.5. Replicative stress

The notion that disturbances in proliferation can promote tumorigenesis does not relate only to the fact that unbalanced proliferation of initiated cells may stimulate clonal expansion, it may be related to the initiation itself. The process of DNA replication, inherent to mitosis, must be finely regulated to faithfully transmit the genetic information to daughter cells. The imperfection of this process can lead to genomic aberrations, including both point mutations and gene fusions, what is considered by several authors as an early step of tumorigenesis (GELOT; MAGDALOU; LOPEZ, 2015).

Replicative stress may be defined as a perturbation of DNA replication that interferes with timely and error-free completion of the S phase, possessing aberrant replication fork structures as a major hallmark. Once replication forks are halted, the replicative minichromosome maintenance (MCM) helicase continues to unwind the double-stranded DNA for a few hundred base pairs creating an unstable segment of exposed single-stranded DNA (ssDNA). Replication protein A (RPA) coats the ssDNA, triggering the activation of the serine/threonine protein kinase ATR (Ataxia telangiectasia and Rad3 related). The subsequent ATR signaling cascade includes the phosphorylation of checkpoint kinase 1 (CHK1), the cell cycle checkpoint protein RAD17 and histone H2AX. The occurrence of these events is frequently described as the experimental demonstration of replicative stress (DOBBELSTEIN; SØRENSEN, 2015).

There are hundreds of specific genomic regions throughout all chromosomes that are particularly sensitive to the effects of replicative stress, usually presenting breaks and gaps after treatment with partial DNA replication inhibitors. These regions have been named ‘chromosomal fragile sites’ and are classified as common (CFS) or rare (RFS) depending on their prevalence in the population and further classified by the genotoxic stressor that induces their “expression” (GLOVER; WILSON; ARLT, 2017). Molecular biologists frequently use the confusing term “fragile site expression” to designate the breaks occurring in specific fragile sites. Those sites were first observed in 1984 by conventional cytogenetics, when human cultured lymphocytes were treated with aphidicolin (an inhibitor of the replicative alpha DNA polymerase)

and chromosomal breaks were observed in specific loci in a clear nonrandom fashion (GLOVER *et al.*, 1984). The reason why those regions are prone to breakage rely on both structural and functional peculiarities.

An important structural feature is gene size. Common fragile sites usually contain abnormally large genes, often measuring about 300 kbp, but reaching up to 2,000 kbp, while the average size of a human gene is 20 kbp (LE TALLEC *et al.*, 2014). However, not all the CFS are associated with very large genes. Several examples are known, such as FRA2G (locus 2q31) and FRA7G (locus 7q31.2), that span only small genes of less than 50 kbp (SMITH *et al.*, 2007). Another interesting explanation for gene fragility that relates to gene size has been proposed recently. Completion of transcription of very large genes (over 800 kbp) usually lasts more than one cell cycle. So, replicative and transcriptional machinery will certainly work on the same strand at the same time on those genes. As replication enzymes travel through the DNA strand, it may collide with R-loops formed by transcriptional machinery, creating DNA damage (AGUILERA; GARCÍA-MUSE, 2013). This mechanism also helps to explain an important feature of fragile sites; its tissue specificity. Fragile genes in one cell type may not be fragile in other tissues. Hence, differential gene expression among different tissues may play a role in their fragility.

Another characteristic of CFS is the presence of large initiation-poor regions. Once a replication fork stalls, a neighbor progressing fork can rescue the halted fork and prevent that the onset of mitosis occur with under replicated DNA (ZEMAN; CIMPRICH, 2014). However, in initiation-poor regions, the probability of rescuing stalled forks significantly diminishes. One more trait of CFS is the high frequency of flexible AT-rich sequences that ensure the formation of secondary structures, which may slow fork progression or even cause forks to collapse (ZLOTORYNSKI *et al.*, 2003). However, as fragile sites are tissue-specific, nucleotide sequence (and their inherent secondary structures) cannot be the only reason responsible for its fragility. Nevertheless, no individual feature seems sufficient to induce fragility of a given gene, so most authors suggest that fragility arises as a consequence of many, if not all, of these characteristics (LE TALLEC *et al.*, 2014).

The role of fragile sites in cancer biology has been extensively studied. Indeed, 52% of the recurrent translocations associated with cancer have at least one gene mapped to a fragile site (BURROW *et al.*, 2009). Interestingly, all the genes involved in RET/PTC1 and RET/PTC3 rearrangements are also located within common fragile sites of the chromosome 10 **(Figure 8)**. Both *RET* and *NCOA4* are mapped to FRA10G, a common fragile site (CFS) associated with locus q11.2 that presents breaks upon treatment with aphidicolin (i.e., CFS/APH-type). On the other hand, *CCDC6* is mapped to FRA10C, a fragile site sensitive to BrdU (i.e., CFS/BrdU-type) at locus q21.

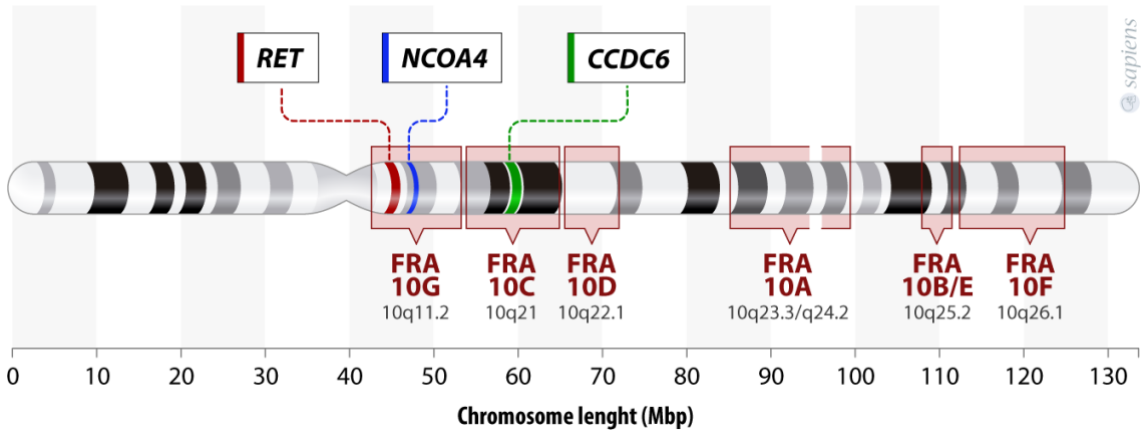

Figure 8. Fragile sites of chromosome 10. Multiple fragile sites (A-G) have been characterized in chromosome 10. Both *RET* and *NCOA4* (involved in RET/PTC3) are mapped to FRA10G while *CCDC6* (involved in RET/PTC1) is mapped to FRA10C. (Data from NCBI's Gene databank [www.ncbi.nlm.nih.gov/gene/] and NCBI's Map Viewer [www.ncbi.nlm.nih.gov/projects/mapview/]).

Importantly, the characterization of FRA10G in locus q11.2 does not mean that all genes comprised within locus q11.2 are essentially fragile nor that locus q11.2 is fragile in all cell types. It means that some genes with experimentally-confirmed fragility have been mapped to these loci and may even be flanked by non-fragile genes.

In the original paper from 1990 that first described RET/PTC1 (GRIECO *et al.*, 1990), the existence of a fragile site had already been suggested due to the high frequency of rearrangements observed in the same locus. However, only in 2010 the role of fragile sites in RET/PTC formation in the thyroid was demonstrated. In a very important work in the field, Gandhi and colleagues showed that the treatment of NTHY-ori3.1 cells (a SV40-transformed human thyroid cell lineage from normal origin) with a

combination of fragile site-inducing chemicals (aphidicolin (APH), the ATM and ATR kinases inhibitor 2-aminopurine (2-AP) and thymidine analog bromodeoxyuridine (BrdU)) induced breaks in chromosome 10 precisely at *RET* gene location, as observed by fluorescence *in situ* hybridization (FISH) (Figure 9A). Moreover, they analyzed the frequency of breaks not only in *RET*, but also in *NCOA4* and *CCDC6*, with three different drug combinations and confirmed the sensitivity of FRA10G (CFS where *RET* and *NCOA4* are located) to APH, and the sensitivity of FRA10C (*CCDC6*'s CFS) to BrdU (Figure 9B). Importantly, they observed that although *NCOA4* is mapped to FRA10G, this gene does not present breaks, denoting it is not fragile at least in the thyroid tissue. Next, the authors used RT-PCR to detect RET/PTC1 and RET/PTC3 transcripts in thyroid cells after treatment with a drug combination that targets simultaneously FRA10G and FRA10C but, consistent with *NCOA4* non-fragile nature, only RET/PTC1 was detected (Figure 9C) (GANDHI *et al.*, 2010).

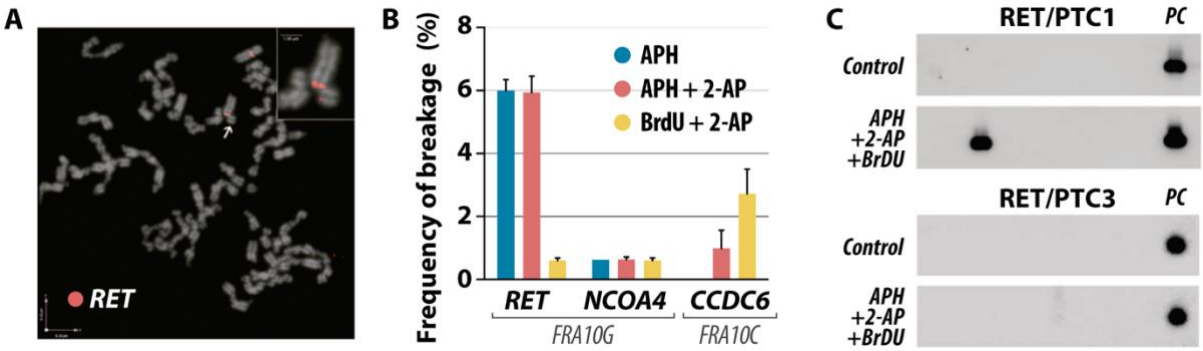

Figure 9. Fragile site expression in thyroid cells. The main findings published by Gandhi and colleagues are depicted here. (A) Fluorescence in situ hybridization (FISH) on metaphase chromosomes of NTHY cells after exposure to APH, 2-AP and BrdU resulting in chromosomal break in *RET* (red signal). (B) Frequency of chromosomal breaks in *RET*, *NCOA4* and *CCDC6* after treatment with fragile site-inducing chemicals. (C) Detection of RET/PTC1 but not RET/PTC3 rearrangements through RT-PCR after treatment with APH, 2-AP and BrdU. APH; aphidicolin, 2-AP; 2-aminopurine, BrdU; bromodeoxyuridine, PC; positive control (RET/PTC1-positive TPC1 cell lineage or RET/PTC3-positive tumor sample). All data are adapted from *Gandhi M, et al. 2009 (Oncogene)*.

These results enlighten the role of fragile sites in RET/PTC1-positive PTC etiology. However, the structural properties conferring fragility to these genes are not well understood. As depicted in Figure 4, although larger than average, neither *RET* nor *CCDC6* as exceptionally large genes, as they have 53 and 177 kbp, respectively.

The clash between replicative and transcriptional machinery is also very unlikely since *RET* is not expressed in thyroid follicular cells. Hence, more functional and structural studies are needed to investigate the replication dynamics of thyroid cells.

Even though the traits discussed above make fragile sites prone to breakage, they are not unstable unless replication stress occur. Replicative stress has multiple causes, both endogenous and exogenous. One common cause is the lack of important factors for proper DNA replication, such as replicative enzymes, histones, chaperones and free nucleotides. It is well documented in the literature that cells lacking appropriate amounts of nucleotides to fuel replication undergo severe replicative stress. This condition is frequently reproduced experimentally by the use of hydroxyurea (HU), a reversible inhibitor of the catalytic domain of the nucleotide-producing enzyme *ribonucleotide reductase* (RNR), responsible for the conversion of ribonucleotides to deoxyribonucleotide triphosphates (dNTPs) (ALVINO *et al.*, 2007). Cells treated with HU have their dNTP pool concentration significantly diminished and, consequently, present high levels of genomic instability.

Several other dysfunctional cellular mechanisms can lead to replicative stress; the misincorporation of ribonucleotides (rNTPs) during DNA replication, untimely loading of helicases outside late G1-phase leading to re-replication, interaction with transcription machinery and even the excessive firing of origins of replications behind oncogene activation are possible sources of replication stress (AGUILERA; GARCÍA-MUSE, 2013; GELOT; MAGDALOU; LOPEZ, 2015; ZEMAN; CIMPRICH, 2014). However, reactive oxygen species now figure as an emerging important endogenous cause of replicative stress.

1.6. Oxidative stress

Reactive oxygen species (ROS) comprise a large group of oxygen-derived small molecules that include radicals and non-radical species. Radicals such as superoxide ($O_2^{\bullet-}$), hydroxyl ($OH^{\bullet}$), and peroxyl ($RO_2^{\bullet}$) are short-lived, highly electrophilic, and reactive molecules with an unpaired electron in its outer shell. Non-radical reactive molecules of oxygen include hypochlorous acid (HOCl), ozone (O_3), singlet oxygen ($^1O_2$), and the most biologically relevant, hydrogen peroxide (H_2O_2) (HALLIWELL;

GUTTERIDGE, 2007). The availability of ROS in a given site results from the balance between its production, from various sources, and its disposal, by enzymatic and non-enzymatic antioxidants. The imbalance of this system can lead to a pro-oxidant environment, which has long been characterized as oxidative stress. This may be achieved by an overproduction of ROS or by insufficient antioxidant activity (HECHT; CAZARIN; *et al.*, 2016). However, this concept has been refined to more stringent terms. Oxidative stress will occur whenever some changes in the mechanisms of production and/or degradation of ROS disrupts the normal functioning of the redox-sensitive mechanisms, even if these changes do not cause irreversible oxidative damage or do not lead to a widespread pro-oxidant status in the cell (HECHT; PESSOA; *et al.*, 2016). ROS avidly interact with a large spectrum of cellular constituents, including small inorganic molecules, proteins, lipids, and nucleic acids. This reaction can reversibly or irreversibly alter the structure and function of these compounds and depending on the extent of the phenomenon can cause loss of important cellular functions (MENG *et al.*, 2006).

Several ROS sources work simultaneously in cells to produce ROS either as a by-product of cellular metabolism or specifically **(Figure 10)**. Enzymes such as xanthine oxidase, uncoupled endothelial nitric oxide synthase (eNOS), P450 enzymes, lipoxygenase, and cyclooxygenase generate high levels of ROS as an unavoidable consequence of their main functions (MEUNIER; DE VISSER; SHAIK, 2004; SOSA *et al.*, 2013; VALKO *et al.*, 2007) In contrast, NADPH oxidases produce ROS as their exclusive function and these molecules are recognized as major co-factors and second messengers of several physiological mechanisms (BEDARD; KRAUSE, 2007). More recently, the role of NADPH oxidases in pathology, particularly in cancer, is gaining attention (AMEZIANE-EL-HASSANI; SCHLUMBERGER; DUPUY, 2016; BLOCK; GORIN, 2012).

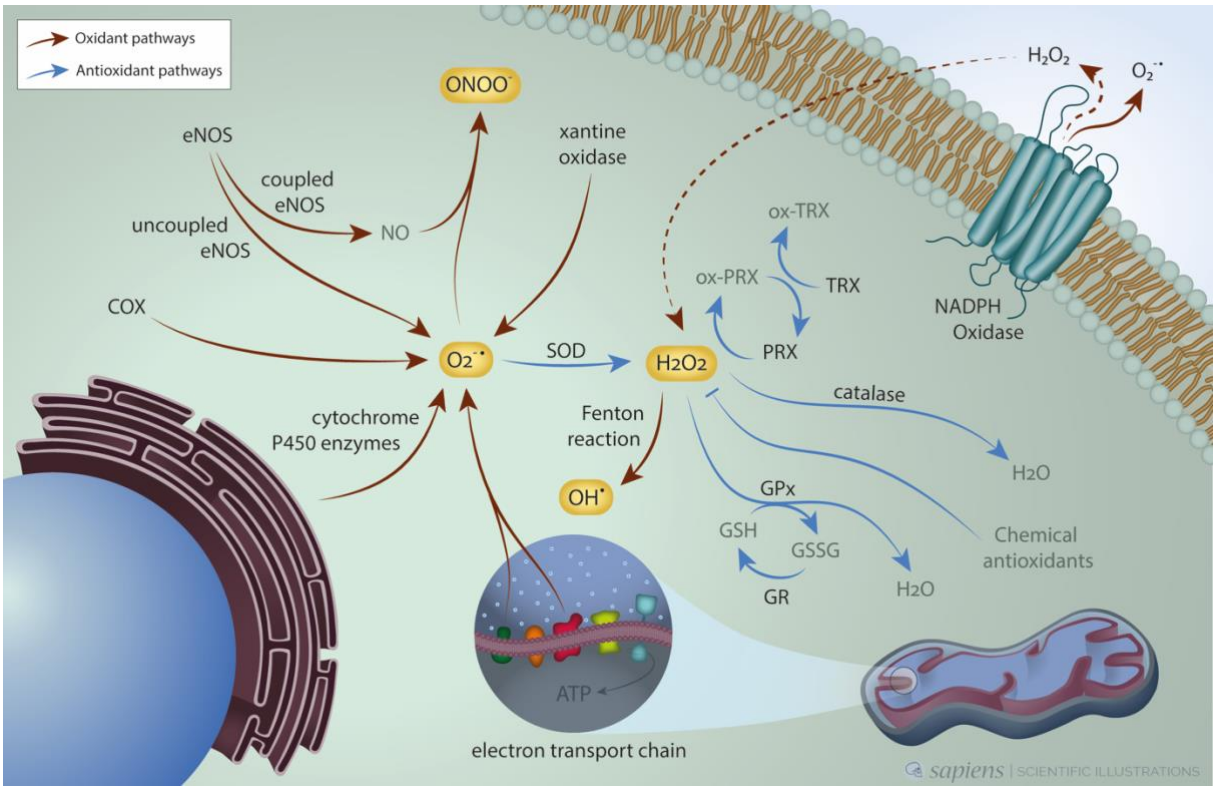

Figure 10. Cellular mechanisms of ROS generation and elimination. Schematic representation of redox homeostasis of eukaryotic cells (eNOS; endothelial nitric oxide synthase, COX; cyclooxygenase, SOD; superoxide dismutase, GPx; glutathione peroxidases, TRX; thioredoxin reductase, PRX; peroxiredoxins, $O2^{-\bullet}$; superoxide radical, $OH^{\bullet}$; hydroxil radical, H_2O_2; hydrogen peroxide, $ONOO^{-}$; peroxynitrite). Reproduced from Hecht et al., 2016b.

Oxidative DNA damage comprises a large variety of lesions, including nitrogenous bases and sugars lesions, DNA breaks and DNA-protein cross-links. There are over a hundred different types of oxidative base modifications characterized in the human genome, however, the most relevant, and most studied, is certainly 7,8-dihydro-8-oxo-guanine (8-oxo-G) (COOKE *et al.*, 2003; VAN LOON; MARKKANEN; HÜBSCHER, 2010). Due to its exceptionally low redox potential, guanosine is particularly vulnerable to oxidation. The resulting 8-oxo-G structure slows fork progression and contributes to genome instability. Moreover, 8-oxo-G efficiently mimics thymine (T) structure. Hence, during replication, DNA polymerases often bypass 8-oxo-G and inaccurately incorporates adenine (A) opposite to the oxidized guanine (8-oxo-G) instead of cytosine (C), creating the dangerous A:8-oxo-G

mismatches, subsequently resulting in C:G to A:T transversion mutations (MARKKANEN *et al.*, 2012). Most of these damages are repaired by multiple enzymes of the base excision repair (BER) pathway. While the removal of C:8-oxo-G lesions is performed by OGG1 (8-oxo-G DNA glycosylase 1), the repair of the mutagenic A:8-oxo-G mismatches is made by MUTYH (MutY glycosylase homologue) and APE1 (AP endonuclease 1) (VAN LOON; MARKKANEN; HÜBSCHER, 2010). Besides the mutagenic nitrogenous base modification, the oxidation of DNA-associated proteins involved in DNA replication and repair are also a possible source of replication stress. It has been shown that the oxidation of PCNA (proliferating cell nuclear antigen) impairs fork progression contributing to replicative stress (MONTANER *et al.*, 2007).

There is also a great collection of exogenous sources of replicative stress that may perturb proper replication progression. Fragile-site inducing chemical agents include chemotherapeutic agents (such as 5-azacytidine, actinomycin-D, bleomycin, busulfan, chlorambucil, cytosine arabinoside, FUdR, methotrexate and others), dietary (caffeine, ethanol), drugs (atenolol, dimethyl sulfate), and several factors from modern daily environment (cigarette smoke, pesticides, benzene, diethylnitrosamine, carbon tetrachloride) (DILLON; BURROW; WANG, 2010). Ionizing radiation may also be considered an exogenous source of replicative stress due to its known ability to induce DNA damage (GANDHI *et al.*, 2010). Indeed, the high prevalence of RET/PTC, a translocation between genes located within fragile sites, in patients with ionizing radiation exposure corroborates this statement.

The consequences of ionizing radiation in human cells are not limited to the immediate effects of energetic particles and waves that interact with biological molecules in a stochastic fashion. Radiation triggers several biological responses that lasts for long periods of time after the irradiation event and are even inherited by daughter cells. Our team has already begun unveiling the role of ionizing radiation in RET/PTC development in immortalized thyroid cells many years ago. First, using NTHYori3.1 cells as a paradigm, our group performed an experiment in which plated cells were exposed to a single dose of 5 Gy of X-rays and analyzed the presence of RET/PTC1 translocations 15 days later. The results showed a strong and clear induction of RET/PTC1 in NTHY cells, however, as widely known, ionizing radiation also induces the radiolysis of water, forming, among other products, H_2O_2 and even

the highly reactive radical $OH^{\bullet}$. Thus, it was reasonable to imagine that at least part of the effects attributed to the irradiation are, in fact, due to oxidative damage secondary to radiolysis. To investigate that, it was also shown that if the 5 Gy-irradiation was executed in the presence of the antioxidant enzyme catalase, RET/PTC1 formation was almost entirely abrogated. To further demonstrate the contribution of ROS to RET/PTC1 formation, it was shown that the incubation of non-irradiated cells with low doses of H_2O_2 was enough to induce RET/PTC1 formation, suggesting that water radiolysis represents an important part of the effects attributed to radiation (AMEZIANE-EL-HASSANI *et al.*, 2010).

Thus, radiation also triggers long-term biological responses that greatly differ from the immediate responses observed within minutes of the irradiation event. These delayed effects have been known for decades and are composed mainly of persistent genomic instability (MARDER; MORGAN, 1993; WATSON *et al.*, 2000) and persistent oxidative stress (TULARD *et al.*, 2003). However, they were mostly attributed to mitochondrial dysfunctions (AZZAM; JAY-GERIN; PAIN, 2012; KIM; FISKUM; MORGAN, 2006). In this context, our group published a subsequent in which the long-term effects elicited by irradiation was assessed (AMEZIANE-EL-HASSANI *et al.*, 2015).

In this work, it was observed that within 48 to 96h after a 10 Gy-irradiation, an important increase in the expression of the NADPH Oxidase DUOX1 occurred. This upregulation led to the overproduction of ROS that caused persistent DNA damage in thyroid cells. Next, it was observed that the ROS produced during the oxidative burst elicited by water radiolysis was involved in DUOX1 surge, since the irradiation in the presence of catalase prevented DUOX1 late-upregulation. Moreover, it was demonstrated that radio-induced thyroid tumors have a significantly higher expression of DUOX1 than normal tissues (AMEZIANE-EL-HASSANI *et al.*, 2015).

Therefore, knowing that one of the main effects elicited by irradiation in thyroid cells is the persistent oxidative stress promoted by DUOX1 late-onset upregulation and that ROS are genotoxic stressors capable of inducing RET/PTC1, our aim is to discover whether there is a replicative stress condition after irradiation, if the DUOX1-

derived ROS is involved in the replicative stress and if the replicative stress favors the formation of RET/PTC1.

2. OBJECTIVES

2.1. Main objective

Investigate the role of replicative stress in the formation of DNA damage and RET/PTC1 translocations in thyroid cells after irradiation and its possible relation with reactive oxygen species.

2.2. Specific objectives

- Characterize the redox homeostasis of NTHY-ori3.1 cells at different time points after irradiation;
- Investigate the effects of 5 Gy-irradiation on the proliferation of thyroid cells;
- Evaluate the possible existence of a replicative stress condition after irradiation;
- Explore the possible role of reactive oxygen species in replicative stress induction;
- Study the timing of DNA strand breaks generation in genes involved in RET/PTC translocation.

3. MATERIALS AND METHODS

3.1. Cell culture

The experimental model used in the present work was the cell lineage NTHY-ori-3-1, a human thyroid follicular epithelial cell developed in 1989 by the transfection of human primary cells with a plasmid containing an origin-defective SV40 genome (SVori-). The transformed cells were found to have factor-independent growth but are non-tumorigenic in nude mice (LEMOINE *et al.*, 1989). This cell present an unstable karyotype, frequently presenting high levels of aneuploidy. In one study published in 2011, NTHY cells were found to have 2, 3 or even 4 or copies of the chromosome 10 (where *RET* is located) (MARIC *et al.*, 2011). The cell used in our work was purchased from the European Collection of Authenticated Cell Cultures (ECACC, United Kingdom) at passage number 16 (Catalog #90011609/Lot #13B007). Cells were usually used until passage 30 and then discarded. Cells were expanded in RPMI 1640 medium (Gibco) without phenol red supplemented with 10% fetal bovine serum (FBS). For experiments, cells were cultivated in RPMI medium supplemented with 3% FBS. The choice of phenol red-free media and lower serum concentration is based on their antioxidant activity that could interfere with our assays. Cells were rigorously plated at the same density and with the same volume of medium in all experiments. Generally, 100,000 cells were plated in wells of 6-wells plates (9.62cm^2/well) with a total volume of 2 mL of fresh RPMI 3% FBS. Vessels of all sizes were used for different experiments, but independently of the surface area, cell number was compensated so density was always maintained. This relatively low cell density at seeding was chosen to avoid excessive confluency at the end of experiment, ensuring that cells remain proliferative. Thus, this optimal density of 10^5 cells/9.62cm^2 will be referred as the standard density for this work.

3.2. Irradiation

Cells were irradiated 24 hours after plating using XRad320 (Precision X-Ray, USA), an X-ray generator operated at 320 KV/4 mA that delivered a dose rate of approximately 1Gy/min. Samples were placed 51.5 cm apart from the source and usually irradiated for 309 seconds. The media of culture flasks was changed few

minutes before irradiation. After irradiation, the medium was not changed until the end of the experiment.

3.3. Whole-cell protein extraction

Plated cells were washed 2 to 3 times with PBS at room temperature and then scraped on ice with cold TEX Buffer, composed of Urea (4 M), Tris/HCl pH 7.0 (100mM), SDS (2.5 %), EDTA (1 mM), EGTA (1 mM), PMSF (100 nM) and protease and phosphatase inhibitors cocktail. Typically, 80-100 μL of TEX buffer was used for a 9.62 cm^2 well. Cell extracts were kept at -20°C until use. The amount of protein present in cell lysates was measured by Pierce BCA Protein Assay Kit (Thermo), according to the manufacturer's instructions.

3.4. Cell fractioning: Chromatin-enriched protein fraction

Chromatin-enriched cell fraction was obtained as previously described with minor adaptations (MÉNDEZ; STILLMAN, 2000). Briefly, $3x10^6$ cells were washed with PBS, trypsinized and centrifuged. Supernatant was discarded and cell pellet was suspended in 100 μL of buffer A (HEPES pH 7.9 10 mM, $MgCl_2$ 1.5 mM, KCl 10mM, Sucrose 0.117g/mL, Glycerol 10%, DTT 1 mM, protease and phosphatase cocktail inhibitor) in a microcentrifuge tube. Triton X-100 was added to the cell suspension and buffer A to reach a final concentration of 0.1%. The tube was vortexed and incubated 5 minutes in ice and then centrifuged for 4 min at 1,300 x g at 4°C. The supernatant that is enriched in cytoplasm soluble proteins was discarded and the pellet was washed with 300uL of solution A and re-centrifuged. To allow nucleus lysis, the pellet was suspended in 100uL of solution B (EDTA 3 mM, EGTA 0.2 mM, DTT 1 mM, protease and phosphatase cocktail inhibitor) vortexed and incubated 10 minutes in ice. The tube was centrifuged for 4 min at 1,700 x g at 4°C, the supernatant discarded, the pellet washed in 300uL of solution B. Once again, the tube was centrifuged for 1 minute at 10,000 × g at 4°C, and the supernatant discarded. Finally, pellet was suspended in TEX buffer and stored at -20°C until analysis. The amount of protein present in cell lysates were measured by Pierce BCA Protein Assay Kit (Thermo), according to the manufacturer's instructions

3.5. Western Blotting

Protein samples (10-30 μg) were mixed with Laemmli sample buffer supplemented with 100mM of DTT and denatured by heating (70ºC during 10 min). Samples were subjected to SDS-PAGE electrophoresis at 150 Volts in Tris-Glycine-SDS buffer (Invitrogen) using NUPAGE western blotting system from Invitrogen. Proteins were electrotransferred to 0.2-mm nitrocellulose sheets (Amersham) for 90-240 minutes at 30 Volts in Tris-Glycine buffer containing 20 % of isopropanol, using the same western blotting system. To avoid unspecific antibody hybridization, membranes were incubated with 5% non-fat milk or 5% bovine serum albumin TBS-T solution for 1h at room temperature. Membranes were probed with primary antibodies overnight at 4ºC, under constant agitation. Membranes were washed 3 times with TBS-T and incubated with goat anti-rabbit IgG-HRP antibody (SouthernBiotech) or goat anti-mouse IgG-HRP antibody (Santa Cruz Biotechnology Inc) for 45 minutes at room temperature. Membranes were washed again 3 times with TBS-T and the proteins were visualized by enhanced chemoluminescence (Amersham) using X-ray films (GE).

Table 2. Antibodies used for Western Blotting.

Antibody	Dilution	Manufacturer	Reference
Actin	1:15,000	Sigma	A2066
ATR	1:2,000	Abcam	ab54793
pATR	1:2,000	Cell Signaling	#2853S
ATM	1:2,000	Cell signaling	#2873S
pATM	1:2,000	Cell signaling	#4526S
Cdc25a	1:1,000	Santa Cruz	sc-65503
pH3	1:1,000	Upstate	#06-570
H3	1:5,000	Abcam	ab12179
Lamin AC	1:2,000	Cell Signaling	sc7292
pChk1-Ser345	1:3,000	Cell Signaling	#2348S
Chk1 (2G1D5)	1;1000	Cell Signaling	#2360
Vinculin	1:20,000	Abcam	ab18058
GFP	1:2,000	Thermo	A11122
P53	1:1,000	Cell Signaling	#9286S
pP53-Ser15	1:1,000	Cell Signaling	#2527S
γH2AX	1:10,000	Millipore	05-636
H2AX	1:5,000	Abcam	ab11175

3.6. Nucleotide Pool measurement

Cells were plated in 10 cm petri dishes at standard density and irradiated as previously described. In the appropriate time point after irradiation, cells were washed 2-3 times with 10 mL of cold PBS and then incubated with 2mL of Acetonitrile (70%) on ice for 5 minutes. During the incubation period, plates were covered and sealed with Parafilm® to minimize evaporation. After 5 minutes, the acetonitrile solution was recovered, transferred to a falcon tube and stored at -80°C until analysis. The concentration of ATP, dATP, dGTP, dCTP and TTP was determined through Mass Spectrometry.

3.7. 8-oxo-G quantification

Cells were plated in 175cm^2 flasks at standard density and irradiated as previously described. At different time points after irradiation, cells were collected by trypsinization, washed with PBS and counted. Next, approximately 8x10^6 cells were pelleted by centrifugation, suspended in 2mL of warm PBS and transferred to a screwcap tube. The cells were again pelleted, the supernatant discarded and the “dry pellet” instantaneously frozen in liquid nitrogen. Tubes were kept at -80°C until analysis. Quantification of 8-oxo-G modifications and total DNA quantification was performed through HPLC (in collaboration with Dr. Jean-Luc Ravanat).

3.8. Extracellular H_2O_2 production by AmplexRed/HRP

Extracellular ROS production has been measured using AmplexRed/HRP, a method that detects the accumulation of oxidized products in the reactional medium. Amplex Red (10-acetyl-3,7-dihydroxyphenoxazine) is oxidized by horseradish peroxidase (HRP) using the H_2O_2 produced by cells as cofactor, and thus becomes a fluorescent molecule called resorufin (Excitation: 571 nm/Emission: 585 nm). For this experiment, cells were plated in multiple 6-well plates and irradiated as previously described. In the appropriate time-point after irradiation, cells were collected by trypsinization, washed with PBS and counted. Next, 10^5 cells were mixed with a reaction mix containing D-glucose (1 mg/mL), horseradish peroxidase (HRP) (0.5

U/mL), Amplex Red (50 μM) and PBS with calcium and magnesium in opaque 96-well plates. The accumulation of resorufin was monitored for approximately 1 hour at 37°C using a fluorescence plate-reader (Victor X4; PerkinElmer, Norwalk, CT). The slope of the curves was then calculated and compared to a H_2O_2 calibration curve and expressed as nM of H_2O_2 produced per minute by 10^5 cells (nM $H_2O_2 \times min^{-1} \times 10^5$ cells).

3.9. Intracellular ROS levels measurement by DCF

Intracellular levels of ROS were assessed using the non-fluorescent lipophilic ester 2',7'-dichlorodihydrofluorescein diacetate (H2-DCF-DA). After crossing the plasma membrane, this compound is de-esterified to the hydrophilic alcohol H_2DCF (dihydrodichlorofluorescein) that may be oxidized to the highly fluorescent molecule DCF (2',7'-dichlorofluorescein) by cellular ROS. For this experiment, cells were plated in multiple 6-well plates and irradiated as previously described. In the appropriate time-point after irradiation, cells were collected by trypsinization, washed with PBS and suspended in RPMI medium containing 5 μM of H_2-DCF-DA. Cells remained for 20 minutes at 37°C in the incubator and were then immediately transferred to ice to stop reaction and minimize sample-to-sample variation. The mean fluorescence of at least 10,000 events was detected using BD Accuri™ C6 (BD Biosciences) and expressed as arbitrary units of fluorescence.

3.10. Mitochondrial superoxide production by MitoSOX

The detection of mitochondrial superoxide production after irradiation was performed by MitoSOX™ Red mitochondrial superoxide indicator (#M36008, Molecular Probes). This live-cell permeant molecule targets mitochondria and is oxidized preferentially by superoxide anions, emitting red fluorescence. For this experiment, cells were plated in multiple 6-well plates and irradiated as previously described. In the appropriate time-point after irradiation, cells were collected by trypsinization, washed with PBS and suspended in RPMI medium containing 5 μM of MitoSOX™. Cells were incubated for 10 minutes at 37°C in the incubator and then immediately transferred to ice to stop reaction and minimize sample-to-sample

variation. The mean fluorescence of at least 10,000 events was detected using BD Accuri™ C6 (BD Biosciences) and expressed as arbitrary units of fluorescence.

3.11. H_2O_2 concentration in extracellular media

The evaluation of H_2O_2 concentration in the minutes following irradiation was performed using AmplexRed/HRP as previously described with adaptations. For each experiment, cells were plated in 12 well-plates with standard density (one well for each time point) and the experiment was performed 24 hours after plating. Before starting, medium was replaced by PBS and cells were placed in the incubator for 30 minutes to stabilize. Next, several wells of a 96-well plate were filled with 100 μL of 2x AmplexRed/HRP mix and kept on ice protected from light in the irradiator room. The wells had 100 μL of medium collected and immediately pipetted into a well with 2x AmplexRed/HRP mix in 12 different time-points: five minutes before irradiation, few seconds before irradiation, 1 minute after irradiation and every 5 minutes after irradiation during the following 45 minutes. After 12 time-points covering 50 minutes of experiment, the plate was read and the H_2O_2 concentration in each time point determined by a H_2O_2 calibration curve.

3.12. Real-time qPCR

Total RNA was extracted from cells using Nucleospin RNA plus (Macherey-Naegel) extraction kit according to the manufacturer's instructions. The quality of RNA preparation, based on 28S/18S rRNA bands visualization, was assessed by agarose electrophoresis. Total RNA (2 μg) was reverse-transcribed using Maxima Reverse Transcriptase (Thermo Fisher Scientific) and oligo(dT) primers in a total reaction volume of 20 μL of PCR buffer, according to the manufacturer's instructions. Reverse transcription reaction was performed in a thermocycler (Applied Biosystems) for 120 min at 50 °C. Human *DUOX1*, *DUOX2, DUOXA1* and *NOX4* qPCR were performed with TaqMan methodology using Universal Master Mix (Applied Biosystems). Reaction was performed in a total volume of 20 μL containing 9 μL of diluted cDNA sample, 350 nM of reverse and forward specific primers and TaqMan specific probe. For ChIP-qPCR assays, real-time qPCR was performed with SyBr Green methodology using

FastStart Universal SYBR Green Master Mix (Roche). Reaction was performed in a total volume of 25 μL containing 2,5 μL of diluted cDNA sample, 300 nM of reverse and forward specific primers. All primers and TaqMan probe oligonucleotide sequences are listed in Table 3. Real-time PCR reactions were performed in Applied Biosystems 7300 machine using the following thermal cycle profile: 50°C for 2 minutes, 95°C for 10 minutes, 42 cycles of 95°C for 10 seconds followed by 60°C for 1 minute. mRNA relative expression of was determined by ΔΔCt methodology (LIVAK; SCHMITTGEN, 2001).

Table 3. Primers and probes used in qPCR

Target		Sequence	Method
DUOX1	5’ primer	CCAGCAATCATCTATGGGGGC	TaqMan
	3’ primer	TGGGGCCGCTGGAACC	
	Probe	5′ FAM-ATCAGCGTGGTGAAGGCGGAGC-3′ TAMRA	
DUOX2	5’ primer	CCGGCAATCATCTATGGAGGT	TaqMan
	3’ primer	CCTTGGGGCCTCTGGAATT	
	Probe	ATCAGCGTGGTGAAGGCGGAGC	
NOX4	5’ primer	TGTCTTCTACATGCTGCTGACGTT	TaqMan
	3’ primer	CTGAGAGCTGGTTCGGTTAAGACT	
	Probe	5′-FAM-CAAACTAATTTAGATACCCACCCTCCCGGC-TAMRA	

3.13. Immunofluorescence

Cells were plated in 6-well plates in which each well received 5 circular coverslips. Irradiation and medium change was executed as usual. Three days after irradiation, cells were fixed with pre-warmed 4 % paraformaldehyde (PFA) in PBS for 10 minutes. Next, fixed cells were washed with Washing Buffer (PBS-Tween 0.05 %) and permeabilized with PBS-Triton X-100 (0.1 %) for 5 minutes at room temperature. Cells were washed 3 times with Washing Buffer and then saturated with Blocking Buffer (goat serum 5%) for 1 hour. Cells were then incubated overnight at 4°C in a humid chamber with primary antibodies diluted in Dilution Buffer (2% goat in PBS-Tween 0.05 %). After 3 washing steps, secondary antibodies were added for 1 hour at room temperature. Three more washing steps were performed and nuclei were stained

with DAPI (300 nM) for 5 minutes. Finally, slides were assembled by placing the coverslips in glass slides with VectaShield.

Table 4. Antibodies used for immunofluorescence.

Primary antibodies				
Antibody	**Host**	**Ref.**	**Brand**	**Dilution**
anti-γH2AX	Mouse	05-636	Millipore	1:1,000
anti-pRPA32	Rabbit	A300-246A	Bethyl Laboratories	1:1,000
anti-FANCD2	Rabbit	ab2187	Abcam	1:1,000
Secondary antibodies				
Antibody	**Host**	**Ref.**	**Brand**	**Dilution**
anti-Mouse IgG AF568	Goat	A11031	Invitrogen	1:1,000
anti-Rabbit IgG AF488	Goat	A11008	Invitrogen	1:1,000

3.14. DNA combing

Cells were plated in 6 cm petri dishes at standard confluence and irradiated as previously described. Three days after irradiation, cells were labeled with the nucleotide analogs IdU and CldU to track replication speed and fork asymmetry. First, 20 μM of IdU was added to culture media so proliferating cells would incorporate it into newly synthetized DNA strands. After exactly 30 minutes, the medium was rapidly discarded and the plate washed. Hence, proliferating cells had at this point a segment of IdU-labeled DNA corresponding to 30 minutes of replication. Immediately after the discard of IdU medium, 20 μM of CldU was added for more 30 minutes. After this period, proliferating cells had a second labeled DNA segment corresponding to another 30 minutes of replication. The third and last incubation was made with 1mM of thymidine to stop labeling. The cells were finally collected by trypsinization, washed, counted and suspended in PBS at $2{,}5x10^6$/mL. DNA extraction of these cells was performed using a very slow and gentle protocol to minimize the break of DNA fibers, since proper analysis of DNA combing results depend on the measurement of long and unbroken DNA. So, 750,000 cells (300μL of cell suspension) were mixed with 300 μL of 2% Low-Melting Agarose (2-Hydroxyethylagarose, #A4018-Sigma) and placed into plug molds at 4°C to form solid blocks. After trapping cells into agarose blocks, they

were treated with 2 mL of Proteinase K Mix (SDS 1%, EDTA 0.25 M, Proteinase K 1 mg/mL) for 48 h (re-adding Proteinase K after 24h) at 42°C. This step is meant to digest cells entirely, gently liberating unbroken DNA fibers. The blocks undergo 3 washing steps at room temperature with TE buffer of 30 minutes each. Finally, agarose blocks will be digested to liberate DNA fibers. To do so, blocks are initially melted by heating at 68°C for 15 minutes. After lowering the temperature to 42°C, Agarose (Promega) is added for 1 hour. After this initial digestion, Agarose is added again and digestion occurs for more 48h. After the 2-days treatment, MES Buffer is added, the solution is heated at 65°C for 30 minutes to dissolve any solid agarose fragment and then cooled to 4°C. This solution must be kept at 4°C in dark for at least one month so the tangled DNA fibers will spontaneously stretch as demanded for proper analysis. After this long incubation period, the solution is gently poured into a small container where treated coverslips will be vertically plunged to “collect” linear DNA fibers from the solution. Coverslips are them assembled with glass slides and stored at -20°C until immunodetection. The visualization of IdU and CldU tracks was performed by immunofluorescence. First, the slides were defrosted and the DNA denatured in 1 M NaOH for 7 minutes. Next, slides were washed once with PBS and other 3 times with crescent concentrations of ethanol (70 %, 85 % and 100 %) for 5 minutes each. Then, a blocking solution was added to the slides for 30 minutes at 37°C. There are no commercial antibodies for CldU and IdU detection, thus, their detection is made using anti-BrdU antibodies. Although there is a crossed-detection of both probes, IdU is preferentially detected by mouse-anti-BrdU-FITC while CldU is preferentially detected by rat-anti-BrdU. After 30 minutes of incubation with both antibodies at 37°C, slides were washed with a Washing Buffer (0.5 M NaCl, 20 mM Tris, 0.5 % Tween-20, pH 7.8) to minimize the cross-detection between IdU and CldU. Fluorochrome-coupled secondary antibodies against rat and mouse (Table 5) diluted in Blocking Buffer were added to the slides and incubated for 30 minutes at 37°C. After washing, the detection of single-stranded DNA was performed to ensure that fibers were not undamaged. Theoretically, fibers should always contain red and green tracks flanked by blue tracks on both ends. If blue fluorescence is absent in one or both sides, it is uncertain whether the end of green/red tracks really represents how far the fork progressed or an artefact due to a broken DNA fiber. So, to detect ssDNA, slides were incubated with primary

antibodies anti-ssDNA, washed as previously described and incubated sequentially with two layers of fluorochrome-labeled antibodies to increase signal.

Table 5. Antibodies used for DNA combing.

Target	Antibody	Dilution	Brand	Reference
IdU	mouse-anti-BrdU-FITC	1:5	BD Biosc.	347583
CldU	rat-anti-BrdU	1:25	Serotec	OBT0030
ssDNA	mouse-anti-ssDNA	1:25	Millipore	MAB3034
Secondary for IdU	goat-anti-mouse-Alexa488	1:50	Invitrogen	A11029
Secondary for CldU	goat-anti-rat-Alexa555	1:50	Invitrogen	A21434
Secondary for ssDNA	goat-anti-mouse-Cy5.5	1:100	Abcam	ab6947
Tertiary for ssDNA	donkey-anti-goat-Cy5.5-5	1:100	Abcam	ab6951

After all hybridizations, slides were mounted with VectaShield and stored at 4°C until imaging. The analysis was performed by automated scanning of at least 5 different areas of the slide. For each area, between 100 and 120 pictures were taken with 10% of overlap and assembled using Metamorph software to form a single image. To determine replication speed, green and red tracks were individually measured (in μm) using a ruler tool from the same software and converted to kilobases (1 μm = 2 Kb). The length of individual tracks (in kilobases) was divided by the duration of the incubations with CldU and IdU (in minutes) to discover replication speed in Kb/min. Fork asymmetry was determined by the ratio between the length of green and red tracks. A representative image of red and green tracks with measurements is shown in **Figure 11.**

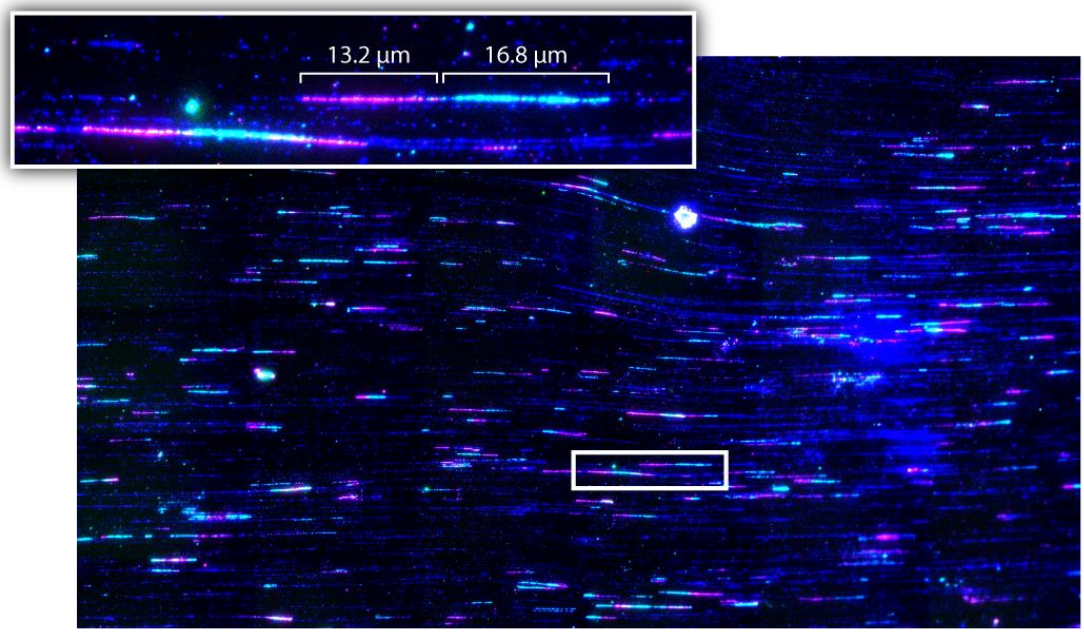

Figure 11. DNA combing analysis. Representative image of combed DNA from non-irradiated NTHY cells. The larger image is a section (~10%) of the original composition created by the combination of at least 100 photos. The smaller rectangle depicts an analyzable fiber (containing blue stained ssDNA at both ends) and the measured length of CldU and IdU tracks.

3.15. Cell cycle

Cells were plated in 6-well plates at standard density and irradiated as previously explained. In the appropriate time-point after irradiation, cells were collected by trypsinization, washed with PBS and suspended in 500 µL of PBS. Next, 2 mL of cold 100% ethanol were slowly added while vortexing to achieve a final concentration of 80% and stored at -20°C until analysis. DNA detection was performed after incubating fixed cells with IP solution (200 mg/mL DNAse-free RNase A, 20 mg/mL propidium iodide, and 0.1% Triton X-100 in PBS) for 30 minutes and then analyzed using BD Accuri™ C6 (BD Biosciences).

3.16. ChIP-qPCR

In order to perform ChIP-qPCR of cells 4 days after irradiation, cells were plated in 175cm^2 flasks at standard density and irradiated as previously described.

Exceptionally, the cells in which ChIP-qPCR was performed only 30 minutes after irradiation were plated differently ($5x10^6$ cells per $175cm^2$ flask) to avoid the use of dozens of flasks to achieve optimal cell number. At appropriate time points, cells were trypsinized, washed and counted. For each condition, around $10x10^6$ cells were cross-linked for 10 minutes in 0.37% formaldehyde solution and then the cross-link reaction was stopped by the addition of Glycine (125 mM). After washing cells twice with PBS, the nuclei of cells were isolated using hypotonic lysis buffer. Nuclei were then sonicated in Covaris® for 10 minutes at 4°C and DNA was broken down to fragments ranging from 250 to 1000 bp, but averaging 400 bp. Next, 30 μg of shredded DNA was precipitated using γH2AX antibody or IgG isotype control and magnetic beads overnight (Magna ChIP™ Protein A+G Magnetic Beads).

.

Table 6. Antibodies used in ChIP

Target	Antibody	Mass	Brand	Reference
γH2AX	mouse-anti-γH2AX (ChIP grade)	3μg	Millipore	05-636
Isotype control	mouse-IgG1 (monoclonal) – BSA and Azide-free	3μg	Abcam	ab81032

Immunoprecipitated DNA fragments were collected with a magnetic rack and washed five times with Low and High Salt Washing Buffer, LiCl Washing Buffer and 2 times with TE Buffer. Then, cells underwent crosslink reversal to detach proteins by treatment with RNAse, Proteinase K and heated at 65°C overnight. DNA was finally purified using the Active Motif's ChIP DNA Purification Kit and used in qPCR.

Table 7. Primers used in ChIP-qPCR

Target	Sequence 3'	Sequence 5'	Method
RET	GCCTTTGGGATCAGTGGACA	AAGATCCGGCATGTGTGGTT	SYBR Green
CCDC6	AAGGAAACCTGATGCCCCAC	GCCACAACACGGTAGAGGAT	SYBR Green
CCDN2	Primer Set CCND2. Activ Motif catalog reference: 71008		SYBR Green
GAPDH	Primer Set GAPDH-1. Activ Motif catalog reference: 71004		SYBR Green
FRA3B	GACCCTTCTCTTTGACCACTTCA	CCTCCCTGACTGGCATCCT	SYBR Green

3.17. BrdU-γH2AX staining

Cells were plated in 6-well plates at standard density and irradiated as previously explained. In the third day after irradiation, cells were exposed to 10μM of BrdU for 10 minutes and then collected by trypsinization and fixed with 80% ethanol and stored at -20°C for 24h. Next, fixed cells were denatured with pepsin (HCl 30 mM, Pepsin 0.5 mg/mL) for 20 minutes at 30°C followed by an incubation with HCl (2 M) for 20 minutes at room temperature. After pelleting cells and discarding the supernatant, a staining solution composed of primary antibodies against γH2AX and BrdU diluted in Dilution Buffer (FBS 0.5 %, Tween-20 0.5 % and HEPES 20 mM) was added to the pellets and incubated for 45 minutes in the dark. Next, cells were washed with PBS and secondary antibodies were added to the pellets for 30 minutes in the dark. After a final washing step, the cells were analyzed using BD Accuri™ C6 (BD Biosciences) and the mean fluorescence of γH2AX of BrdU-positive and BrdU-negative cells were compared.

Table 8. Antibodies used for BrdU-γH2AX staining

Antibody	Dilution	Brand	Reference
Rabbit-anti-γH2AX	1:4000	Abcam	ab11174
Mouse-anti-BrdU	1:50	Dako	M0744
Horse-anti-mouse-FITC	1:100	Vector Labs	FI-2001
Goat-anti-rabbit-AlexaFluor 647	1:3000	Thermo Fisher	A21244

3.18. Plasmid transfection

NTHY cells were transfected 48 hours after irradiation with 1 μg of H2B-YFP plasmid DNA in 6-well plates using X-tremGENE HP DNA transfection reagent (Roche), following the manufacturer's protocol. Differently from most experiments, in which medium was not changed until the day of analysis, when transfection was performed the culture medium was replaced by fresh medium right before transfection to minimize toxicity. Transfection efficiency was confirmed by cell-cytometry and were considered efficient when >50% of cells were YFP-positive.

3.19. Statistical analysis

Statistical analyses were carried out with Graph-Pad Prism (GraphPad Software, version 6.0c) in all data performed with 3 or more independent experiments. The statistical significance was evaluated by t test, one-way or two-way analysis of variance (ANOVA), depending on experimental design. Multi-comparison post-tests were eventually performed depending on experimental design and indicated in the figure legends. Error bars are SEM. Statistical significance was represented by the symbol * as following: *$p<0.05$, **$p<0.01$, ***$p<0.001$ and ****$p<0.0001$. Absence of symbols means no statistical significance.

4. RESULTS

Previous studies from our group suggested the existence of two distinct phenomena, an early oxidative burst immediately after irradiation and a late persistent oxidative damage related to the induction NADPH oxidase expression. To characterize the first phenomenon in our model, we quantified the H_2O_2 concentration in the medium at different time-points before and after a single dose of 5Gy. The result represented in Figure 12A shows that when NTHY cells in PBS receive a 5Gy dose of irradiation, an immediate increase in ROS is observed in the extracellular medium (PBS). However, this experiment does not clarify whether this increase is due to a cellular response to the irradiation or simply the radiolysis of water. Thus, we repeated the same experiment in the absence of cells. Identical plates containing nothing but PBS were irradiated and the same increase is observed, endorsing that the early oxidative burst observed after irradiation is virtually entirely due to water radiolysis. However, while in cell-free wells the H_2O_2 concentrations remains constantly high, the concentration in cell-containing wells the H_2O_2 rapidly decreases reaching control levels within 45 minutes, probably due to detoxification by antioxidants secreted by the cells, the oxidation of cells themselves and by the cell entry of extracellular ROS.

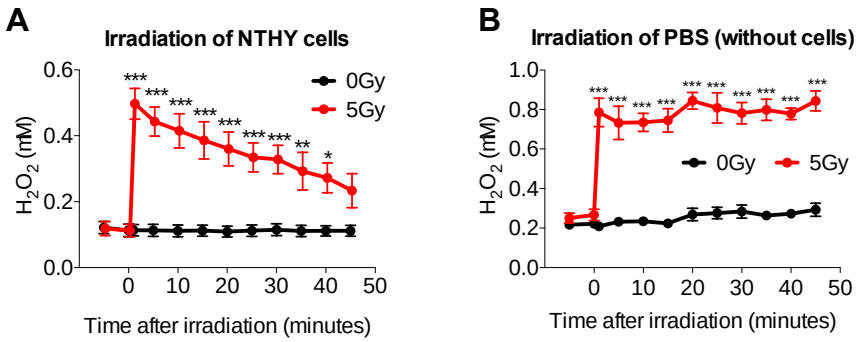

Figure 12. Early effects of irradiation. A) Monitoring of extracellular H_2O_2 concentration in plates with irradiated and non-irradiated NTHY cells in PBS. B) Monitoring of extracellular H_2O_2 concentration in wells containing nothing but PBS, confirming the water radiolysis. Graphs represent the mean of 4 independent experiments, each conducted with 2 technical replicates. Statistical analysis performed by 2-way ANOVA. *p<0.05, **p<0.01, ***p<0.001.

Irradiation is also known to elicit long-term effects on irradiated cells. To investigate that, we analyzed ROS levels in different cell compartments and by 3

different methods. Extracellular ROS production, was measured by the accumulation of oxidized probes in the extracellular medium, what is usually considered as a marker of NADPH Oxidase enzymes activities, since the catalytic site of these enzymes face the extracellular space. As seen in Figure 13A, extracellular ROS production increases in a time-dependent fashion after irradiation. Note that this experiment is essentially different from the one depicted in Figure 12A, although the same probe was used (more details can be found in the section *Materials and Methods*). Similarly, intracellular ROS levels were measured (Figure 13B) and a very similar pattern was observed. The detection of ROS, mainly superoxide anions, by mitochondria using the MitoSOX probe (Figure 13C) also revealed a time-dependent increase, but differently from the 2 other methods, mitochondrial ROS was the only to present a mild, but statistically significant, response in 30 minutes after irradiation. This further confirms that the early oxidative burst relates to water radiolysis and not a cellular adaptation. As described in a previous work (AMEZIANE-EL-HASSANI *et al.*, 2015), NADPH Oxidase DUOX1 has been identified as an important source of ROS after irradiation. Our results (Figure 13D) confirm this finding as we observe a time-dependent increase in DUOX1 mRNA expression while NOX4, another NADPH Oxidase expressed in the thyroid, is not modulated.

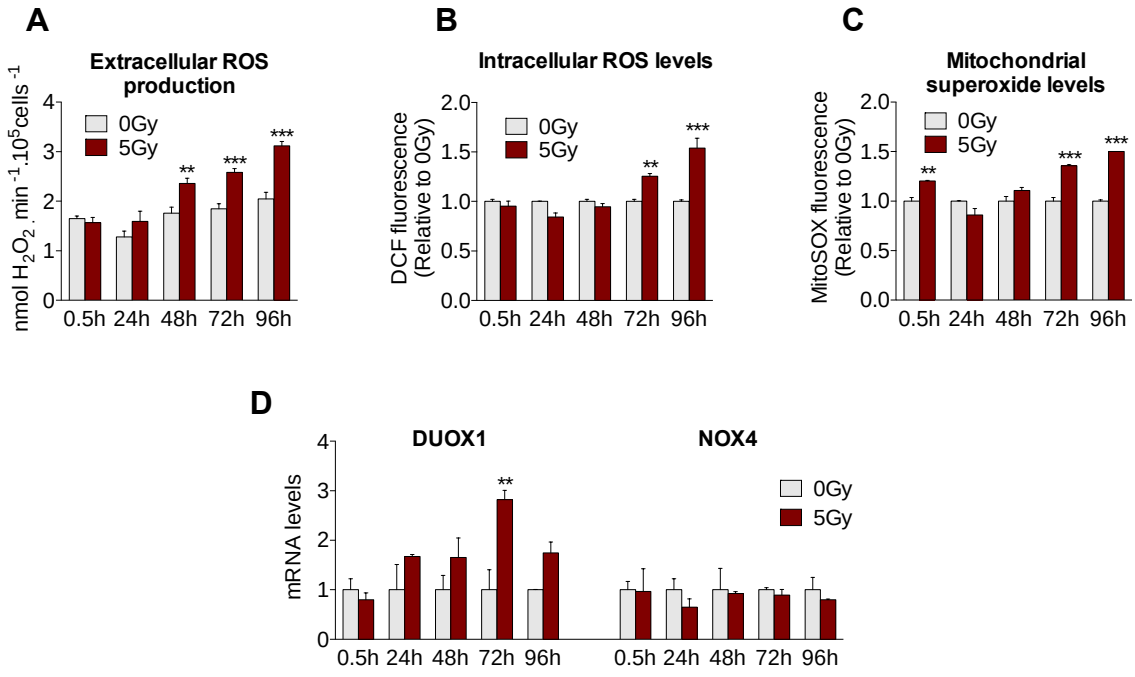

Figure 13. Time course of ROS production following irradiation of NTHY cells. Several probes were used to detect ROS production in live NTHY cells at different time periods after irradiation. A) Extracellular H_2O_2 production measured by AmplexRed/HRP assay. B) Intracellular ROS levels

measured with the probe H_2DCFDA. C) Mitochondrial superoxide ($O2^{\bullet-}$) levels detected by MitoSOX. D) mRNA levels of the NADPH Oxidases DUOX1 and NOX4 in NTHY cells measured by qPCR. Graphs represent the mean of 3 (Figure 13A) or 2 (Figures B, C and D) independent experiments, each conducted with at least 3 technical replicates. Statistical analysis performed by 2-way ANOVA. *p<0.05, **p<0.01, ***p<0.001.

After characterizing two distinct peaks of oxidative stress, we decided to explore the consequences of these phenomena to DNA damage. Thus, we performed a time-course analysis of the double strand breaks (DSB) marker γH2AX by Western Blotting at several time points before and after irradiation and observed a 2-wave pattern (Figure 14A). First, we observe a sharp increase of γH2AX that disappears within the first 24 h, and later it starts to increase again, resulting in a pattern that perfectly correlates with the two distinct waves of oxidative stress showed in Figures 12 and 13. Moreover, we analyzed the occurrence of oxidative damage by the presence of the most common oxidative DNA lesion, 7,8-dihydro-8-oxo-guanine (8-oxo-G). As shown in Figure 14B, an increase trend in 8-oxo-G is only observed several days after irradiation. Although ROS and DSB are present both at 30 min and 72 h after irradiation, oxidative DNA damage is only seen in the later, suggesting that the nature of these two phenomena may be completely distinct.

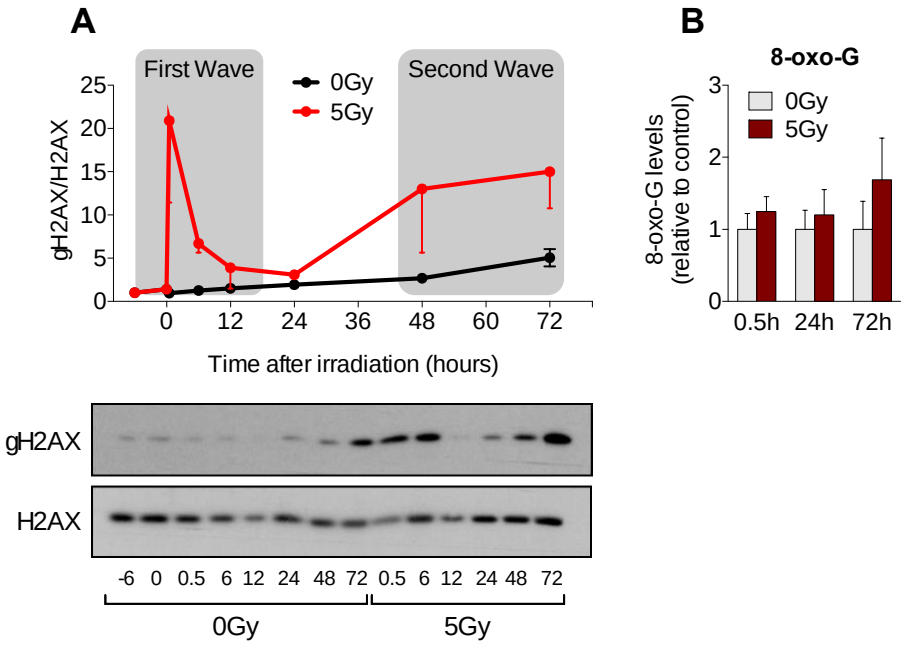

Figure 14. DNA damage in the days following irradiation. A) Western Blotting detection of double-stranded DNA breaks by H2AX (γ)phosphorylation. Numbers shown in Y axis are the relative ratio between γH2AX and total-H2AX in relation to the time point -6 hours (-6 h = 1). Graph A represents the mean of 2 independent experiments. B) Oxidative DNA damage was assessed by the detection of the

most common oxidative DNA lesion, 7,8-dihydro-8-oxo-guanine (8-oxo-G). Graph 14B represents the mean of 2 independent experiments comprising 5 technical replicates. Statistical analysis was performed in 14B by 2-way ANOVA. Absence of symbols indicates no statistical significance.

The sharp increase in γH2AX in the first 30 minutes after irradiation shown in Figure 14A was assumed to be related to irradiation itself but also to ROS derived from water radiolysis. To test this theory, we conducted an experiment in which, besides irradiated and non-irradiated NTHY cells, we analyzed the presence of γH2AX in non-irradiated cells that were incubated during 30 minutes with irradiated medium. A summarized protocol is shown in Figure 15A. The results reveal that the incubation of non-irradiated cells with irradiated medium (rich in ROS, as shown in Figure 12) was not capable of inducing DNA damage (Figure 15B). It is important to note that the conducted experiments only consider the role of extracellular water radiolysis and do not exclude the possibility of water radiolysis in the intracellular compartments. However, although the addition of exogenous H_2O_2 in cell cultures undeniably induces DNA damage, we show that the amount of ROS produced by radiolysis of the extracellular medium in our model is not enough to enter cell nuclei and damage DNA.

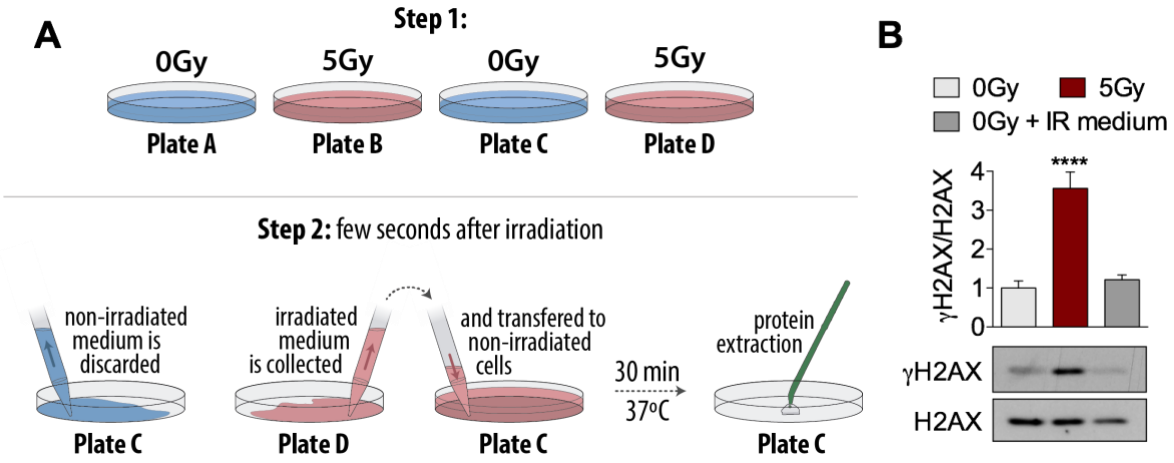

Figure 15. The role of water radiolysis in DNA damage. A) Brief representation of the protocol used in this analysis. B) Western Blotting detection of γH2AX 30 minutes after irradiation. Samples consist of non-irradiated cells (first lane), irradiated cells (second lane) and non-irradiated cells that received irradiated medium for 30 minutes (third lane). Numbers shown in Y axis are the relative ratio between γH2AX and total-H2AX in relation to the group 0Gy. Graph represents the mean of 2 independent experiments conducted each with 3 technical replicates. Statistical analysis performed by one-way ANOVA followed by Bonferroni's multiple comparisons test. ****p< 0.0001.

A second approach has been used to find evidences of oxidative damage in the nuclei of cells 72h after irradiation. The modified histone H2B with a coupled YFP tag can be transfected in NTHY cells and serves as a nucleus-specific oxidation sensor. As shown in Figure 16A, redox-western-blotting analysis indicates that irradiation increases the oxidized portion of H2B in a dose-dependent manner. A similar effect was observed after incubation of cells with low doses of H_2O_2 (100 μM) for 1 hour before extraction. The treatment of irradiated cells with catalase showed little or no effect on H2B oxidation. However, as seen in more detail in Figure 16B, even the reduced form of H2B protein is highly modulated by irradiation. This modulation occurs in a very specific fashion, since transfected GFP protein levels are unchanged. Of note, this experiment analyzes only transfected and not endogenous H2B since we detect it by anti-YFP antibody. Although the results suggest the presence of an oxidative environment in the nucleus of irradiated cells, the unexpected irradiation-related modulation of H2B indicates that this may be an inappropriate experimental protocol to investigate this issue.

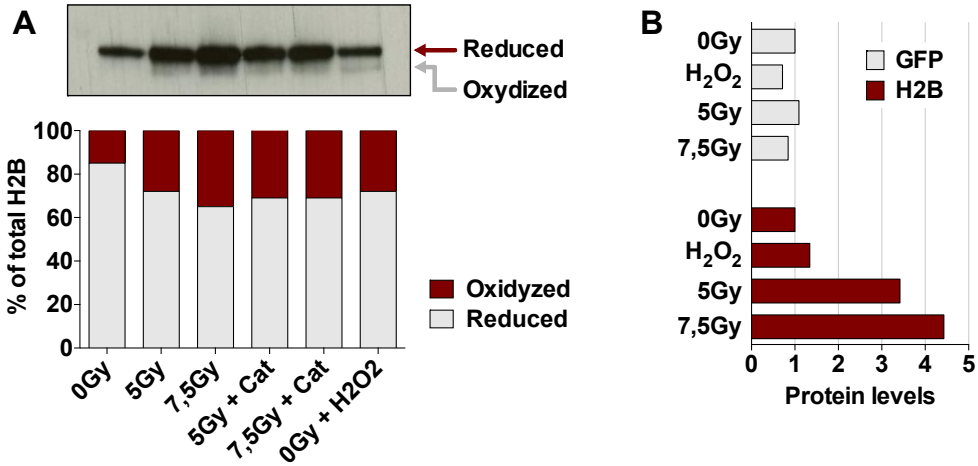

Figure 16. Evidence of oxidative damage in the nucleus. A) Western Blotting analysis of transfected histone H2B-YFP oxidation in native cell lysates of NTHY cells 72h after irradiation and after treatment with Catalase (250 U/mL for the last 4h) or H_2O_2 (100 μM for the last 1h). B) Protein expression of the reduced form of H2B-YFP and GFP (intern control) showing that transfected H2B-YFP is highly induced after irradiation. Graphs represent the mean of 3 (Figure 16A) or 1 (Figure 16B) independent experiments.

In order to address the possible existence of replicative stress in NTHY cells after irradiation, we first analyzed parameters of cell replication and its relationship with

DNA damage. Propidium Iodide (IP)-based cell cycle analysis revealed that 5 Gy irradiation exerts only mild effects on cell proliferation. After a significant cell cycle arrest in G2/M observed 12h after irradiation, the cells seem to recover at 24 and 48h. Finally, at 72h a significant effect is again observed; the proportion of G0/G1 cells slightly decreases concomitantly with an increase of aneuploidy (Figure 17A). The analysis of cell cycle through IP and BrdU coupled analysis was attempted but due to the high rate of aneuploidy of NTHY cells, it was impossible to discriminate between 4n diploid and 2n tetraploid cell populations, thus, proper analysis was not possible. To further investigate whether the irradiated cells are still proliferative and thus subjected to the possible effects that a replicative stress could induce, we analyzed the presence of DNA damage, measured by the presence of γH2AX, in the proliferative (BrdU-positive) and non-proliferative (BrdU-negative) fractions of the whole cell population in irradiated and control cells. As shown in Figure 17B, proliferative and non-proliferative irradiated cells possess similar increased levels of γH2AX, confirming that the irradiated (and damaged) cells did not stop cycling. The analysis of the proportion of BrdU-positive in whole population also indicates that the dose of radiation used (5 Gy) does not trigger drastic effects on cell replication in NTHY cells (Figure 17C). Lastly, concomitant analysis of cell cycle and γH2AX shows a consistent increase in γH2AX fluorescence in all phases of the cell cycle (Figure 17D).

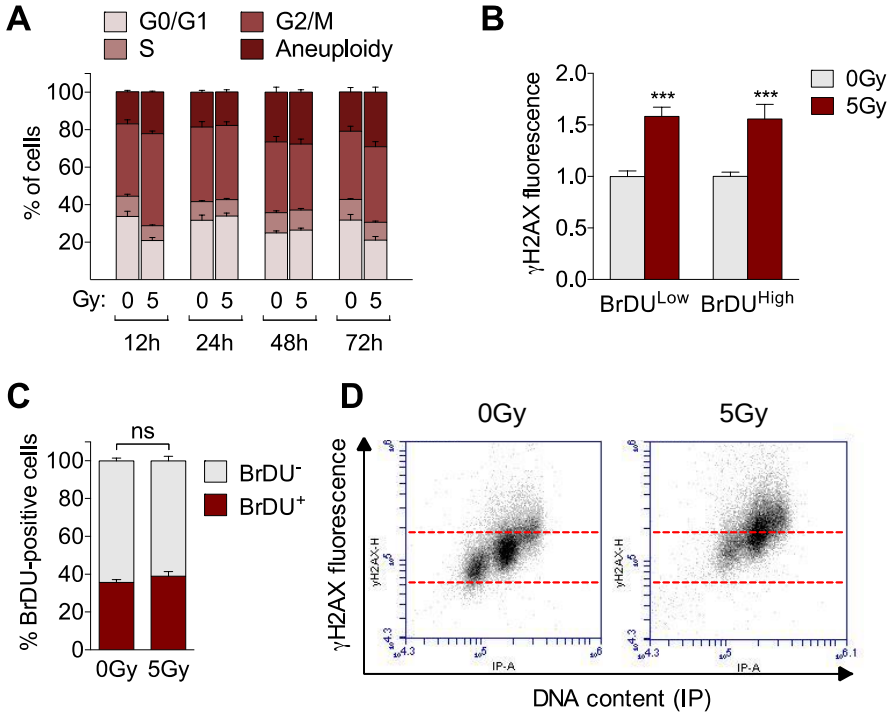

Figure 17. Cell cycle and proliferation status of irradiated NTHY cells. A) Cell cycle analysis of irradiated cells using iodide propidium. At 24h, statistical significance (***) was observed in G0/G1 and G2/M. At 72h, statistical significance (**) was observed only in G0/G1. B) Detection of DNA damage (γH2AX) in proliferative (BrdU^{positive}) and non-proliferative (BrdU^{negative}) cells by flow cytometry. C) Quantification of the proportion of proliferative cells in the whole population by BrdU incorporation. D) Representative experiment of γH2AX and IP coupled analysis revealing that DNA damage is present in cells across all cell phases. Graphs represent the mean of 3 (Figures 17A, B and C) or 2 (D) independent experiments conducted with at least 3 technical replicates each. Statistical analysis performed by 2-way ANOVA. *p<0.05, **p<0.01, ***p<0.001.

To evaluate if the irradiation causes a replicative stress in NTHY cells, we analyzed several molecular markers of this phenomenon. The analysis of Chk1 phosphorylation (Ser345) in whole-cell extracts by Western blotting revealed a pattern similar to the “2 waves profile” observed in γH2AX (Figure 18A). This activation was accompanied by ATR and ATM phosphorylation in chromatin-enriched fractions of NTHY cells 72h after irradiation, an effect that was partially reversed by short-duration (4h) treatment with low doses of the antioxidant catalase and the flavoprotein inhibitor DPI (Figure 18B).

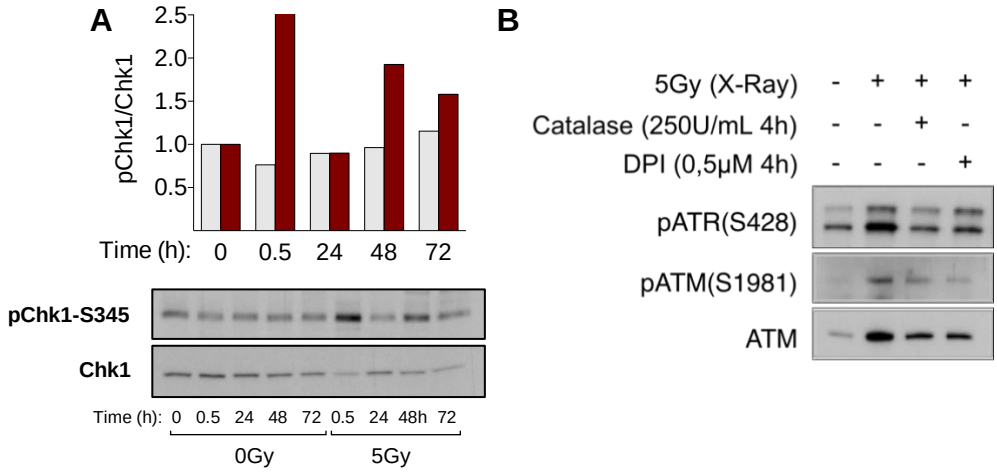

Figure 18. Evaluation of proteins associated with replication stress through Western Blotting. A) Protein levels of pChk1-Ser345 evaluated by Western Blotting using whole-cell extracts of NTHY cells. B) Protein levels of pATR, pATM and total ATM in chromatin-enriched fractions of NTHY cells measured by Western Blotting. Graph A represents one experiment and B depicts a representative image of 2 independent experiments.

Further analysis of replicative stress markers was performed by immunofluorescence. The presence of single-stranded DNA (Ser33-pRPA32), double-stranded DNA breaks (γH2AX) and fragile site expression (FANCD2) were analyzed in NTHY cells 72h after irradiation with or without antioxidant treatment in the last 4h. Results show a great increase in merged foci of γH2AX/pRPA after irradiation and a partial reversion by antioxidants. The presence of pRPA in double-strand breaks may suggest a replicative stress-related damage, since the pRPA coating of single strands is a known hallmark of the typical stalled replication forks observed under replicative stress conditions. The partial reversion of this phenomenon by antioxidants suggests a role for reactive oxygen species in this scenario (Figure 19A). Likewise, the increase observed in merged foci between γH2AX and FANCD2, a protein known to translocate to fragile sites under genotoxic stress (TÉCHER *et al.*, 2017), suggests that the 5Gy irradiation of NTHY cells are indeed promoting the DNA damage in fragile sites (Figure 19B). Morphological analysis of the nucleus of irradiated cells also depict classical features of genomic instability, such as the presence of micronuclei (Figure 19C) and severe nuclear deformation (Figure 19D).

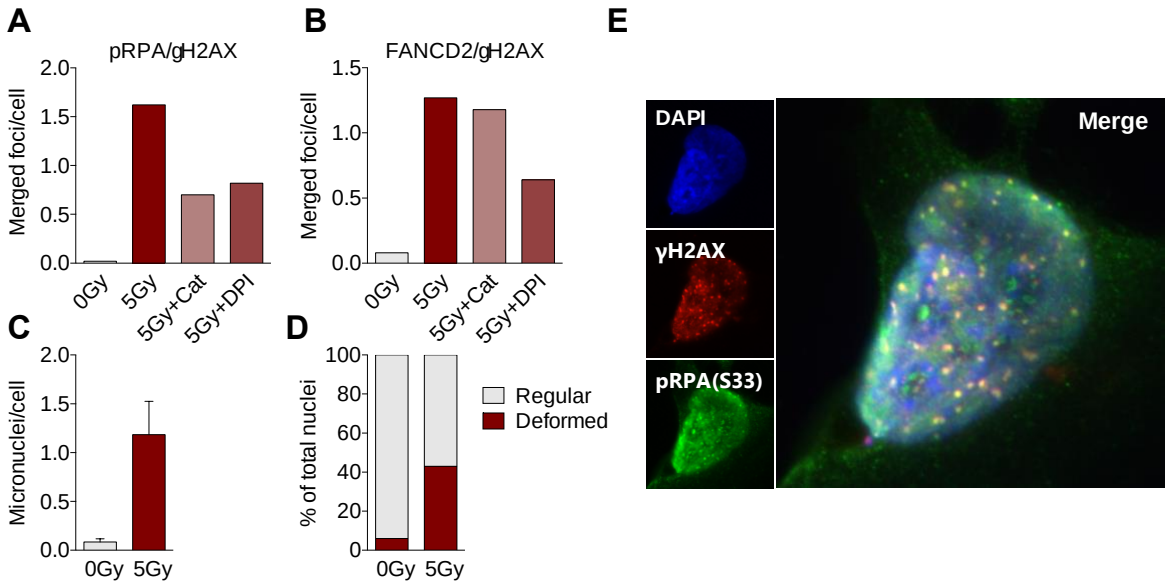

Figure 19. Evaluation of proteins associated with replication stress through immunofluorescence 72 hours after irradiation. A) Quantification of immunofluorescence analysis of γH2AX/pRPA merged foci. B) Quantification of immunofluorescence analysis of γH2AX/FANCD2 merged foci. C) Quantification of relative number of micronuclei per nucleus. D) Circularity evaluation of nuclei. E) Representative image of γH2AX/pRPA foci in irradiated cell. Graphs represent the mean of 2 independent experiments, in which at least 100 cells were analyzed.

Afterwards, we continued to investigate the molecular features of replicative stress in irradiated NTHY cells. Unsynchronized replication is a major cause of genetic instability since the presence of under replicated DNA during the onset of mitosis will frequently produce gaps and breaks. Thus, we performed *DNA combing* to investigate replicative dynamics, more specifically replication speed and fork asymmetry. In this preliminary result, we observed that 5 Gy irradiation provoked a slight decrease (-20%) in replication speed 72h after irradiation. Interestingly, that was reversed by the treatment with low doses (0.5 μM) of the antioxidant DPI (Figure 20A). The analysis of fork asymmetry, a measure of the presence of obstacles to fork progression using the ratio of CldU and IdU track lengths, did not show any alteration (Figure 20B).

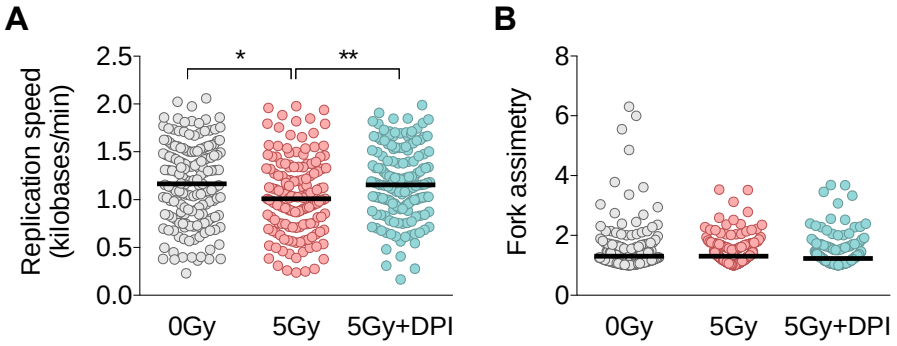

Figure 20. DNA combing of NTHY cells 72h after irradiation. A) Replication speed of irradiated cells is reduced but can be reversed by low doses (0.5 μM) of the antioxidant DPI. B) Fork asymmetry is calculated by the ratio between CldU and IdU tracks to evidence obstacles to fork progression. Irradiated NTHY cells did not present any alteration in fork asymmetry, although basal levels are considered very high. Graphs represent one experiment in which at least 120 fibers were analyzed.

Alongside protein markers, several other cellular features are used to evaluate replicative stress. The pool of nucleotides in a cell is considered a key-factor for proper and error-free replication. Unbalanced amounts of free nucleotides are known to be a cause of replicative stress in several models. To address this question, we performed acetonitrile-based extractions in NTHY cells at different time points after irradiation and analyzed dATP, dGTP, dCTP, TTP and ATP by mass-spectrometry. The results show that a consistent increase is observed in all nucleotides over time after irradiation (Figure 21).

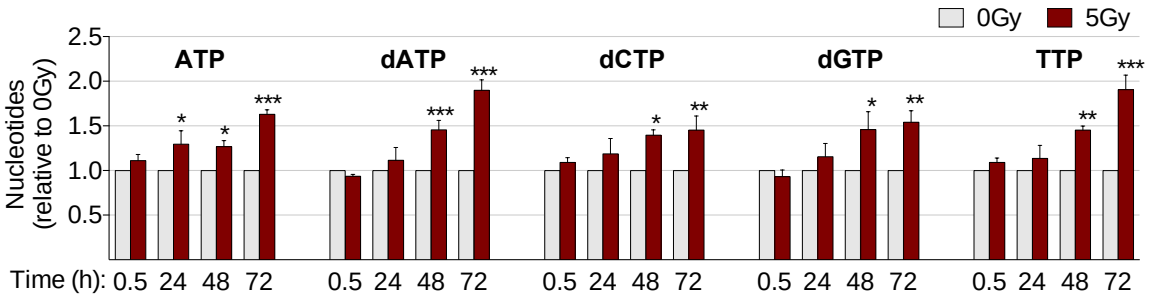

Figure 21. Time course of cellular nucleotides pool after NTHY irradiation. Intracellular nucleotides (dGTP, dATP, dCTP, TTP and ATP) concentration of NTHY cells measured by mass spectrometry after acetonitrile-based extraction at different time points post-irradiation. Graphs represent the mean of 5 independent experiments. Statistical analysis performed by 2-way ANOVA. *p<0.05, **p<0.01, ***p<0.001.

It’s well known that both paucity and overload of nucleotides are detrimental to genome integrity and may lead to increased mutagenesis. Thus, the dNTP pool increase observed after irradiation can contribute to genomic instability. Importantly, the increase in ATP concentrations was a very interesting observation that could be a link between irradiation and molecular pathways with direct influence on ROS and NADPH Oxidases. First, a study revealed that DUOX1 can be activated by extracellular ATP (BOOTS *et al.*, 2009). Second, a recent paper has described that irradiated cells increase their ATP production in a mechanism mediated by CDK1 with direct implications in DNA repair and genome integrity (QIN *et al.*, 2015).

Following this hypothesis, we tested whether ATP could stimulate ROS production in NTHY cells and also the role of CDK1. As seen in Figure 22A and B, neither the addition of exogenous ATP nor the removal of ATP by the ATP-consuming enzyme Apyrase exerted any effect on H_2O_2 generation. Likewise, the treatment of cells with the CDK1 inhibitor RO3306 did not change radio-induced ROS production, even though it exerts a stimulatory effect in non-irradiated cells. We also investigated the inactivation of CDK1 and the activation of its activator, cdc25a, by Western Blotting at several time-points after irradiation and did not observe any effect. As seen in Figure 22E, the mitosis marker pH3 was also not changed after irradiation. Although coherent with our model, this molecular pathway does not seem to be involved in thyroid DNA damage response.

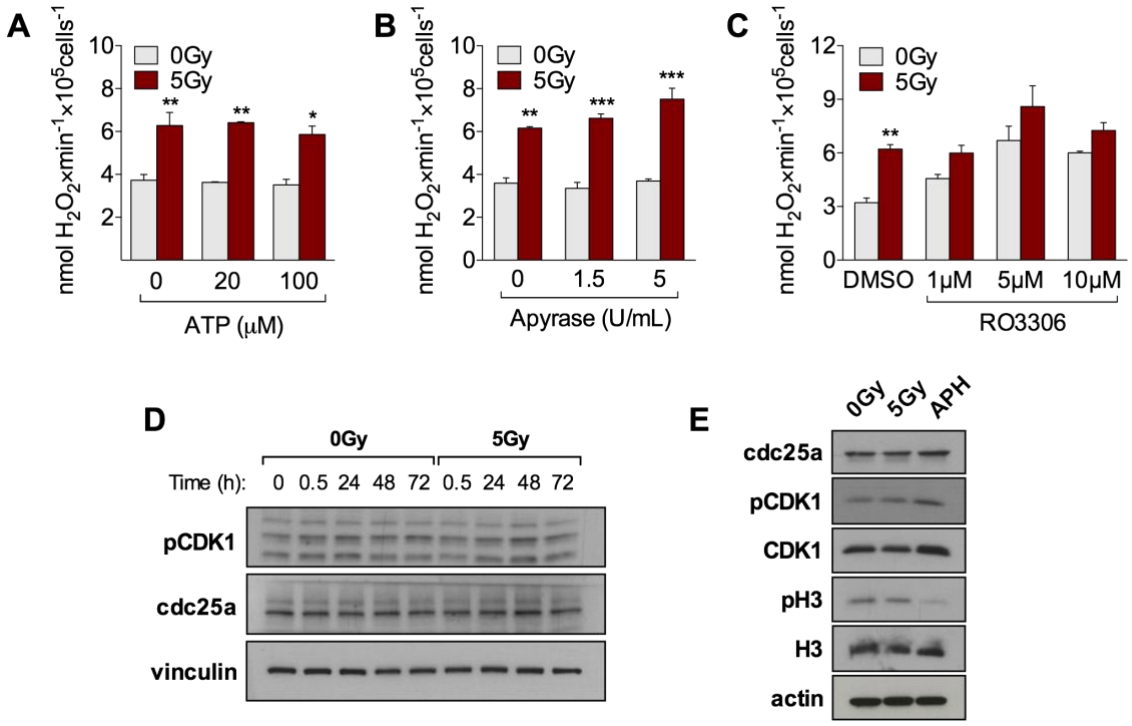

Figure 22. Role of CDK1 and ATP in radio-induced ROS production. A) Irradiated (72 h) and non-irradiated NTHY cells were pre-incubated for 1h with exogenous ATP and then analyzed by AmplexRed/HRP still in the presence of ATP. B) Irradiated (72 h) and non-irradiated NTHY cells were treated with the ATP-consuming enzyme Apyrase for 2h. C) Irradiated (72 h) and non-irradiate NTHY cells were treated for 20h with different concentrations of the CDK1 inhibitor RO3360. D) Protein expression of CDK1 and CDC25a by Western Blotting at different time points after irradiation (n = 2). E) Protein expression of proteins involved in CDK1-pathway 72 hours after irradiation or after treatment with 0.4 μM of aphidicolin (APH) for 24h. Graphs 22A, B and C represent the mean of 3 independent experiments conducted with at least 2 technical replicates each. Statistical analysis performed by 2-way ANOVA followed by Sidak's multiple comparisons test. *p<0.05, **p<0.01, ***p<0.001. Graphs 22D and E portray representative images of one experiment each.

Preliminary analysis of our results suggests that irradiation is indeed capable of causing a mild replicative stress condition in NTHY cells. Importantly, it is worth noticing that, regarding replicative stress features, the effects observed after irradiation in our model are not as intense as those observed in the literature by authors using genotoxic drugs to cause a severe replicative stress. Indeed, analysis of ROS production (Figure 23A) and DUOX1/2 mRNA expression (Figure 23B) in NTHY cells treated with those drugs produce extremely different effects from those observed after irradiation. This discrepancy suggests that the use of genotoxic drugs to study fragile sites expression and replication dynamics is a very useful tool but does not reflect physiological conditions and thus requires careful interpretation.

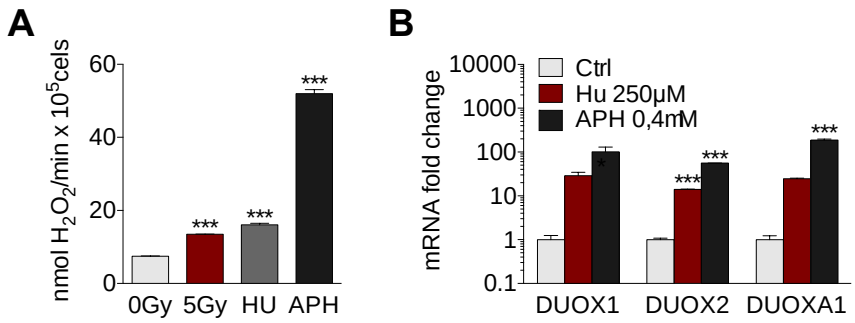

Figure 23. Pharmacological induction of replication stress stimulates oxidative stress. A) Extracellular ROS production measured by AmplexRed/HRP in NTHY cells 4 days after irradiation or after a 4-day treatment with the genotoxic drugs aphidicolin (APH) (0.4 μM) or hydroxyl-urea (HU) (250 μM). B) mRNA analysis by qPCR of *DUOX1*, *DUOX2* and *DUOXA1* genes in the exact same conditions (log scale). Graph represents the mean of 3 biological replicates. Statistical analysis were performed by ordinary one-way ANOVA in (A) and two-way ANOVA followed by Tukey's multiple comparisons test in (B). *p<0.05, **p<0.01, ***p<0.001.

Finally, we aimed to understand whether the DNA breaks that lead to RET/PTC1 formation happen shortly after irradiation (in the first wave of ROS) or several days after irradiation (second wave). To do so, we irradiated NTHY cells and conducted chromatin extraction 30 minutes after irradiation or 4 days after irradiation (96 h). Then, we performed ChIP analysis using γH2AX antibody, in an attempt to identify which genes present double-strand breaks, a mandatory step for gene inversion. We ran qPCR for *RET* and *CCDC6*, partners in RET/PTC1 translocation, *FRA3B*, one of the most active common fragile site in the genome, and two endogenous genes with no known relation to genomic instability, *GAPDH* and *CCDN2*. As shown in Figure 24, all genes seem to break 30 minutes after irradiation, consistent with the stochastic nature of irradiation. However, at 96h, *RET* (and possibly *CCDC6*) still present γH2AX while neither *FRA3B* or *GAPDH* do so. These results suggest that DNA breaks in these genes either persist after the first wave of lesions or arise only days after irradiation. However, due to the enormous variability inherent to this method, more experiments are needed to confirm these results.

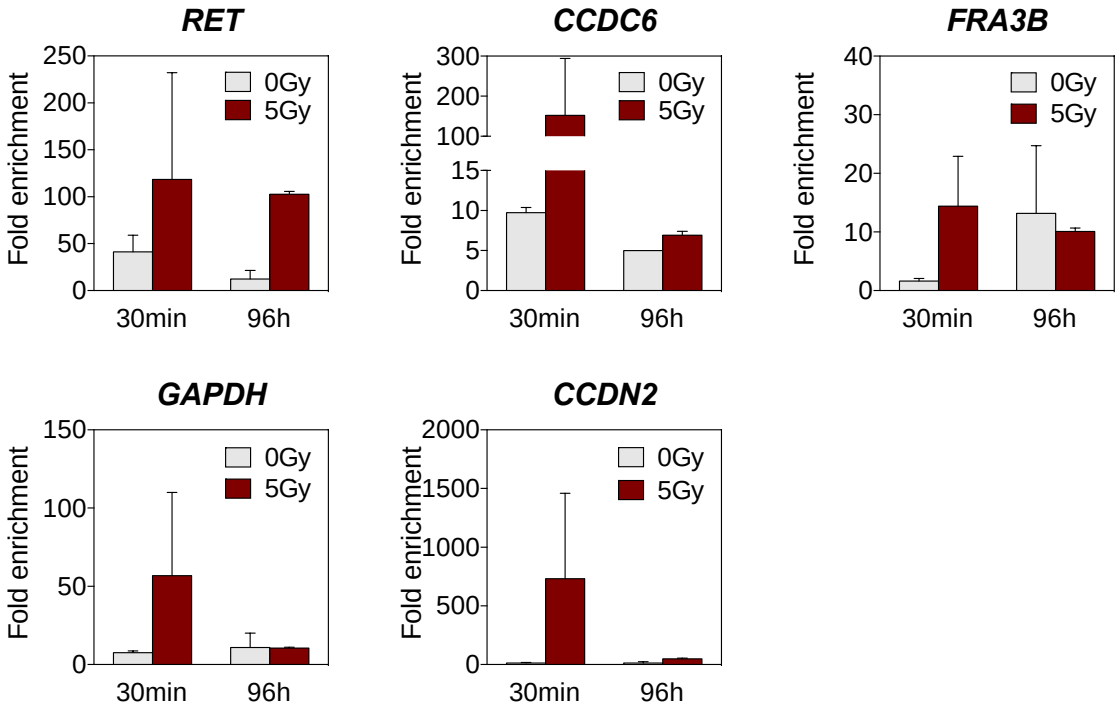

Figure 24. ChIP-qPCR analysis of genes involved in RET/PTC1 translocation and controls. Immunoprecipitation of γH2AX-bound DNA fragments revealed which genes present double-stranded DNA breaks. Chromatin was extracted 30 minutes or 4 days after the irradiation. *RET* and *CCDC6* are the two genes involved in RET/PTC1 translocation. *FRA3B*, a common fragile site, *GAPDH* and *CCDN2* were used as intern controls Data represents the mean of 4 biological replicates from 2 independent experiments. Statistical analysis performed by 2-way ANOVA.

5. DISCUSSION

Since the discovery of RET/PTC1 by Grieco in 1990, significant advances have been achieved in understanding the role of radiation in thyroid cancer incidence and the clinical features of RET/PTC tumors. However, evidence of the molecular mechanisms governing *RET* breakage still lack, making the comprehension of this cancer's etiology still very elusive. Progress has been made by a few groups that reported the induction of breaks in RET/PTC-related genes upon pharmacological inhibition of replication (GANDHI *et al.*, 2010) and the characterization of the unusual gene separation in thyroid interphase nuclei (NIKIFOROVA, 2000). More recently, our group has published papers that also indicates a crucial role for reactive oxygen species in RET/PTC formation (AMEZIANE-EL-HASSANI *et al.*, 2010, 2015). Thus, the aim of this work was to investigate the formation of RET/PTC1 translocation in the context of replicative stress and dissect its possible relation with oxidative stress in radio-induced thyroid cancer.

Our investigation starts by a characterization of the so-called first wave of oxidative stress induced upon cellular radiation exposure. As expected, irradiation efficiently induced water radiolysis, generating a substantial amount of H_2O_2 that rapidly disappears as its reacts with both surface and intracellular organic matter of cells. This experiment supports previous reports from our group that revealed an important role of irradiation-derived reactive oxygen species in RET/PTC1 formation. In the mentioned work, cells were irradiated with a single 10 Gy dose of X-Rays and RET/PTC1 translocation was detected by nested-PCR 15 days after the irradiation event. Interestingly, when irradiation was conducted in the presence of the extracellular antioxidant enzyme catalase, RET/PTC formation was almost entirely abrogated. Moreover, the study also shows that the treatment of non-irradiated cells with H_2O_2 mimics the effects of irradiation, as the induction of RET/PTC translocations was also detected after 15 days in a similar extent to those observed in irradiated cells (AMEZIANE-EL-HASSANI *et al.*, 2010). Thus, the authors hypothesized that irradiation-derived extracellular ROS could be responsible for the DNA damage that causes RET/PTC1 *in vitro*.

Another study from the same group revealed that the secretion of several cytokines, such as interleukin 1α (IL-1α), interleukin 1β (IL-1β), interleukin 6 (IL-6) and interleukin 13 (IL-13), occur a few days after irradiation. IL-13 is a well-known positive regulator of NADPH Oxidase DUOX1 expression in a variety of models, such as the respiratory epithelial cells (HARPER *et al.*, 2005) and keratinocytes (HIRAKAWA *et al.*, 2011). Accordingly, Ameziane El-Hasani (2015) showed that IL-13 increases ROS production of thyrocytes in a pP38-dependent manner and leads to a persistent oxidative environment some days after irradiation (i.e., the second wave of oxidative stress) that ultimately results in DNA damage. Corroborating these previous findings, after 5Gy irradiation we also observed the late onset upregulation of DUOX1 mRNA and a consistent oxidative stress, as shown by the augmented extracellular, intracellular and mitochondrial ROS productions.

Thus, our model consists of two events that are temporally separated from each other by some days. While the first wave of oxidative stress lasts no longer than one hour, the second wave of oxidative stress appears only after 48 hours. As the presence of RET/PTC1 in these previous works was evaluated only 15 days after irradiation for technical reasons, it is impossible to determine whether the DNA damage-causing event happened in the first wave or in the second wave of oxidative stress.

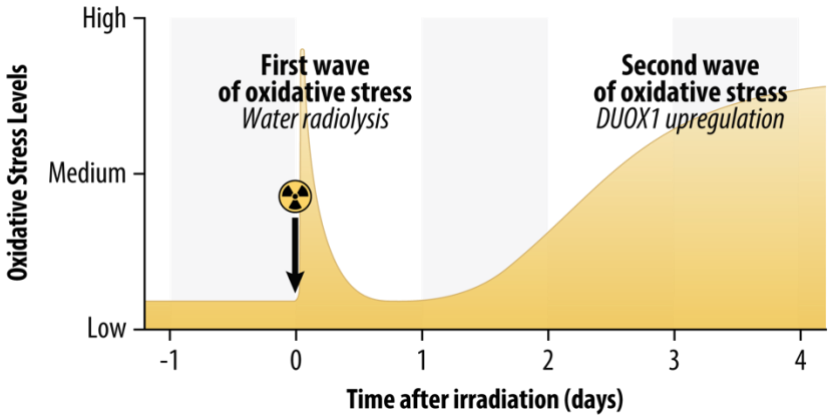

Figure 25. Oxidative stress response after cellular irradiation. X-Ray irradiation of thyroid cells elicit two temporally separated phenomena: first, an oxidative burst mediated by water radiolysis, and, second, a persistent oxidative stress mediated by DUOX1 upregulation through IL-13 pathway. Radioactivity symbol represents the moment of irradiation.

In an attempt to clarify this issue, we performed a very simple experiment that is shown in Figure 15. In this experiment, we transferred irradiated medium (containing H_2O_2 from water radiolysis) to non-irradiated cells, incubated for 30 minutes and immediately performed protein extraction. Analysis revealed that 30 minutes of exposition to the amount of H_2O_2 produced by water radiolysis is not enough to induce DNA damage. As said, previous work revealed that treatment of cells with exogenous H_2O_2 induced RET/PTC while irradiation in the presence of catalase, a H_2O_2-consuming enzyme that is unable to cross the plasma membrane, protected cells from RET/PTC formation, suggesting that extracellular ROS could be the cause of damage. However, the absence of DNA damage in our experiment challenges this assumption. Moreover, it was demonstrated that the treatment of non-irradiated cells with H_2O_2 upregulates DUOX1 after a few days (i.e., triggers the second wave of oxidative stress), an effect also abrogated by catalase (AMEZIANE-EL-HASSANI *et al.*, 2015). Thus, in the light of these findings, it seems that the real role of the first wave of oxidative stress after irradiation (i.e., water radiolysis) is to trigger the molecular mechanisms involved in the onset of the second wave of replicative stress, and that second wave would probably be directly implicated in RET/PTC formation.

The delayed but persistent oxidative stress observed *in vitro* may help us understand another important feature of radio-induced thyroid cancers; its long latency time. As discussed, the first reports of thyroid tumors from Chernobyl begun to appear just a few years after the accident. However, Chernobyl-related cancers continued to appear in the exposed population for decades and, interestingly, their molecular profiles seem to have changed over time. In the first years following the accident, reports showed a clear predominance of RET/PTC3-positive tumors. Over time, the proportion of tumors with a *RET* rearrangement dropped, but in the *RET*-positive tumors the proportion with RET/PTC1 has increased while the proportion RET/PTC3 has declined (RABES *et al.*, 2000). These shifts have been comprehensively reviewed by Dillwyn Williams (WILLIAMS, 2008b), who proposed the model depicted in Figure 26.

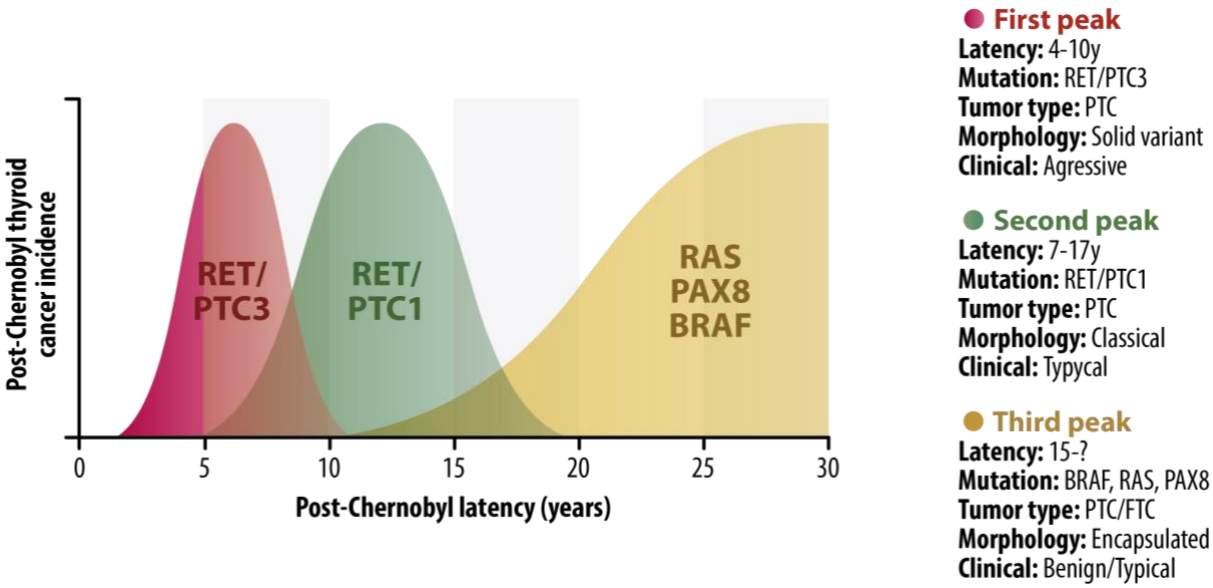

Figure 26. Hypothetical model for the molecular profile shift of thyroid tumors after the Chernobyl accident over time. Few years after the accident, RET/PTC3 was the predominant translocation found in these radio-induced thyroid tumors. As longer latency tumors were unveiled, the proportion of RET/PTC1 translocations rose while RET/PTC3 declined. Nowadays, other abnormalities are more prevalent. Adapted from Williams D, 2008.

The distinct latency of RET/PTC tumors allow us to draw hypothesis about its etiology. As demonstrated by *in vitro* studies, the RET/PTC3 translocation delivers a significantly higher mitogenic signal than RET/PTC1 (BASOLO *et al.*, 2002), possibly explaining why RET/PTC3 tumors presented such a rapid onset after the Chernobyl accident. Conversely, it is possible to hypothesize that the longer latency of RET/PTC1 tumors may be consistent with a potential replication-related origin. As thyrocytes have an extremely slow proliferation rate, several years would be needed for ROS-related replication defects to be clinically evidenced. The hypothesis that a persistent oxidative and replicative stress could be implicated in long latency thyroid tumors is supported by the previous report showing that DUOX1 mRNA is increased in a cohort of 20 patients bearing radio-induced thyroid tumors (not only PTCs) with median latency of 17 years (AMEZIANE-EL-HASSANI *et al.*, 2015). Still, these hypothesis do not help explaining the etiology of even longer latency tumors lacking *RET* translocations. It is tempting to speculate that apart from the oxidative stress generated by DUOX1, other factors might interact and predispose the occurrence of one mutation or the other, as time passes.

Recently, a controversial paper estimated the influence of *hereditary*, *environmental* and *replicative* factors in the etiology of several cancer types and concluded that, overall, replicative factors would be responsible for up to 66% of all cancers. These so-called replicative mutations are referred to as unavoidable, inherent to the tissue physiology, and could help explain the natural difference in the incidence among different tumors. More specifically, while replication errors would be responsible for only 33% of lung cancers, it would represent 98% of thyroid cancers (TOMASETTI; LI; VOGELSTEIN, 2017).

A relevant fact that places replication stress as an important player in thyroid cancer etiology has been observed in patients with *Werner Syndrome*, an autosomal recessive progeroid disorder associated with a greater susceptibility to a few cancers, most notably thyroid cancer (LAUPER et al., 2013). *WRN* encodes a nuclear protein with helicase and exonuclease activity involved in DSB repair and genomic stability (PIRZIO et al., 2008). In our model, a preliminary experiment showed that silencing *WRN* in NTHY cells using siRNA induces DNA damage and magnifies the DNA damage caused by irradiation and the genotoxic agent HU (data not shown). Yet, the significance of *WRN* defects in thyroid replication stress is not fully understood.

Evidently, replicative stress only arises in proliferative cells. Thus, using IP-based cell cycle and BrdU incorporation, we have confirmed that cells remain proliferative even 72 hours after a single 5 Gy dose of X-ray. However, also at this time point, several protein hallmarks of replicative stress were present and, interestingly, their presence was partially counteracted by antioxidants, suggesting a role for ROS in the establishment of a replication stress. Moreover, we observed important morphological repercussions on the nuclei of irradiated cells, including both nuclei deformation and micronuclei. Indeed, nuclear architecture defects (e.g., nuclear blebs, chromatin strings, and micronuclei) are hallmarks of genetic instability (GISSELSSON *et al.*, 2001). Likewise, it has been shown in fibroblasts that oxidative stress activates p38, leading to the accumulation of Lamin B1, a major component of nuclear lamina that governs nuclear shape. The authors show that the loss of nuclear architecture is a preliminary step of senescence (BARASCU *et al.*, 2012). Even though we did observe nuclear deformation, our cells are clearly not senescent, as seen by cell cycle

analysis and strong BrdU incorporation even in γH2AX-positive cells (Figure 17B). In the paper published by Ameziane El-Hasani *et al* in 2015, the standard X-ray dose used for NTHY cells was 10 Gy. As a consequence, several markers of senescence were observed, such as growth arrest and senescence-associated secretory phenotype (SASP). Hence, in the present work, we deliberately used a moderate irradiation dose (5 Gy) that seems to be under the threshold necessary to induce senescence.

To fully understand the role of irradiation on replicative stress in our model, the investigation of replication dynamics was imperative. Using DNA combing, we studied fork progression velocity and fork asymmetry. First, we observed that irradiated cells present a slightly lower replicative fork speed than non-irradiated cells. Moreover, this reduction in progression speed was fully reversed by the treatment with the flavoprotein inhibitor DPI, suggesting an important role for ROS, and more specifically, DUOX1, in this context. Indeed, mounting evidence suggests that ROS control fork progression. As said earlier, it is known that proteins from the replicative machinery, such as PCNA, can be have its function compromised by oxidation (MONTANER *et al.*, 2007). Likewise, in a recent paper, Kumar Somyajit *et al* (2017) reported a novel role for the redox-sensitive peroxiredoxin 2 (PRDX2) as a major modulator of replicative fork progression in response to ROS. Under normal situations, PRDX2 forms oligomers that binds to TIMELESS, a fork-accelerator protein that takes part in the *replisome* (i.e., protein complex formed in replication forks edges for control of progression speed, DNA unwinding, etc.). When subjected to reactive oxygen species, PRDX2 is oxidized and becomes monomeric, causing TIMELESS to dissociate from the replisome. The dissociation slows down fork progression and leads to replication stress (SOMYAJIT *et al.*, 2017). Likewise, another recent paper associates fork progression speed control to cellular redox state. The authors show that homologous recombination (HR) defective cells are naturally under oxidative stress, that in turn, deaccelerates fork speed. The treatment of these cells with antioxidants rescues fork speed and genomic stability. Also, the exposure of wild-type (HR-competent) cells to H_2O_2 efficiently mimics the oxidative stress phenotype and also diminishes fork speed while it creates genomic instability (WILHELM *et al.*, 2016).

Altogether, these findings strongly suggest that reactive oxygen species are major regulators of fork progression velocity.

In our investigation about replication dynamics we also measured fork asymmetry. Fork asymmetry is a mean of calculating perturbations to fork progression and this analysis is the reason why we need two different thymidine analogs (CldU and IdU) in this experiment. If during the first 30 minutes of experiment (CldU incubation) the replication fork progressed 18 μm and in the second 30 minutes (IdU incubation) the same fork progressed only 12 μm, it implies that the fork faced obstacles that kept it from progressing during the second pulse, lowering its velocity. Thus, the greater the difference in track length, the greater the asymmetry ratio. Our analysis did not reveal any differences among the analyzed groups. Nevertheless, the median asymmetry rate observed even in non-irradiated cells (ratio = 1.3) is considered markedly high, probably resulting from the natural great genomic instability of this cell lineage. Hence, this abnormally elevated asymmetry might mask minor variations in this parameter.

As discussed earlier, replicative stress is a multifactorial condition that may result from the contribution of dozens of factors acting simultaneously in the nucleus. Hence, pointing an exact cause for its occurrence is often a difficult task. We started pursuing this answer by analyzing a recurrent source of replicative stress: free deoxyribonucleoside triphosphates (dNTPs) concentrations. Cells finely regulate the concentration of the dNTP pool mostly by *de novo* synthesis mediated by the ribonucleotide reductase (RNR) enzyme. Unbalanced dNTP concentrations can lead to DNA strand breaks, enhanced mutagenesis, stimulation of genetic recombination, chromosomal abnormalities, DNA breaks, and even cell death (MATHEWS, 2006). The uncoordinated cell proliferation of tumor cells, for example, can rapidly make cells run out of dNTPs and further promote genomic instability. Conversely, excessive dNTP pools can contribute to increased mutagenesis. The accumulation of only one nucleotide or even the proportional increase of all four nucleotides can seriously impact genomic stability. As shown by elegant studies using *E. coli*, the proportional increase of dNTPs can augment the frequency of spontaneous mutations up to 40-fold (WHEELER; RAJAGOPAL; MATHEWS, 2005). Excessive dNTP pools boost mutagenesis primarily by DNA misinsertion and impaired proofreading of DNA Polymerase. DNA misinsertion results from the competition between dNTPs for pairing

with the template base, and a dNTP present in excess can be readily misincorporated. Proofreading activity is reduced by elevated dNTP concentrations through the *next-nucleotide effect*, a phenomenon characterized by the illegitimate extension of a DNA chain following a misinserted base, before the mismatch could be repaired (AYE *et al.*, 2015). Indeed, PCR reactions are routinely run at low dNTP concentrations to maximize polymerase proofreading and minimize replication errors. In our work, we did observe a proportional increase in all nucleotides in a time-dependent manner after irradiation. This increase is followed by the activation of several replicative stress markers (e.g., pChk1, pRPA, pATR) and also DNA damage markers (e.g., γH2AX). Nevertheless, this association is only hypothetical since we did not demonstrate experimentally whether the increased nucleotides impair proofreading or increase mutagenesis in our model, nor if it is directly implicated in the activation of replicative stress markers.

A recent report linking reactive oxygen species to nucleotide pool regulation goes in an opposite direction. While treatment of Chinese hamster lung cells with H_2O_2 decreased nucleotide pool, treatment with the antioxidant NAC increased it (WILHELM *et al.*, 2016). Of note, free nucleotides are necessary to fuel not only replication but also DNA repair, so, since our irradiated cells are under severe DNA damage (as illustrated by the presence of high levels of γH2AX 3 days after the irradiation) it would be reasonable to hypothesize that the augmented nucleotide pool could be a homeostatic cell response to DNA damage. However, this overload may, as a collateral effect, increase genomic instability and contribute to replicative stress.

The unexpected increase in ATP levels evoked new hypothesis that were further explored. As discussed earlier, previous findings from the literature revealed that irradiation could boost ATP synthesis through CDK1/Cyclin B activation (QIN *et al.*, 2015) and another study reported that ATP could positively regulate *DUOX1* expression via purinergic receptor activation (BOOTS *et al.*, 2009). As in our model we observe a simultaneous rise in both ATP and *DUOX1*, this hypothesis could reveal the mechanism responsible for the increase in ATP in our irradiated thyroid cells and suggest a new mechanism for *DUOX1* upregulation. Regarding ATP-dependent modulation of *DUOX1*, the production of extracellular ROS in NTHY cells did not respond to ATP fluctuations not even after irradiation, when *DUOX1* levels are already

augmented. Considering the role of CDK1, previous studies showed that CDK1/Cyclin B1 complex is translocated to mitochondria after irradiation and stimulates ATP production through the phosphorylation of mitochondrial electron transport chain (ETC) complex I. The overproduction of ATP would then fuel the highly ATP-consuming repair machinery and allow cells to cope with extensive DNA damage (QIN *et al.*, 2015). However, our results suggest no involvement of this pathway as both inactive pCDK1 (inactivated by phosphorylation) and the CDK1-activating phosphatase cdc25a were unchanged after irradiation. Also, the inhibition of CDK1 by RO3306 did not counteract the stimulus of irradiation upon ROS production. CDK1 and Cyclin B1 complex to form M-Cdk, the kinase responsible for triggering several events related to mitosis initiation like nuclear lamina disintegration and chromatin condensation. Thus, modulations of CDK1 would probably result in changes in mitosis entry. Consistent with the absence of modulation of CDK1, phosphorylated histone H3, a marker of mitosis entry, was not over activated.

Ultimately, to better understand the nature of radio-induced DNA damage that leads to RET/PTC, we investigated whether the breaks in RET/PTC related genes were originated during the first or the second wave of oxidative stress. Immediately after irradiation, breaks could be formed by the direct deleterious effects of ionizing radiation itself and also through intracellular or extracellular ROS derived from water radiolysis. Conversely, 4 days after irradiation, damage would probably result from the persistent oxidative/replicative stress. Hence, we immunoprecipitated the damaged chromatin of irradiated and non-irradiated NTHY cells using γH2AX antibodies at these two-time points and quantified the presence of the RET/PTC-related genes among the precipitated chromatin. Their detection would reveal that these genes presented double stranded breaks (DSB). However, the stochastic effect of ionizing radiation generated double-stranded breaks in all analyzed genes, including both RET/PTC-related and unrelated genes. Remarkably, 4 days after, RET/PTC unrelated genes did not present the same extent of breaks, suggesting that these genes had their DSBs repaired. Indeed, as seen in Figure 14A, the profile of H2AX γ-phosphorylation (i.e., the occurrence of DSB) clearly shows that after the first wave, the cells completely repair their DNA. However, it apparently does not happen with the RET/PTC-related genes. Both *RET* and *CCDC6* still present breaks 4 days after the irradiation. It is

unclear, however, whether the original breaks created during the first wave remain unrepaired or if they are repaired and then damaged again.

Notably, the absence of fragile site expression of FRA3B four days after irradiation is intriguing. This common fragile site is probably the most frequently expressed in the human genome. It comprises the gene *FHIT*, a tumor suppressor gene related to carcinogenesis of several human cancers, such as esophageal, breast, cervical and lung cancers (ARLT *et al.*, 2006). The demonstration that oxidative stress preferentially induces breaks in FRA10C (*RET*) and FRA10G (*CCDC6*), while sparing FRA3B, could mean a unique specificity of these loci for oxidative damage, introducing a novel subcategory of fragile sites. However, with available data this hypothesis remains somehow speculative until these results are reproduced and more robust data about the nature of these sites can be obtained.

6. CONCLUSIONS

The present study aimed to understand the role of oxidative and replicative stress in thyroid radio-carcinogenesis, more specifically, their role in formation of the recurrent RET/PTC1 translocation. Using state-of-art methods, we analyzed parameters of both oxidative and replicative stress, gene expression and replication dynamics. Based on current data, we propose that RET/PTC1 formation is a consequence of ROS-induced replicative stress. The mechanistic model would be the following: upon irradiation, the oxidative burst mediated by water radiolysis activates several molecular pathways that will ultimately create a persistent oxidative stress produced by DUOX1 upregulation. The reactive oxygen species would, then, regulate replication fork speed by direct and indirect mechanisms, leading to replicative stress. The untimely replication would favor breaks in fragile sites, specially FRA10C and FRA10G, enabling the formation of RET/PTC1 translocation. Yet, more studies are needed to fully characterize this phenomenon. We expect this work will provide significant contributions to the field of adult and pediatric thyroid carcinogenesis bringing new insights into RET/PTC etiology.

7. REFERENCES

AGUILERA, A.; GARCÍA-MUSE, T. Causes of Genome Instability. *Annual Review of Genetics*, v. 47, n. 1, p. 1–32, 23 Nov. 2013.

AKIBA, S. *et al. Thyroid cancer incidence among atomic bomb survivors, 1958-79*. . [S.l: s.n.]. , 1992

ALVINO, G. M. *et al.* Replication in Hydroxyurea: It's a Matter of Time. *Molecular and Cellular Biology*, v. 27, n. 18, p. 6396–6406, 15 Sep. 2007.

AMERICAN CANCER SOCIETY. *Cancer Facts & Figures 2013*. Atlanta: American Cancer Society, 2013.

AMEZIANE-EL-HASSANI, R. *et al.* NADPH oxidase DUOX1 promotes long-term persistence of oxidative stress after an exposure to irradiation. *Proceedings of the National Academy of Sciences*, v. 112, n. 16, p. 5051–5056, 2015.

AMEZIANE-EL-HASSANI, R. *et al.* Role of H2O2 in RET/PTC1 Chromosomal Rearrangement Produced by Ionizing Radiation in Human Thyroid Cells. *Cancer Research*, v. 70, n. 10, p. 4123–4132, 15 May 2010.

AMEZIANE-EL-HASSANI, R.; SCHLUMBERGER, M.; DUPUY, C. NADPH oxidases: new actors in thyroid cancer? *Nature Reviews Endocrinology*, v. 12, n. 8, p. 485–494, 13 May 2016.

ARIGHI, E.; BORRELLO, M. G.; SARIOLA, H. RET tyrosine kinase signaling in development and cancer. *Cytokine & growth factor reviews*, v. 16, n. 4–5, p. 441–67, 2005.

ARLT, M. F. *et al. Common fragile sites as targets for chromosome rearrangements*. *DNA Repair*. [S.l: s.n.]. , 2006

AYE, Y. *et al.* Ribonucleotide reductase and cancer: biological mechanisms and targeted therapies. *Oncogene*, v. 34, n. 16, p. 2011–2021, 9 Apr. 2015.

AZZAM, E. I.; JAY-GERIN, J.-P.; PAIN, D. Ionizing radiation-induced metabolic oxidative stress and prolonged cell injury. *Cancer letters*, v. 327, n. 1–2, p. 48–60, 31 Dec. 2012.

BARASCU, A. *et al.* Oxydative stress alters nuclear shape through lamins dysregulation: a route to senescence. *Nucleus (Austin, Tex.)*, v. 3, n. 5, p. 411–417, 2012.

BARKER, R. J. *et al.* High levels of genetic change in rodents of Chernobyl. *Nature*, v. 380, n. 6576, p. 707–708, 25 Apr. 1996.

BARTALENA, L. Diagnosis and management of Graves disease: a global overview. *Nature Reviews Endocrinology*, v. 9, n. 12, p. 724–734, 15 Oct. 2013.

BASOLO, F. *et al.* Potent Mitogenicity of the RET/PTC3 Oncogene Correlates with Its Prevalence in Tall-Cell Variant of Papillary Thyroid Carcinoma. *The American Journal of Pathology*, v. 160, n. 1, p. 247–254, Jan. 2002.

BAVERSTOCK, K. *et al.* Thyroid cancer after Chernobyl. *Nature*, v. 359, n. 6390, p. 21–22, 3 Sep. 1992.

BEDARD, K.; KRAUSE, K.-H. The NOX family of ROS-generating NADPH oxidases: physiology and pathophysiology. *Physiological reviews*, v. 87, n. 1, p. 245–313, Jan. 2007.

BINDER-FOUCARD, F. *et al. Estimation nationale de l'incidence et de la mortalité par cancer en France entre 1980 et 2012. Partie 1 – Tumeurs solides.* Saint-Maurice: [s.n.], 2013.

BLOCK, K.; GORIN, Y. Aiding and abetting roles of NOX oxidases in cellular transformation. *Nature reviews. Cancer*, v. 12, n. 9, p. 627–37, Sep. 2012.

BOAVENTURA, P. *et al.* Genetic alterations in thyroid tumors from patients irradiated in childhood for tinea capitis treatment. *European journal of endocrinology*, v. 169, n. 5, p. 673–9, Nov. 2013.

BOOTS, A. W. *et al.* ATP-mediated Activation of the NADPH Oxidase DUOX1 Mediates Airway Epithelial Responses to Bacterial Stimuli. *Journal of Biological Chemistry*, v. 284, n. 26, p. 17858–17867, 26 Jun. 2009.

BOUTZIOS, G. *et al.* Higher Incidence of Tall Cell Variant of Papillary Thyroid Carcinoma in Graves' Disease. *Thyroid*, v. 24, n. 2, p. 347–354, Feb. 2014.

BURROW, A. A. *et al.* Over half of breakpoints in gene pairs involved in cancer-specific recurrent translocations are mapped to human chromosomal fragile sites. *BMC genomics*, v. 10, n. 1, p. 59, 30 Jan. 2009.

CANCER GENOME ATLAS RESEARCH NETWORK. Integrated genomic characterization of papillary thyroid carcinoma. *Cell*, v. 159, n. 3, p. 676–90, 23 Oct. 2014.

CAUDILL, C. M. *et al.* Dose-Dependent Generation of RET / PTC in Human Thyroid Cells after in Vitro Exposure to γ-Radiation: A Model of Carcinogenic Chromosomal Rearrangement Induced by Ionizing Radiation. *The Journal of Clinical Endocrinology & Metabolism*, v. 90, n. 4, p. 2364–2369, Apr. 2005.

CELETTI, A. *et al.* H4(D10S170), a gene frequently rearranged with RET in papillary thyroid carcinomas: functional characterization. *Oncogene*, v. 23, n. 1, p. 109–21, 8 Jan. 2004.

CHEN, A. Y.; JEMAL, A.; WARD, E. M. Increasing incidence of differentiated thyroid cancer in the United States, 1988-2005. *Cancer*, v. 115, n. 16, p. 3801–3807, 2009.

CHEN, Y.-K. *et al.* Cancer risk in patients with Graves' disease: a nationwide cohort study. *Thyroid : official journal of the American Thyroid Association*, v. 23, n. 7, p. 879–84, 2013.

COCLET, J. *et al.* Cell population kinetics in dog and human adult thyroid. *Clinical endocrinology*, v. 31, n. 6, p. 655–65, Dec. 1989.

COLLINS, B. J. *et al.* RET expression in papillary thyroid cancer from patients irradiated in childhood for benign conditions. *The Journal of clinical endocrinology and metabolism*, v. 87, n. 8, p. 3941–6, Aug. 2002.

COOKE, M. S. *et al.* Oxidative DNA damage: mechanisms, mutation, and disease. *FASEB*, v. 17, n. 10, p. 1195–214, 1 Jul. 2003.

CORDIOLI, M. I. C. V. *et al.* Are we really at the dawn of understanding sporadic pediatric thyroid carcinoma? *Endocrine-related cancer*, v. 22, n. 6, p. R311-24, Dec. 2015.

COSTA, E. O. A. *et al.* The effect of low-dose exposure on germline microsatellite mutation rates in humans accidentally exposed to caesium-137 in Goiânia. *Mutagenesis*, v. 26, n. 5, p. 651–5, 1 Sep. 2011.

DILLON, L. W.; BURROW, A. A.; WANG, Y.-H. DNA instability at chromosomal fragile sites in cancer. *Current genomics*, v. 11, n. 5, p. 326–37, 2010.

DOBBELSTEIN, M.; SØRENSEN, C. S. Exploiting replicative stress to treat cancer. *Nature reviews. Drug discovery*, v. 14, n. 6, p. 405–23, 2015.

DOM, G. *et al.* A gene expression signature distinguishes normal tissues of sporadic and radiation-induced papillary thyroid carcinomas. *British journal of cancer*, v. 107, n. 6, p. 994–1000, 4 Sep. 2012.

ELLEGREN, H. *et al.* Fitness loss and germline mutations in barn swallows breeding in Chernobyl. *Nature*, v. 389, n. 6651, p. 593–596, 9 Oct. 1997.

FAGIN, J. A.; WELLS, S. A. Biologic and Clinical Perspectives on Thyroid Cancer. *New England Journal of Medicine*, v. 375, n. 11, p. 1054–1067, 15 Sep. 2016.

FLAVIN, R. *et al.* RET/PTC rearrangement occurring in primary peritoneal carcinoma. *International journal of surgical pathology*, v. 17, n. 3, p. 187–97, 1 Jun. 2009.

FRANSSILA, K. O.; HARACH, H. R. Occult papillary carcinoma of the thyroid in children and young adults. A systemic autopsy study in Finland. *Cancer*, v. 58, n. 3, p. 715–9, 1 Aug. 1986.

FUSCO, A. *et al.* A new oncogene in human thyroid papillary carcinomas and their lymph-nodal metastases. *Nature*, v. 328, n. 6126, p. 170–172, 9 Jul. 1987.

GANDHI, M. *et al.* DNA breaks at fragile sites generate oncogenic RET/PTC rearrangements in human thyroid cells. *Oncogene*, v. 29, n. 15, p. 2272–2280, 2010.

GELOT, C.; MAGDALOU, I.; LOPEZ, B. S. Replication stress in Mammalian cells and its consequences for mitosis. *Genes*, v. 6, n. 2, p. 267–98, 22 Jan. 2015.

GISSELSSON, D. *et al.* Abnormal nuclear shape in solid tumors reflects mitotic instability. *American Journal of Pathology*, v. 158, n. 1, p. 199–206, 2001.

GLOVER, T. W. *et al.* DNA polymerase alpha inhibition by aphidicolin induces gaps and breaks at common fragile sites in human chromosomes. *Human genetics*, v. 67, n. 2, p. 136–42, 1984.

GLOVER, T. W.; WILSON, T. E.; ARLT, M. F. Fragile sites in cancer: more than meets the eye. *Nature reviews. Cancer*, v. 17, n. 8, p. 489–501, 25 Jul. 2017.

GRIECO, M. *et al.* PTC is a novel rearranged form of the ret proto-oncogene and is frequently detected in vivo in human thyroid papillary carcinomas. *Cell*, v. 60, n. 4, p. 557–563, 1990.

GRUBBS, E. G. *et al.* RET fusion as a novel driver of medullary thyroid carcinoma. *The Journal of clinical endocrinology and metabolism*, v. 100, n. 3, p. 788–93, Mar. 2015.

GUIHARD-COSTA, A.-M.; MÉNEZ, F.; DELEZOIDE, A.-L. Organ weights in human fetuses after formalin fixation: standards by gestational age and body weight. *Pediatric and developmental pathology*, v. 5, n. 6, p. 559–78, 2002.

HALLIWELL, B.; GUTTERIDGE, J. *Free Radicals in Biology and Medicine*. 4a. ed. [S.l.]: Oxford University Press, 2007.

HARPER, R. W. *et al.* Differential regulation of dual NADPH oxidases/peroxidases, Duox1 and Duox2, by Th1 and Th2 cytokines in respiratory tract epithelium. *FEBS Letters*, v. 579, n. 21, p. 4911–4917, 29 Aug. 2005.

HECHT, F.; CAZARIN, J. M.; *et al.* Redox homeostasis of breast cancer lineages contributes to differential cell death response to exogenous hydrogen peroxide. *Life Sciences*, v. 158, p. 7–13, 2016.

HECHT, F.; PESSOA, C. F.; *et al.* The role of oxidative stress on breast cancer development and therapy. *Tumor Biology*, v. 37, n. 4, p. 4281–4291, 2016.

HENDERSON, Y. C. *et al.* High Rate of BRAF and RET/PTC Dual Mutations Associated with Recurrent Papillary Thyroid Carcinoma. *Clinical Cancer Research*, v. 15, n. 2, p. 485–491, 15 Jan. 2009.

HIRAKAWA, S. *et al.* Dual oxidase 1 induced by Th2 cytokines promotes STAT6 phosphorylation via oxidative inactivation of protein tyrosine phosphatase 1B in human epidermal keratinocytes. *Journal of immunology (Baltimore, Md. : 1950)*, v. 186, n. 8, p. 4762–70, 15 Apr. 2011.

INSTITUTO NACIONAL DE CÂNCER. *Estimativa 2018: incidência de câncer no Brasil*. Rio de Janeiro: Instituto Nacional de Câncer, 2017.

INTERNATIONAL ATOMIC ENERGY AGENCY. *The Radiological Accident in Goiânia*. Vienna: IAEA, 1988.

IYAMA, K. *et al.* Identification of Three Novel Fusion Oncogenes, SQSTM1/NTRK3 , AFAP1L2/RET , and PPFIBP2/RET , in Thyroid Cancers of Young Patients in Fukushima. *Thyroid*, v. 27, n. 6, p. 811–818, Jun. 2017.

JHIANG, S. M. *et al.* Targeted expression of the ret/PTC1 oncogene induces papillary thyroid carcinomas. *Endocrinology*, v. 137, n. 1, p. 375–8, Jan. 1996.

KIM, G. J.; FISKUM, G. M.; MORGAN, W. F. A Role for Mitochondrial Dysfunction in Perpetuating Radiation-Induced Genomic Instability. *Cancer Research*, v. 66, n. 21, p. 10377–10383, 1 Nov. 2006.

LAUPER, J. M. *et al.* Spectrum and Risk of Neoplasia in Werner Syndrome: A Systematic Review. *PLoS ONE*, v. 8, n. 4, p. e59709, 1 Apr. 2013.

LE TALLEC, B. *et al.* Updating the mechanisms of common fragile site instability: how to reconcile the different views? *Cellular and Molecular Life Sciences*, v. 71, n. 23, p. 4489–4494, 24 Dec. 2014.

LEMOINE, N. *et al.* Characterisation of human thyroid epithelial cells immortalised in vitro by simian virus 40 DNA transfection. *British Journal of Cancer*, v. 60, n. 6, p. 897–903, Dec. 1989.

LEMYZE, M.; FAVORY, R. Enlarged tonsils and fatigue. *American family physician*, v. 82, n. 6, p. 669, 15 Sep. 2010.

LIVAK, K. J.; SCHMITTGEN, T. D. Analysis of Relative Gene Expression Data Using Real-Time Quantitative PCR and the 2−ΔΔCT Method. *Methods*, v. 25, n. 4, p. 402–408, Dec. 2001.

MARDER, B. A.; MORGAN, W. F. Delayed chromosomal instability induced by DNA damage. *Molecular and cellular biology*, v. 13, n. 11, p. 6667–77, 1 Nov. 1993.

MARIC, I. *et al.* Centrosomal and mitotic abnormalities in cell lines derived from papillary thyroid cancer harboring specific gene alterations. *Molecular Cytogenetics*, v. 4, n. 1, p. 26, 2011.

MARKKANEN, E. *et al.* A switch between DNA polymerases δ and λ promotes error-free bypass of 8-oxo-G lesions. *Proceedings of the National Academy of Sciences of the United States of America*, v. 109, n. 50, p. 20401–6, 11 Dec. 2012.

MARONGIU, F. *et al.* Cell turnover in the repopulated rat liver: distinct lineages for hepatocytes and the biliary epithelium. *Cell and tissue research*, v. 356, n. 2, p. 333–40, May 2014.

MATHEWS, C. K. DNA precursor metabolism and genomic stability. *The FASEB Journal*, v. 20, n. 9, p. 1300–1314, Jul. 2006.

MEMON, A. *et al.* Dental x-rays and the risk of thyroid cancer: A case-control study. *Acta Oncologica*, v. 49, n. 4, p. 447–453, 16 Jan. 2010.

MÉNDEZ, J.; STILLMAN, B. Chromatin association of human origin recognition complex, cdc6, and minichromosome maintenance proteins during the cell cycle: assembly of prereplication complexes in late mitosis. *Molecular and cellular biology*, v. 20, n. 22, p. 8602–12, 15 Nov. 2000.

MENG, T. *et al.* Cys-Oxidation of Protein Tyrosine Phosphatases : Its Role in

Regulation of Signal Transduction and Its Involvement in Human Cancers. p. 9–16, 2006.

MEUNIER, B.; DE VISSER, S. P.; SHAIK, S. Mechanism of oxidation reactions catalyzed by cytochrome p450 enzymes. *Chemical reviews*, v. 104, n. 9, p. 3947–80, Sep. 2004.

MONTANER, B. *et al.* Reactive oxygen-mediated damage to a human DNA replication and repair protein. *EMBO reports*, v. 8, n. 11, p. 1074–1079, 12 Nov. 2007.

MORRIS, L. G. T.; MYSSIOREK, D. Improved detection does not fully explain the rising incidence of well-differentiated thyroid cancer: A population-based analysis. *American Journal of Surgery*, v. 200, n. 4, p. 454–461, 2010.

MULLIGAN, L. M. *et al.* Germ-line mutations of the RET proto-oncogene in multiple endocrine neoplasia type 2A. *Nature*, v. 363, n. 6428, p. 458–60, 3 Jun. 1993.

NIKIFOROV, Y. E. Thyroid carcinoma: molecular pathways and therapeutic targets. *Modern Pathology*, v. 21, n. December 2007, p. S37–S43, May 2008.

NIKIFOROVA, M. N. Proximity of Chromosomal Loci That Participate in Radiation-Induced Rearrangements in Human Cells. *Science*, v. 290, n. 5489, p. 138–141, 2000.

NUNES, H. F. *et al.* Assessment of BCL2/J(H) translocation in healthy individuals exposed to low-level radiation of 137CsCl in Goiânia, Goiás, Brazil. *Genetics and Molecular Research*, v. 12, n. 1, p. 28–36, 16 Jan. 2013.

PIEROTTI, M. A *et al.* Characterization of an inversion on the long arm of chromosome 10 juxtaposing D10S170 and RET and creating the oncogenic sequence RET/PTC. *Proceedings of the National Academy of Sciences of the United States of America*, v. 89, n. 5, p. 1616–1620, 1992.

PIRZIO, L. M. *et al.* Werner syndrome helicase activity is essential in maintaining fragile site stability. *Journal of Cell Biology*, v. 180, n. 2, p. 305–314, 2008.

PORTELLA, G. *et al.* Development of mammary and cutaneous gland tumors in transgenic mice carrying the RET/PTC1 oncogene. *Oncogene*, v. 13, n. 9, p. 2021–6, 7 Nov. 1996.

QIN, L. *et al.* CDK1 Enhances Mitochondrial Bioenergetics for Radiation-Induced DNA Repair. *Cell Reports*, v. 13, n. 10, p. 2056–2063, 2015.

RABES, H. M. *et al.* Pattern of radiation-induced RET and NTRK1 rearrangements in 191 post-chernobyl papillary thyroid carcinomas: biological, phenotypic, and clinical implications. *Clinical cancer research : an official journal of the American Association for Cancer Research*, v. 6, n. 3, p. 1093–103, Mar. 2000.

RHODEN, K. J. *et al.* RET/Papillary Thyroid Cancer Rearrangement in Nonneoplastic Thyrocytes: Follicular Cells of Hashimoto's Thyroiditis Share Low-Level Recombination Events with a Subset of Papillary Carcinoma. *The Journal of Clinical Endocrinology & Metabolism*, v. 91, n. 6, p. 2414–2423, Jun. 2006.

ROMEI, C. *et al.* Modifications in the papillary thyroid cancer gene profile over the last 15 years. *The Journal of clinical endocrinology and metabolism*, v. 97, n. 9, p. E1758-65, Sep. 2012.

ROMEI, C.; CIAMPI, R.; ELISEI, R. A comprehensive overview of the role of the RET proto-oncogene in thyroid carcinoma. *Nature reviews. Endocrinology*, v. 12, n. 4, p. 192–202, 2016.

ROMEI, C.; ELISEI, R. RET/PTC Translocations and Clinico-Pathological Features in Human Papillary Thyroid Carcinoma. *Frontiers in Endocrinology*, v. 3, n. APR, p. 1–8, 2012.

RON, E. *et al.* Thyroid cancer after exposure to external radiation: a pooled analysis of seven studies. *Radiation research*, v. 141, n. 3, p. 259–77, Mar. 1995.

SAAD, A. G. *et al.* Proliferative activity of human thyroid cells in various age groups and its correlation with the risk of thyroid cancer after radiation exposure. *The Journal of clinical endocrinology and metabolism*, v. 91, n. 7, p. 2672–7, 2006.

SADETZKI, S. *et al.* Risk of thyroid cancer after childhood exposure to ionizing radiation for tinea capitis. *Journal of Clinical Endocrinology and Metabolism*, v. 91, n. 12, p. 4798–4804, 2006.

SANTORO, M. *et al.* Development of thyroid papillary carcinomas secondary to tissue-specific expression of the RET/PTC1 oncogene in transgenic mice. *Oncogene*, v. 12, n. 8, p. 1821–6, 18 Apr. 1996.

SANTORO, M. *et al.* Involvement of RET oncogene in human tumours: specificity of RET activation to thyroid tumours. *British journal of cancer*, v. 68, n. 3, p. 460–4, Sep. 1993.

SANTORO, M. *et al.* Molecular characterization of RET/PTC3; a novel rearranged version of the RETproto-oncogene in a human thyroid papillary carcinoma. *Oncogene*, v. 9, n. 2, p. 509–16, Feb. 1994.

SANTORO, M.; MELILLO, R. M.; FUSCO, A. RET/PTC activation in papillary thyroid carcinoma: European Journal of Endocrinology Prize Lecture. *European journal of endocrinology*, v. 155, n. 5, p. 645–53, Nov. 2006.

SCHUCHARDT, A. *et al.* Defects in the kidney and enteric nervous system of mice lacking the tyrosine kinase receptor Ret. *Nature*, v. 367, n. 6461, p. 380–383, 27 Jan. 1994.

SHY, R. Tinea Corporis and Tinea Capitis. *Pediatrics in Review*, v. 28, n. 5, p. 164 LP-174, 1 May 2007.

SINGLA, S. *et al.* Should asymptomatic enlarged thymus glands be resected? *The Journal of Thoracic and Cardiovascular Surgery*, v. 140, p. 977–983, 2010.

SMITH, D. I. *et al.* Large common fragile site genes and cancer. *Seminars in Cancer Biology*, v. 17, p. 31–41, 2007.

SOARES, P. *et al.* BRAF mutations and RET/PTC rearrangements are alternative events in the etiopathogenesis of PTC. *Oncogene*, v. 22, n. 29, p. 4578–4580, 17 Jul. 2003.

SOMYAJIT, K. *et al.* Redox-sensitive alteration of replisome architecture safeguards genome integrity. *Science*, v. 358, n. 6364, p. 797–802, 10 Nov. 2017.

SOSA, V. *et al.* Oxidative stress and cancer: An overview. *Ageing Research Reviews*, v. 12, n. 1, p. 376–390, Jan. 2013.

STANIFORTH, J. U. L.; ERDIRIMANNE, S.; ESLICK, G. D. Thyroid carcinoma in Graves' disease: A meta-analysis. *International Journal of Surgery*, v. 27, p. 118–125, Mar. 2016.

TAKAHASHI, M.; RITZ, J.; COOPER, G. M. Activation of a novel human transforming gene, ret, by DNA rearrangement. *Cell*, v. 42, n. 2, p. 581–8, Sep. 1985.

TÉCHER, H. *et al.* The impact of replication stress on replication dynamics and DNA damage in vertebrate cells. *Nature Reviews Genetics*, v. 18, n. 9, p. 535–550, 17 Jul. 2017.

TOMASETTI, C.; LI, L.; VOGELSTEIN, B. Stem cell divisions, somatic mutations, cancer etiology, and cancer prevention. *Science (New York, N.Y.)*, v. 355, n. 6331, p. 1330–1334, 24 Apr. 2017.

TULARD, A. *et al.* Persistent oxidative stress after ionizing radiation is involved in inherited radiosensitivity. *Free radical biology & medicine*, v. 35, n. 1, p. 68–77, 1 Jul. 2003.

VALKO, M. *et al.* Free radicals and antioxidants in normal physiological functions and human disease. *The international journal of biochemistry & cell biology*, v. 39, n. 1, p. 44–84, Jan. 2007.

VAN LOON, B.; MARKKANEN, E.; HÜBSCHER, U. Oxygen as a friend and enemy: How to combat the mutational potential of 8-oxo-guanine. *DNA Repair*, v. 9, n. 6, p. 604–616, 2010.

VERSTEYHE, S. *et al.* Comparative analysis of the thyrocytes and T cells: responses to H2O2 and radiation reveals an H2O2-induced antioxidant transcriptional program in thyrocytes. *The Journal of clinical endocrinology and metabolism*, v. 98, n. 10, p. E1645-54, Oct. 2013.

WATSON, G. E. *et al.* Chromosomal instability in unirradiated cells induced in vivo by a bystander effect of ionizing radiation. *Cancer research*, v. 60, n. 20, p. 5608–11, 15 Oct. 2000.

WHEELER, L. J.; RAJAGOPAL, I.; MATHEWS, C. K. Stimulation of mutagenesis by proportional deoxyribonucleoside triphosphate accumulation in Escherichia coli. *DNA Repair*, v. 4, n. 12, p. 1450–1456, 2005.

WILHELM, T. *et al.* Slow Replication Fork Velocity of Homologous Recombination-Defective Cells Results from Endogenous Oxidative Stress. *PLoS Genetics*, v. 12, n.

5, p. 1–20, 2016.

WILLIAMS, D. Cancer after nuclear fallout: lessons from the Chernobyl accident. *Nature reviews. Cancer*, v. 2, n. 7, p. 543–9, Jul. 2002.

WILLIAMS, D. Radiation carcinogenesis: lessons from Chernobyl. *Oncogene*, v. 27, n. S2, p. S9–S18, Dec. 2008a.

WILLIAMS, D. Thyroid Growth and Cancer. *European Thyroid Journal*, v. 4, n. 3, p. 164–173, 26 Aug. 2015.

WILLIAMS, D. Twenty years' experience with post-Chernobyl thyroid cancer. *Best Practice & Research Clinical Endocrinology & Metabolism*, v. 22, n. 6, p. 1061–1073, Dec. 2008b.

WORLD HEALTH ORGANIZATION. *Health Effects of the Chernobyl Accident and Special Health Care Programmes*. Geneva: [s.n.], 2006.

ZEMAN, M. K.; CIMPRICH, K. A. Causes and consequences of replication stress. *Nature cell biology*, v. 16, n. 1, p. 2–9, 2014.

ZHU, Z. *et al.* Prevalence of RET/PTC rearrangements in thyroid papillary carcinomas: effects of the detection methods and genetic heterogeneity. *The Journal of clinical endocrinology and metabolism*, v. 91, n. 9, p. 3603–10, Sep. 2006.

ZLOTORYNSKI, E. *et al.* Molecular Basis for Expression of Common and Rare Fragile Sites. *Molecular and Cellular Biology*, v. 23, n. 20, p. 7143–7151, 15 Oct. 2003.

ZOU, M.; SHI, Y.; FARID, N. R. Low rate of ret proto-oncogene activation (PTC/retTPC) in papillary thyroid carcinomas from saudi arabia. *Cancer*, v. 73, n. 1, p. 176–180, 1 Jan. 1994.

8. APPENDIX

8.1 Thesis synthesis in french

Les cancers de la thyroïde sont les tumeurs endocrines les plus courantes et représentent 3 à 4% de tous les cancers humains. Bien que les progrès dans le traitement de ce néoplasme aient entraîné une baisse significative de la mortalité au cours des dernières décennies, son incidence augmente rapidement dans le monde entier. Cependant, il est encore largement discuté si l'augmentation observée est simplement due à une amélioration de la détection menant au diagnostic excessif de tumeurs cliniquement non pertinentes ou à une augmentation réelle. Le cancer de la thyroïde peut provenir de cellules folliculaires (thyrocytes) et parafoliculares (cellules C). Alors que les cellules folliculaires néoplasiques peuvent se transformer en tumeurs papillaires ou folliculaires bien différenciées et aussi en tumeurs anaplasiques non différenciées, les cellules néoplasiques parafolliculaires, quand à elles, conduisent toujours à un cancer médullaire. Les carcinomes papillaires représentent le type le plus commun de cancer de la thyroïde, avec près de 80% des cas. Les altérations génétiques les plus pertinentes trouvées dans ces tumeurs sont des mutations ponctuelles et/ou des translocations dans les gènes *RET*, *BRAF* et *RAS*. *RET* est un proto-oncogène de 53kb situé sur le bras long du chromosome 10 (q11.21) qui code pour un récepteur tyrosine kinase qui stimule la prolifération, la croissance cellulaire, la différenciation et la survie par activation des ligands de la famille GDNF.

Plusieurs types de aberrations génomiques ont déjà été décrits dans le gène *RET* et leur rôle dans le développement du cancer a été étudié de manière approfondie pendant plus de 20 ans. Alors que les mutations ponctuelles sur *RET* généralement (mais pas exclusivement) mènent au cancer médullaire, les réarrangements chromosomiques impliquant le gène RET et divers partenaires potentiels conduisent au carcinome papillaire de la thyroïde (CPT). Le premier rapport d'une translocation impliquant RET a été publié en 1990 par Dr. Grieco, inaugurant une liste qui comprend aujourd'hui plus de 25 translocations, chacune avec son gène partenaire respectif. La translocation ainsi identifiée, maintenant connue sous le nom RET/PTC1, résulte d'une inversion intrachromosomique entre *RET* et *CCDC6*, un gène situé aussi sur le chromosome 10 (q21.2) codant pour une protéine exprimée de manière constitutive. Indépendamment du gène partenaire, toutes les translocations entraînent une fusion de la région 3' de *RET*, codant pour la région catalytique du récepteur tyrosine kinase, avec l'extrémité 5' du gène donneur. Ceci génère une protéine cytoplasmique constitutivement active qui favorise la prolifération par l'activation des voies MAPK et PI3K, ce qui augmente considérablement le risque de néoplasie.

Les rayonnements ionisants ont été reconnus pendant des décennies comme le facteur de risque le plus important pour le développement du cancer papillaire de la thyroïde, en particulier pour la formation les translocations RET/PTC. En effet, plusieurs auteurs ont démontré de manière expérimentale une relation de cause à effet entre l'irradiation et la formation de RET/PTC *in vitro*, confirmant ainsi les résultats cliniques qui montrent que les cancers de la thyroïde induits par les rayonnements (par exemple, les survivants de l'accident de Tchernobyl) ont une prévalence plus élevée d'exprimer la translocation RET/PTC que les tumeurs papillaires sans antécédents d'exposition aux rayonnements (tumeurs sporadiques). Conformément à ces résultats, notre groupe a montré qu'une dose unique de 5Gy de rayons X peut induire RET/PTC1 dans la lignée de cellules épithéliales de la thyroïde NTHY-ori3.1. Notre groupe a

également montré que les espèces réactives de l'oxygène (ERO) sont des médiateurs importants de ce processus. Enfin, plus récemment, notre groupe a également montré que l'irradiation favorise l'augmentation de la NADPH oxydase DUOX1, favorisant l'établissement d'un stress oxydatif persistant, accompagné par des lésions à l'ADN et de l'instabilité génomique.

Le rôle des ROS dans la promotion de l'instabilité génomique repose non seulement sur sa capacité à causer des dommages oxydatifs à l'ADN, mais aussi sur la création d'un environnement hostile pour la réplication. Le stress réplicatif peut être définie comme une perturbation dans la réplication de l'ADN avec des fourches de réplication aberrantes contenant des fragments d'ADN simple brin comme caractéristique marquantes qui interfèrent dans la vitesse et l'exactitude de la phase S. . De tels troubles peuvent être provoqués par des sources exogènes (rayonnement ionisant ou des composés génotoxiques tels que l'inhibiteur de la polymérase réplicative alpha) ou par des sources endogènes (espèces réactives de l'oxygène, l'incorporation aléatoire de nucléotides, etc.). Les sites fragiles sont des régions du génome particulièrement sensibles au stress réplicatif. Sous stress, ces régions sont sujettes à des cassures et sont maintenant considérées comme des facteurs clés dans le développement de divers types de cancer. Ainsi, on estime que 52% des translocations chromosomiques liées à la carcinogenèse ont au moins un des gènes localisés sur des sites fragiles. C'est le cas pour *RET* et *CCDC6*, la paire de gènes responsables de la formation de RET/PTC1. *RET* est situé dans FRA10G et *CCDC6* est situé dans FRA10C, deux sites fragiles communs du chromosome 10. Il a été démontré que le traitement des cellules NTHY-ori3.1 avec des inducteurs de stress genotoxic peuvent induire des cassures au niveau de *RET* et induire spécifiquement la formation de RET/PTC1 dans les cellules thyroïdiennes, suggérant un rôle important du stress réplicatif dans la tumorigenèse de cet organe. Dans ce cadre, notre objectif était d'étudier la relation entre le stress oxydatif et le stress réplicatif dans les cellules de la thyroïde après l'irradiation et d'étudier leur rôle dans la formation de la translocation RET/PTC1. La lignée cellulaire humaine NTHYori3.1 (thyrocyte d'origine non-tumorale transformée avec le vecteur SV40) a été utilisée pour montrer que l'irradiation déclenche une augmentation persistante de la production de ROS intra et extracellulaire qui commence plusieurs jours après l'irradiation. Nous avons également observé que, immédiatement après l'irradiation, il y a aussi un pic transitoire de production de ROS qui résulte exclusivement de la radiolyse de l'eau. Ces deux événements, temporellement séparés, conduisent à des dommages à l'ADN. Afin d'étudier l'existence de stress réplicatif, nous avons d'abord confirmée par l'analyse du cycle cellulaire et l'incorporation de BrdU que les cellules irradiées restent proliférantes. Par la suite, nous avons évalué l'existence de marqueurs protéiques de stress réplicatif 3 jours après l'irradiation. L'analyse a révélé une activation de plusieurs marqueurs de stress réplicatifs tels que l'expression des formes phosphoryles de Chk1, ATR et RPA et l'expression de la protéine FANCD2. Par ailleurs, des changements morphologiques nucléaires liés à l'instabilité génétique, tels que la déformation et les micronoyaux, ont été détectés. L'étude de la dynamique de réplication par peignage de l'ADN a également mis en évidence l'existence d'un stress réplicatif, comme le démontre la diminution de la vitesse de réplication. Cette baisse a été contrecarrée par les antioxydants, ce qui suggère l'implication des ERO dans le processus. Afin de comprendre les causes possibles de ce stress, nous avons évalué la concentration des deoxiribonucleotides triphosphate (dNTP) dans les cellules irradiées. Nous avons observé une augmentation de tous les nucléotides d'une manière dépendante du temps, ce qui dans certains modèles est liée à une

augmentation de la mutagenèse et de l'instabilité génétique. Afin de déterminer si la formation de RET/PTC1 *in vitro* est liée aux effets directs des rayonnements ionisants ou est une conséquence d'un stress réplicatif, nous avons évalué l'apparition des cassures double brin dans les deux gènes impliqués dans la translocation RET/PTC1 à deux moments distincts: 30 minutes après l'irradiation ou 4 jours plus tard. L'analyse par ChIP-qPCR utilisant un anticorps dirigé contre γH2AX a révélé qu'immédiatement après l'irradiation les cassures se font, non seulement au niveau des gènes RET et CCDC6, mais également au niveau d'autres gènes analysés et ce, en raison de dommages stochastiques. Par contre, nous observons seulement un enrichissement de gH2AX au niveau des gènes RET et CCDC6 après plusieurs jours. Par conséquent, ces données suggèrent que le stress réplicatif jouerait un rôle important dans l'étiologie du cancer de la thyroïde papillaire induit par le rayonnement ionisant

8.2 Thesis synthesis in portuguese

Os cânceres de tireoide são os tumores endócrinos mais comuns e representam 3-4% de todos os cânceres humanos. Embora os avanços no tratamento dessa neoplasia maligna tenham promovido um declínio significativo da mortalidade nas últimas décadas, sua incidência está aumentando rapidamente em todo o mundo. No entanto, ainda se discute intensamente se o aumento observado se deve simplesmente a uma melhora na detecção que leva ao diagnóstico excessivo de tumores clinicamente irrelevantes ou ao aumento real do número de casos novos. O câncer de tireoide pode se originar das células foliculares (tireócitos) ou parafoliculares (células C). Enquanto as células foliculares neoplásicas podem evoluir para os tumores papilares ou foliculares bem diferenciados e os tumores anaplásicos indiferenciados, as células parafoliculares neoplásicas levarão sempre ao câncer medular. Os carcinomas papilíferos são o tipo mais prevalente de câncer de tireoide, representando quase 80% dos casos. As alterações genéticas mais relevantes encontradas nesses tumores são mutações pontuais e/ou translocações nos genes *RET*, *BRAF e RAS*. *RET* é um proto-oncogene de 53 Kb localizado no braço longo do cromossomo 10 (q11.21) que codifica um receptor tirosina-quinase, normalmente não expresso nas células foliculares da tireóide, que gera estímulo à proliferação, crescimento celular, diferenciação e sobrevivência mediante a ativação por ligantes da família GDNF (fator neurotrófico derivado da linha celular glial).

Vários tipos de alterações genômicas já foram descritos no gene *RET* e seu papel no desenvolvimento do câncer tem sido amplamente estudado há mais de 20 anos. Enquanto mutações pontuais em *RET* geralmente (mas não exclusivamente) levam ao câncer medular, rearranjos cromossômicos envolvendo *RET* e vários possíveis genes parceiros causará os carcinomas papilíferos de tireoide (PTC). O primeiro relato de uma translocação envolvendo *RET* foi feito em 1990 por Grieco e colaboradores, inaugurando uma lista que hoje inclui mais de 25 translocações, cada uma com seu respectivo gene parceiro. A translocação identificada por Grieco, hoje conhecida como RET/PTC1, é uma inversão intracromossômica entre *RET* e *CCDC6*, um gene localizado no cromossomo 10 (q21.2) que codifica uma proteína expressa de maneira constitutiva na célula folicular tireoidiana. Independentemente do gene parceiro, todas as translocações RET/PTC resultam na fusão da porção 3' de *RET*, que codifica a região catalítica do receptor tirosina quinase, com a porção 5' do gene doador. Isto gera uma proteína de fusão citoplasmática constitutivamente ativa que promove o estímulo contínuo à proliferação através da ativação das vias de MAPK e PI3K, aumentando consideravelmente o risco de neoplasia.

À medida que nossa compreensão sobre as consequências funcionais da sinalização das proteínas de fusão RET/PTC evolui, vários fármacos anti-tirosina quinase são desenvolvidos e testados para o manejo de tumores RET/PTC positivos. No entanto, ainda busca-se entender os mecanismos moleculares que controlam a quebra específica nesses genes. A radiação ionizante é reconhecida há décadas como o mais importante fator de risco para o desenvolvimento do câncer papilífero de tireoide, especialmente para translocações RET/PTC. De fato, vários autores demonstraram experimentalmente a relação causal entre a irradiação e a formação de RET/PTC *in vitro*, corroborando achados clínicos que mostram que os cânceres de tireoide radio-induzidos (como por exemplo, os diagnosticados nos sobreviventes do acidente de Chernobyl) têm maior prevalência de RET/PTC do que tumores papilíferos sem histórico de exposição à radiação (tumores esporádicos). Em consonância com

esses resultados, nosso grupo mostrou que uma única dose de 5 Gy de raios-X pode induzir a formação de RET/PTC1 na linhagem de células epiteliais de tireoide NTHY-ori3.1. Nosso grupo mostrou ainda que as espécies reativas de oxigênio (ERO) são importantes mediadores desse processo. Em um trabalho subsequente, nosso grupo também demonstrou que a irradiação promove um aumento persistente da expressão da NADPH Oxidase DUOX1, o que leva à estresse oxidativo, dano ao DNA e instabilidade genômica.

O papel das ERO na promoção da instabilidade genômica não se baseia apenas em sua capacidade de causar danos oxidativos ao DNA, mas também à criação de um ambiente hostil à replicação. O estresse replicativo pode ser definido como uma perturbação da replicação do DNA que interfere com a conclusão pontual e sem erros da fase S, possuindo forquilhas de replicação aberrantes contendo fragmentos de DNA fita-simples como característica principal. Essas perturbações podem ser causadas por fontes exógenas (irradiação ou compostos genotóxicos tais como o inibidor da polimerase replicativa) ou fontes endógenas (espécies reativas de oxigênio, incorporação estocástica de nucleotídeos, etc.). Sítios frágeis são regiões do genoma particularmente sensíveis ao estresse replicativo. Sob estresse, essas regiões são propensas a apresentar quebras e são hoje consideradas como fatores-chave no desenvolvimento de vários tipos de câncer. De fato, estima-se que 52% das translocações cromossômicas relacionadas à carcinogênese têm pelo menos um dos genes mapeados para sítios frágeis. Este é o caso de *RET* e *CCDC6*, o par de genes responsável pela formação de RET/PTC1. *RET* está localizado em FRA10G, enquanto o *CCDC6* está localizado em FRA10C, dois sítios frágeis comuns do cromossomo 10. Foi demonstrado que o tratamento de células NTHY-ori3.1 com indutores de estresse replicativo podem induzem quebras em *RET* e induzir especificamente a formação de RET/PTC1 em células de tireoide, sugerindo um papel importante para o estresse replicativo na tumorigênese tireoidiana. Portanto, nosso objetivo foi estudar a relação entre o estresse oxidativo e o estresse replicativo em células tireoidianas após irradiação e investigar seu papel na formação da translocação RET/PTC.

Usando a linhagem celular humana NTHYori3.1 (tireócito de origem não-tumoral transformada com SV40), verificamos que a irradiação promove um aumento persistente na geração de ERO intra e extracelular que se inicia vários dias após a irradiação. Observamos que imediatamente após a irradiação ocorre também um pico transitório de produção de ERO que resulta exclusivamente da radiólise da água. Estes dois eventos, temporalmente separados, levam a danos ao DNA. A fim de investigar a possível existência de estresse replicativo, primeiramente confirmamos através da análise do ciclo celular e da incorporação de BrdU que as células irradiadas permanecem proliferativas. Posteriormente, avaliamos a existência de marcadores proteicos de estresse replicativo 3 dias após a irradiação. A análise revelou a ativação de importantes marcadores de estresse replicativo como pChk1, pATR, pRPA e FANCD2. Além disso, alterações morfológicas nucleares relacionadas à instabilidade genética, como deformação e micronúcleos, foram detectadas. O estudo da dinâmica de replicação por *DNA combing* também apontou a existência de estresse replicativo, como demonstrado pela diminuição da velocidade de replicação. Interessantemente, esta diminuição foi revertida por antioxidantes, sugerindo a participação das ERO neste processo. Com a intenção de compreender as possíveis causas desse estresse, avaliamos a concentração de deoxiribonucleotídeos trifosfatos (dNTPs) em células irradiadas. Observamos um aumento consistente de todos os nucleotídeos de maneira tempo-dependente, o que em alguns modelos está relacionado a aumento na

mutagênese e instabilidade genética. A fim de compreender se a formação de RET/PTC *in vitro* estaria relacionada aos efeitos diretos da radiação ionizante e das ERO ou seria uma consequência do estresse replicativo, avaliamos a ocorrência de quebras de fita dupla nos genes relacionados à translocação RET/PTC em dois momentos distintos: 30 minutos após a irradiação ou 4 dias depois. A análise por ChIP-qPCR revelou que embora até mesmo genes não relacionados sejam afetados imediatamente após a irradiação, apenas os genes relacionados à RET/PTC continuam danificados vários dias após. Portanto, os dados sugerem que o estresse replicativo exerce um papel importante na etiologia do câncer papilífero de tireoide induzida por radiação que leva à indução tardia da DUOX1 e ao estresse oxidativo.

.

université PARIS-SACLAY
ÉCOLE DOCTORALE
Signalisation et réseaux intégratifs en biologie (BIOSIGNE)

Titre : THE ROLE OF REACTIVE OXYGEN SPECIES IN THYROID RADIO-CARCINOGENESIS

Mots clés : Cancer de la thyroïde, Stress Oxydatif, Stress replicatif, Espèce reactive de l'oxygène

Résumé : Les cancers papillaires de la thyroïde (PTC) sont les tumeurs endocrines les plus courantes et représentent 2-3% de tous les cancers humains. Les altérations génétiques les plus pertinentes trouvées dans ces tumeurs sont des mutations dans les gènes BRAF et RAS, et des translocations du gène RET. Ces translocations oncogéniques, connues sous le nom de RET/PTC, résultent de la fusion de RET avec des gènes partenaires non-apparentés. L'exposition aux radiations ionisantes est le facteur de risque le plus important pour la formation de RET/PTC. Durant ces dernières années, notre groupe a mis en évidence un rôle crucial des espèces réactives de l'oxygène (ROS) dans la formation de RET/PTC dans des cellules thyroïdiennes in vitro et a notamment montré que l'irradiation (IR) induit l'établissement d'un stress oxydatif persistant du aux ROS produites par la NADPH Oxydase DUOX1, laquelle est induite à post-IR. Cela conduit à des dommages à l'ADN. Les enfants présentent un risque significativement plus élevé de développer des cancers radio-induits de la thyroïde exprimant RET/PTC, probablement en raison du taux de prolifération élevé des cellules. Ceci suggère que la dynamique de réplication pourrait être impliquée dans la formation de la translocation RET/PTC1. En effet, il a été montré que l'induction pharmacologique d'un stress réplicatif peut favoriser la formation de RET/PTC in vitro dans les cellules thyroïdiennes. Ainsi, pour déterminer si un stress réplicatif peut contribuer aux effets à long terme de l'irradiation: à savoir une persistance des lésions de l'ADN et la formation de RET/PTC1, nous avons analysé les effets à post-IR dans les cellules NTHY-ori3.1. Nos résultats confirment qu'une irradiation des cellules aux rayons X à la dose de 5 Gy induit deux vagues de stress oxydatif: une première vague forte mais transitoire qui se produit dans les minutes qui suivent l'irradiation et une deuxième vague dont l' augmentation débute 2 jours après l'irradiation pour persister ensuite. Ces deux pics de stress oxydatif conduisent à deux pics de dommages à l'ADN. L'irradiation des cellules à cette dose n'a aucun effet sur la prolifération et sur la progression du cycle cellulaire. Cependant, plusieurs marqueurs de stress réplicatif sont exprimés trois jours après l'irradiation. Par ailleurs, l'analyse de la dynamique de réplication révèle une diminution de la vitesse de réplication à post-IR qui est contrecarrée par les antioxydants, suggérant qu'un stress oxydatif peut contribuer à un stress réplicatif. Enfin, par ChIP-QPCR, nous observons que les gènes impliqués dans RET/PTC1 présentent plus de cassures double brin que des gènes endogènes, et ce, trois jours après l'irradiation. Ainsi, nous proposons qu'un stress réplicatif induit par un stress oxydatif pourrait être potentiellement impliqué dans l'étiologie des tumeurs RET/PTC-positives.

Title : THE ROLE OF REACTIVE OXYGEN SPECIES IN THYROID RADIO-CARCINOGENESIS

Keywords : Thyroid Cancer, Oxidative Stress, Replicative Stress, Reactive oxygen species

Abstract : Papillary thyroid cancers (PTC) are the most common endocrine tumors and account for 2-3% of all human cancers. The most relevant genetic alterations found in these tumors are mutations in the genes BRAF and RAS, and chromosomal translocations in RET, a proto-oncogene activated in 15-20% of PTCs. These oncogenic translocations, known as RET/PTCs, result from the fusion of RET with unrelated partner genes. Ionizing radiation is a major risk factor for RET/PTC formation, however, the molecular mechanisms involved in these radioinduced translocations just begun to be unveiled. In the past few years, our group has reported a critical role for reactive oxygen species (ROS) in the formation of RET/PTC in thyroid cells *in vitro* and has also shown that irradiation can elicit a persistent oxidative stress caused by the upregulation of the NADPH Oxidase DUOX1 that leads to DNA damage, mediating at least part of the effects of radiation. However, how could ROS lead to the formation of RET/PTC is not fully understood. Children are at significantly higher risk of developing radio-induced thyroid tumors, specially RET/PTC positive, probably due to the intense proliferation rate of their follicular thyroid cells. This epidemiological observation prompts the assumption that replication dynamics may be involved in RET/PTC formation. Indeed, it has been shown that the pharmacological induction of replicative stress can stimulate the *in vitro* formation of RET/PTC in thyroid cells. Thus, to investigate whether replicative stress might contribute for the long-term effects of irradiation on DNA damage and RET/PTC formation, we analyzed the effects of radiation in NTHY-ori3.1 thyroid cell lineage in terms of oxidative and replicative stress and replication dynamics. Our results confirm that irradiation triggers two waves of oxidative stress: first, a strong but transient oxidative burst takes place minutes after irradiation and next, a persistently increased oxidative stress that starts only 2 days after irradiation. These two peaks of oxidative stress lead to two peaks of DNA damage. Irradiation caused little or no effect on proliferation nor on cell cycle progression. However, several protein markers of replicative stress, such as pATR, pATM, pChk1 and pRPA are induced three days after irradiation. Moreover, replication dynamics analysis revealed a diminished replication speed that has been reversed by antioxidants, suggesting that oxidative stress may contribute to replication defects. Finally, using ChIP-qPCR, we observed that the genes involved in RET/PTC1 translocation present more double-stranded breaks than RET/PTC-unrelated genes 3 days after irradiation. Hence, we propose that replicative stress is potentially involved in the etiology of RET/PTC-positive tumors.